

# Aerodynamic Design of The STAD-1 Kestrel



Progetto Aerodinamico  
Professor: M. Boffadossi

Baio Matteo  
Magni Thomas  
Matteucci Niccolò  
Nazir Ali  
Rancati Elia  
Schifone Marco

25<sup>th</sup> July 2024



# Presentation Outline

---



1. Introduction and Design Points.
2. Initial Aerodynamic Considerations.
3. Wing Planform Design.
4. Tail Sizing.
5. High-Lift Devices Design.
6. Higher Order Methods Setup.
7. Airfoil Choice.
8. LEX Design.
9. Complete Aircraft Simulations.
10. Adjoint Optimization
11. Conclusions and Open Points.



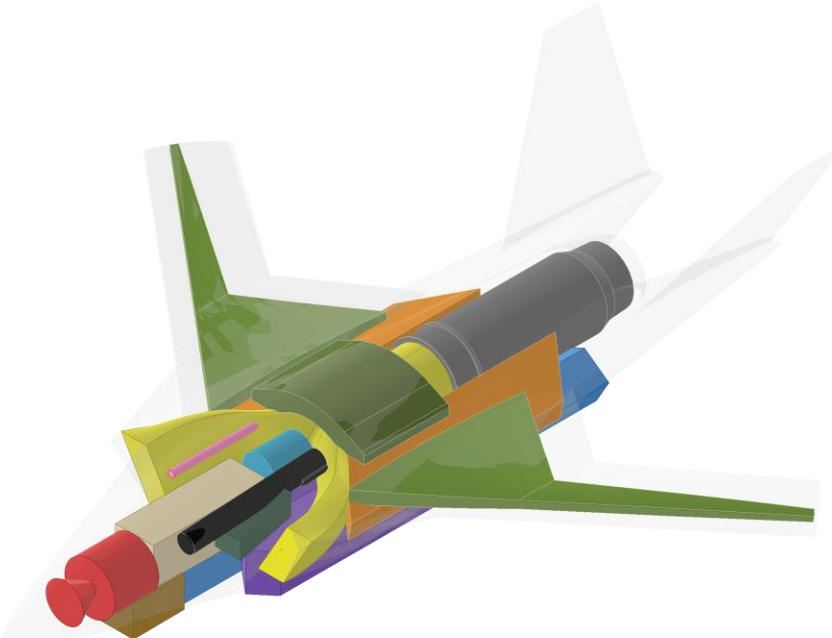
# Introduction and design points: RFP

---

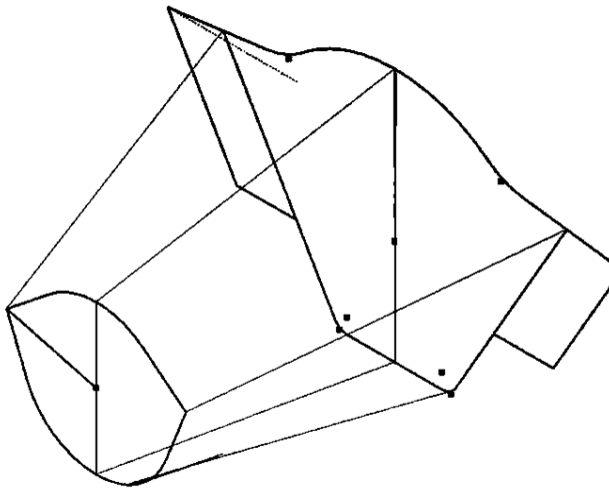


*“Design a **remotely-piloted attack aircraft** for fighting primarily **low-speed manned flying targets**, including **attack helicopters** and **propeller-driven fixed-wing aircraft** (either attack or unarmed/cargo). The aircraft should have also **ground strafing capabilities**. The **range in an operational mission should at least 1,500 km**, including the outbound and return phases. Airborne or land infrastructure and other considerations are required. Target applications are among **current high-tension/open warfare scenarios**.”*

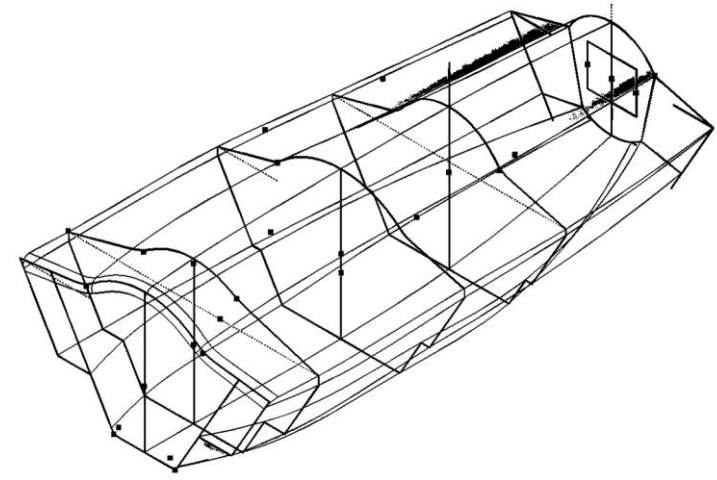
# Introduction and Design Points: Fuselage Design



*Internal Components View.*



*Nose Section Lofting.*



*Central Section Lofting.*

# Introduction and Design Points: Fuselage



## STAD-1 KESTREL

MTOM: 7153 kg + 450 kg (external)

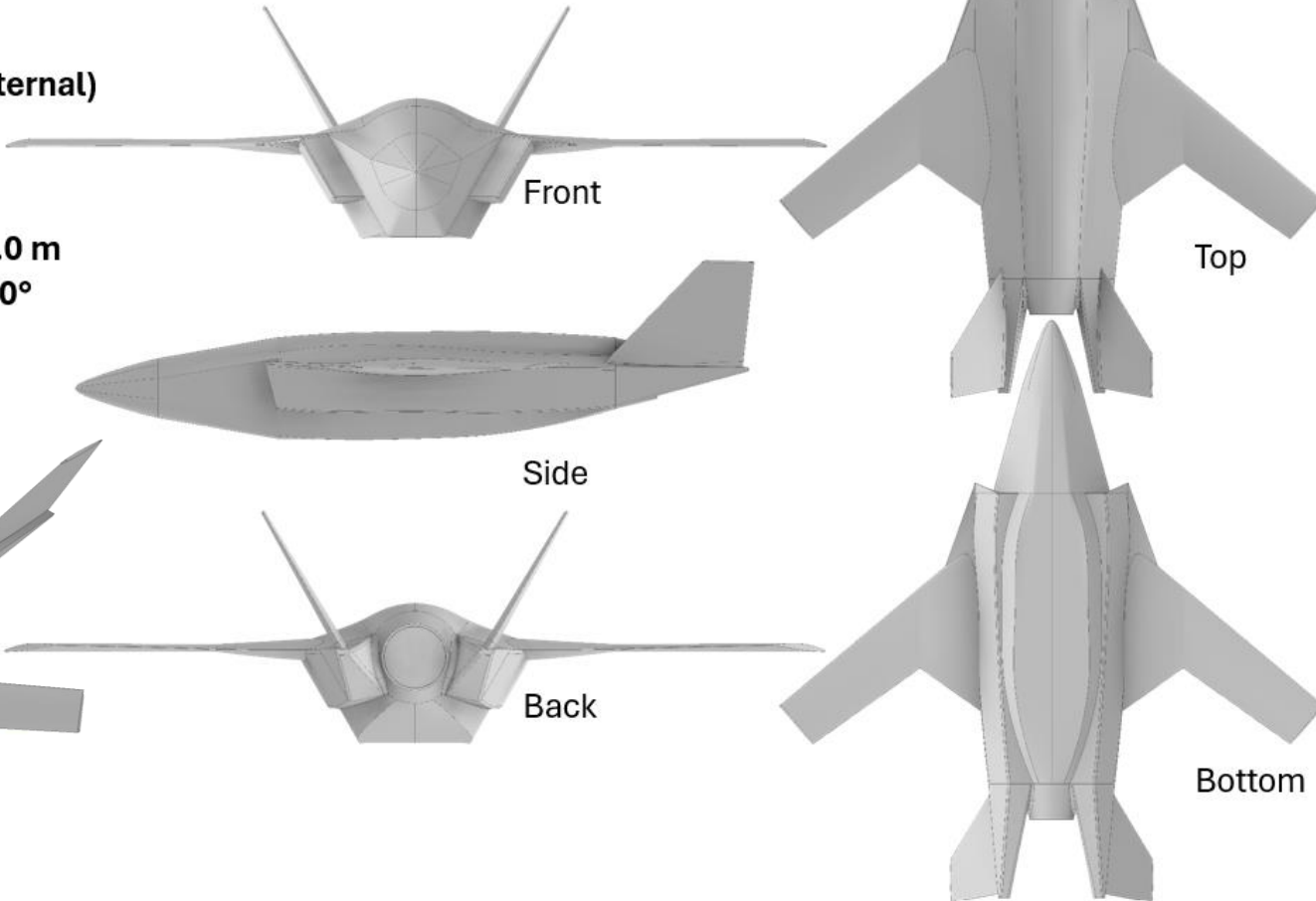
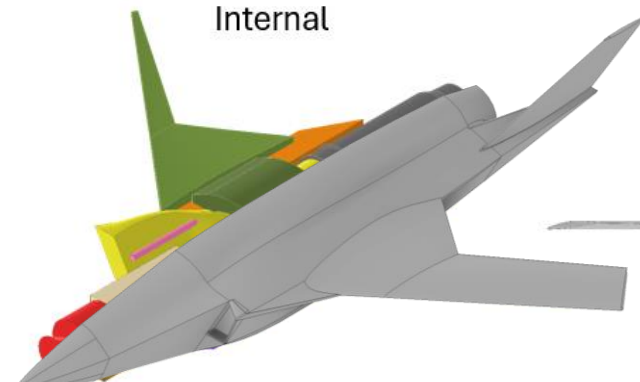
NTOM: 6913 kg

Length: 11.3 m

Span: 10.7m

Height: 3.0 m

Angles: 60°



|                    | Mass [kg] |
|--------------------|-----------|
| Fuel               | 1134      |
| Intake             | 107       |
| Engine             | 971       |
| Landing Gear       | 372       |
| Ammo-box           | 162       |
| Gun                | 105       |
| Free fall Bays     | 520       |
| Side Bays          | 280       |
| Avionics           | 270       |
| EOTS               | 91        |
| Refueling Probe    | 11        |
| APU                | 84        |
| Radar              | 215       |
| Airframe + Systems | 1959      |



# Introduction and Design Points: Design Points



Obtained after a SMP iteration, following the hypothesis of  $AR = 4.198$ .

| Endurance Mission $M_a = 0.50$ and 15,000 ft |               |   |              |                 |
|--|---------------|---|--------------|-----------------|
|  | Consumed Fuel | $\bar{M}/S \left[ \frac{kg}{m^2} \right]$ | $C_L^{wing}$ | $\rho [kg/m^3]$ |
| Initial condition                            | 10.24%        | 255.40                                    | 0.28         | 0.7708          |
| Final condition                              | 65.83%        | 228.92                                    | 0.25         | 0.7708          |

| Rapid Response Mission $M_a = 0.85$ and 10,000 ft |               |   |              |                 |
|---|---------------|---|--------------|-----------------|
|   | Consumed Fuel | $\bar{M}/S \left[ \frac{kg}{m^2} \right]$ | $C_L^{wing}$ | $\rho [kg/m^3]$ |
| Initial condition                                 | 6.32%         | 257.27                                    | 0.07         | 0.9050          |
| Final condition                                   | 9.20%         | 255.90                                    | 0.07         | 0.9050          |

| Sustained Turn $M_a = 0.85$ and 15,000 ft (80% MTOM) |           |                      |                 |
|--|-----------|----------------------|-----------------|
| $\bar{M}/S \left[ \frac{kg}{m^2} \right]$            | $n_{SUS}$ | $n^{sus} C_L^{wing}$ | $\rho [kg/m^3]$ |
| 208.22   | 5.1       | 0.40                 | 0.7708          |

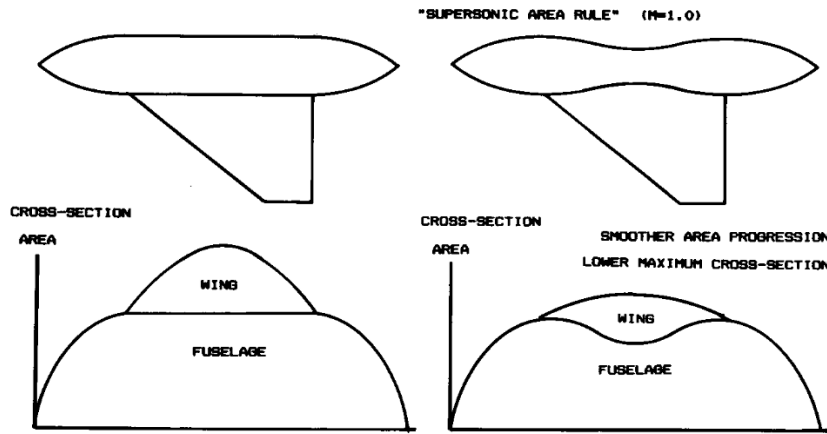
| Instantaneous Turn $M_a = 0.77$ and 15,000 ft (80% MTOM) |           |                      |                 |
|--|-----------|----------------------|-----------------|
| $\bar{M}/S \left[ \frac{kg}{m^2} \right]$                | $n_{INS}$ | $n^{ins} C_L^{wing}$ | $\rho [kg/m^3]$ |
| 208.22   | 8.0       | 0.77                 | 0.7708          |



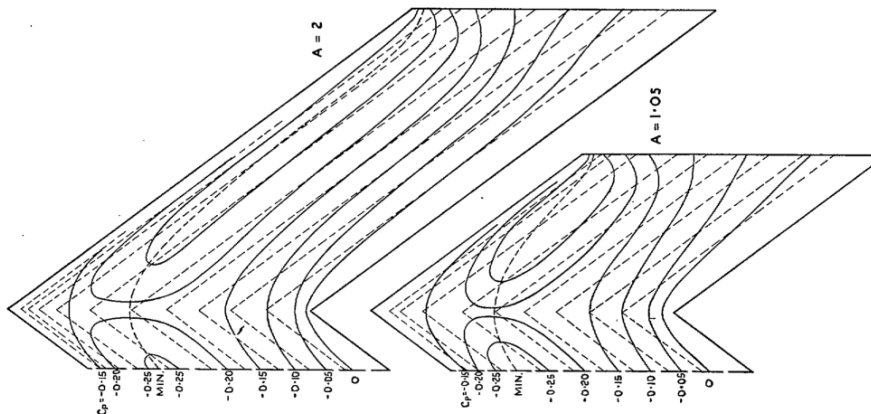
# Initial Aerodynamic Considerations



- The fuselage should have a certain shape to improve the wing-fuselage interaction, defined as the “**Supersonic Area Rule**”.
- Swept wings are affected by “**isobars unsweep**” at the root and tip:
  - Root: **introduction of LEX** to change the pressure distribution at root
  - Airfoil: **higher curvature** to change isobars at tip



Source - *Aircraft Design: A Conceptual Approach*, D. P. Raymer



Source - *Aircraft Design: A Conceptual Approach*, D. P. Raymer



# Wing Planform Design: Procedure

---



Planform is defined by the following procedure:

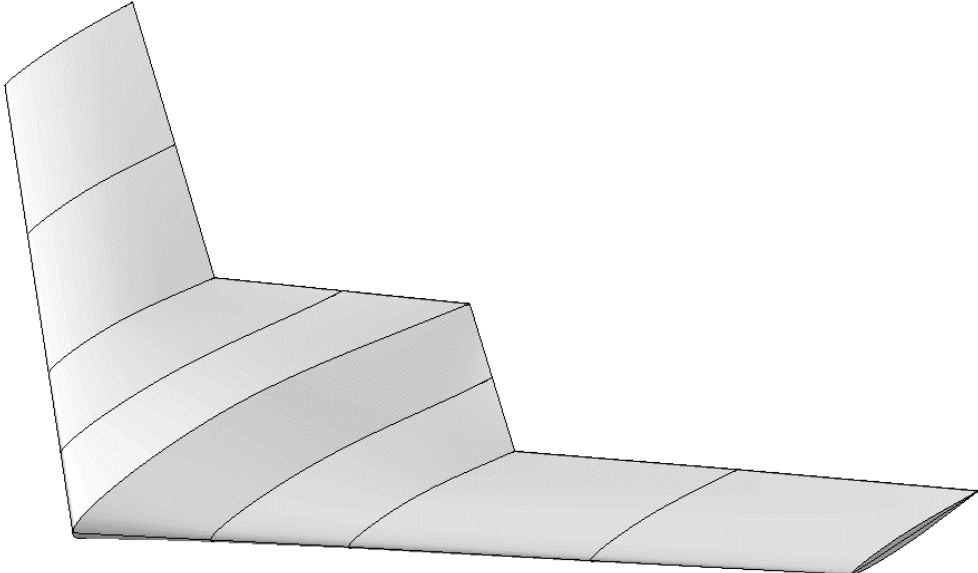
1. **High LE** sweep selected for satisfy Radar Cross Section (RCS) and transonic flight requirements.
2. **Root chord** and **taper ratio** (and so **Tip chord**) closest as possible to 1 in the swept section. Selected iteratively in order to obtain a feasible geometry.
3. **Twist** chosen to achieve as a compromise between elliptical lift distribution and avoiding stall on the external sections.
4. **Incidence** selected as  $0^\circ$ .
5. **Dihedral** set to  $0^\circ$  for RCS considerations.

# Wing Planform Design: Sizing



Planforms designed through OpenVSP and analyzed with its VLM method.

- Stall correction included.
- Viscous and parasite drag obtained by OpenVSP drag tool.
- Prandtl-Glauert correction included.



|                            | Value                |
|----------------------------|----------------------|
| <b>Leading edge sweep</b>  | 40°                  |
| <b>Trailing edge sweep</b> | ±35°                 |
| <b>Reference surface</b>   | 26.56 m <sup>2</sup> |
| <b>Wingspan</b>            | 10.56 m              |
| <b>Mean chord</b>          | 2.65 m               |
| <b>Aspect ratio</b>        | 4.198                |
| <b>Taper ratio</b>         | 0.225                |
| <b>Twist</b>               | 0° to -4°            |

$$(L/D)_{Loiter} = 16.88 \text{ at } M_a = 0.50 \text{ at } 15,000 \text{ ft}$$

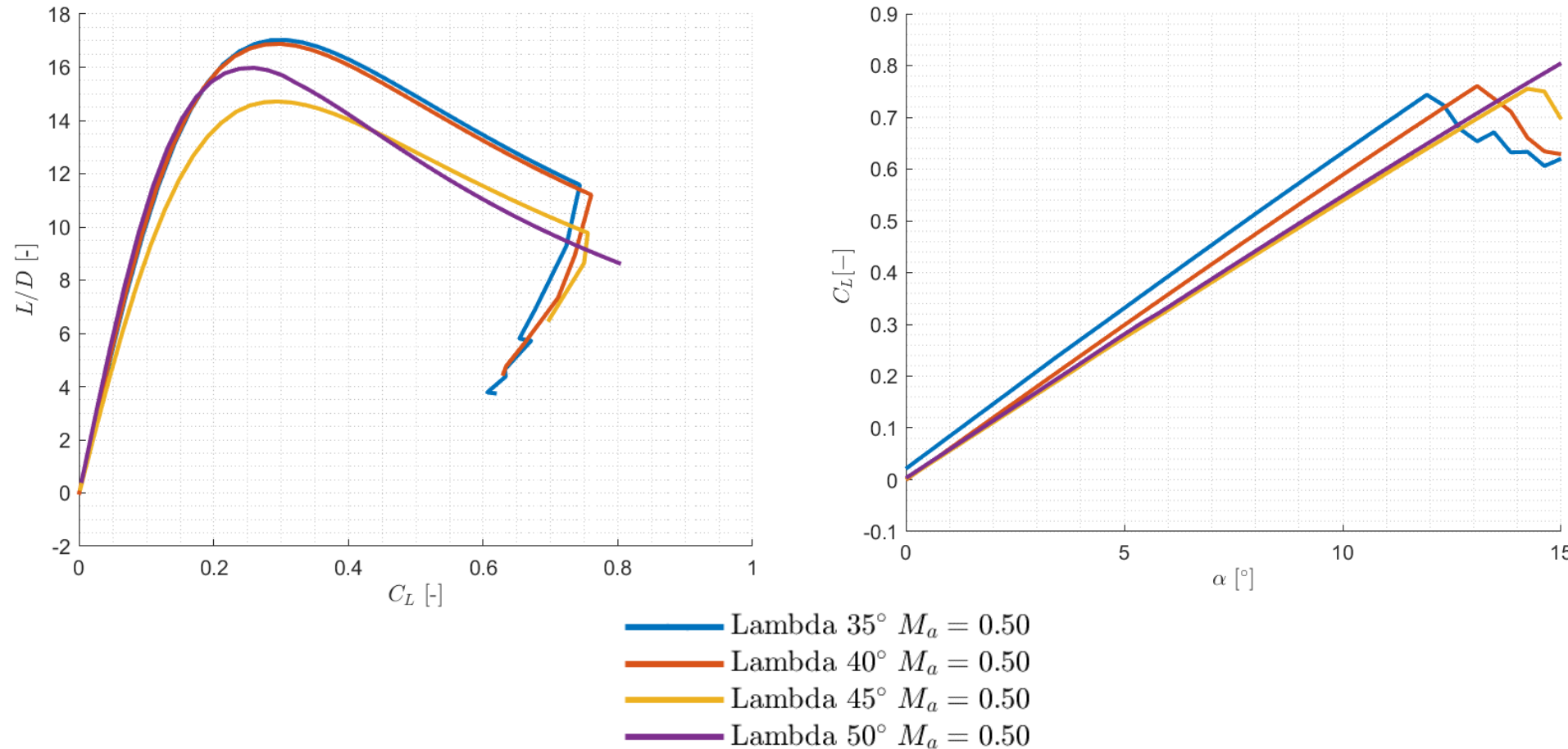
# Wing Planform Design: Sweep Sensitivity



Different configuration tested with the same guidelines

Higher sweep resulted in not feasible geometries

40° configuration chosen for  $L/D$ , RCS and higher stall AOA reasons.



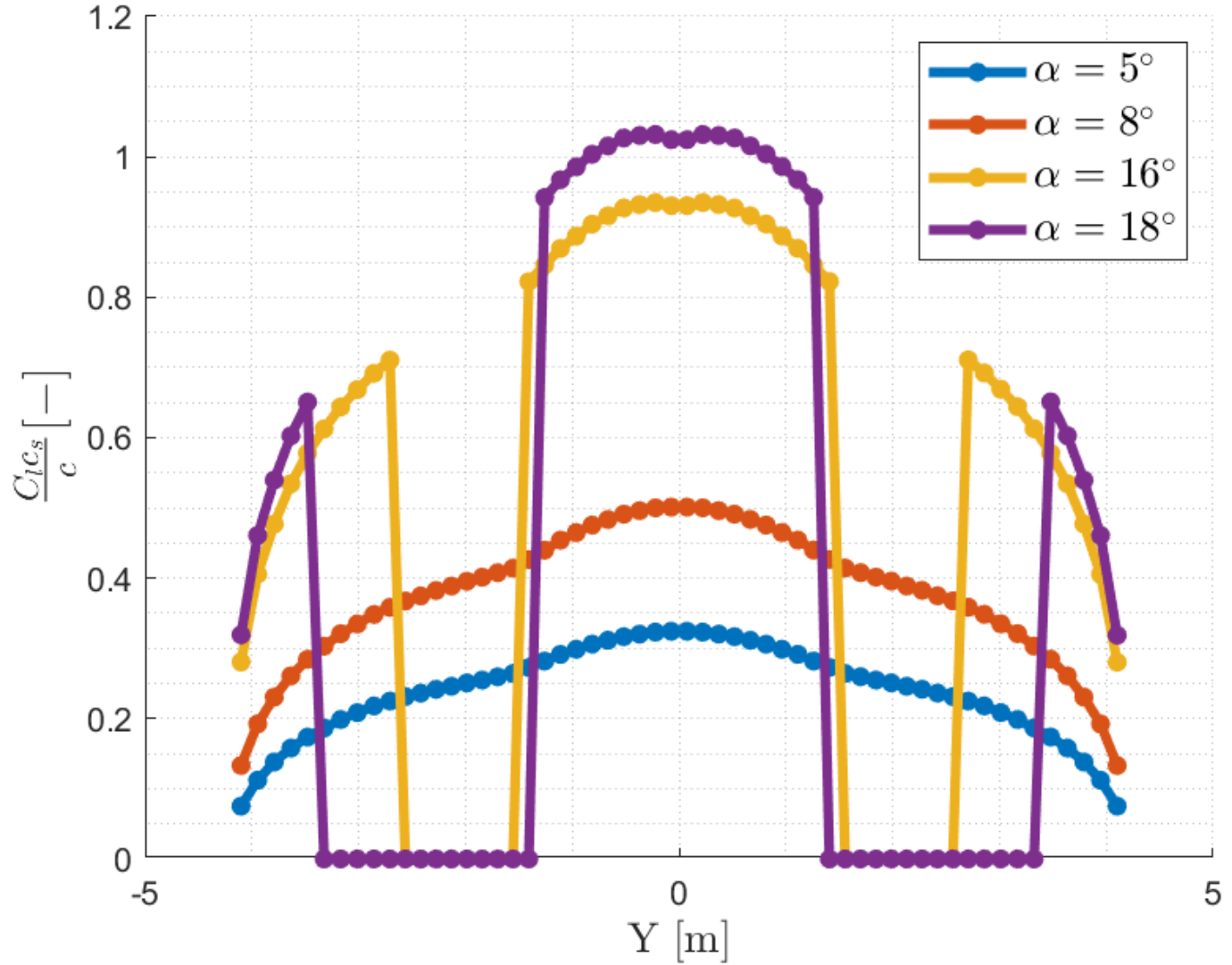
# Wing Planform Design: Spanwise Distribution



It can be verified that the target spanwise distribution behavior has been reached.

The distribution is nearly elliptical (leading to a good  $L/D$ ) while still having wing tip stall delayed.

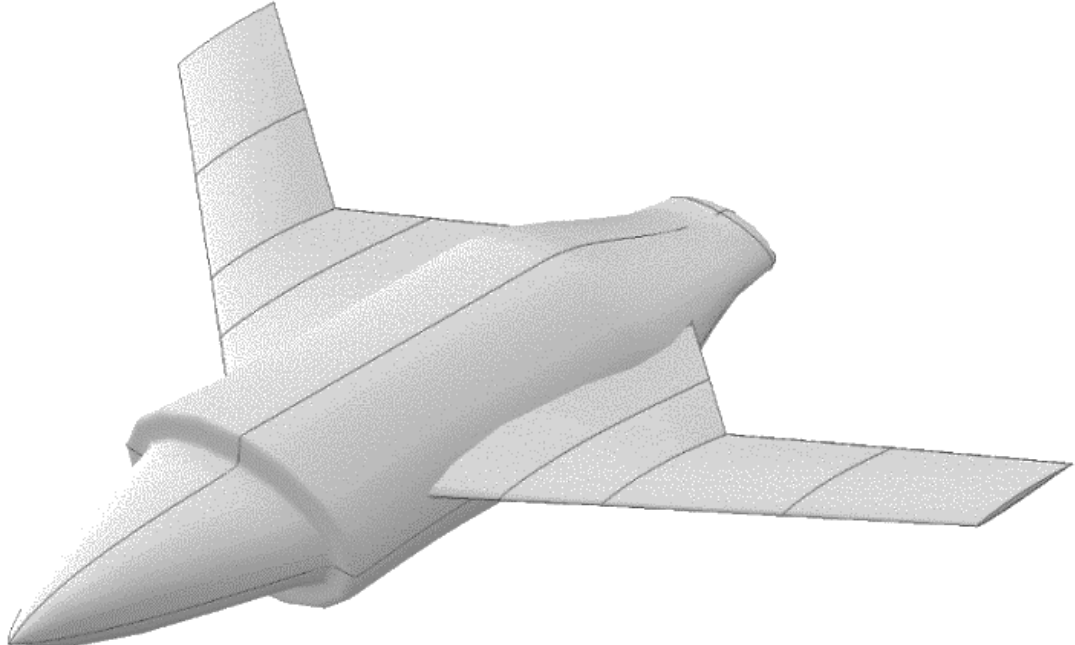
It has been achieved with the combination of twist and curvature of the airfoils.



# Wing Planform Design: Wing Design



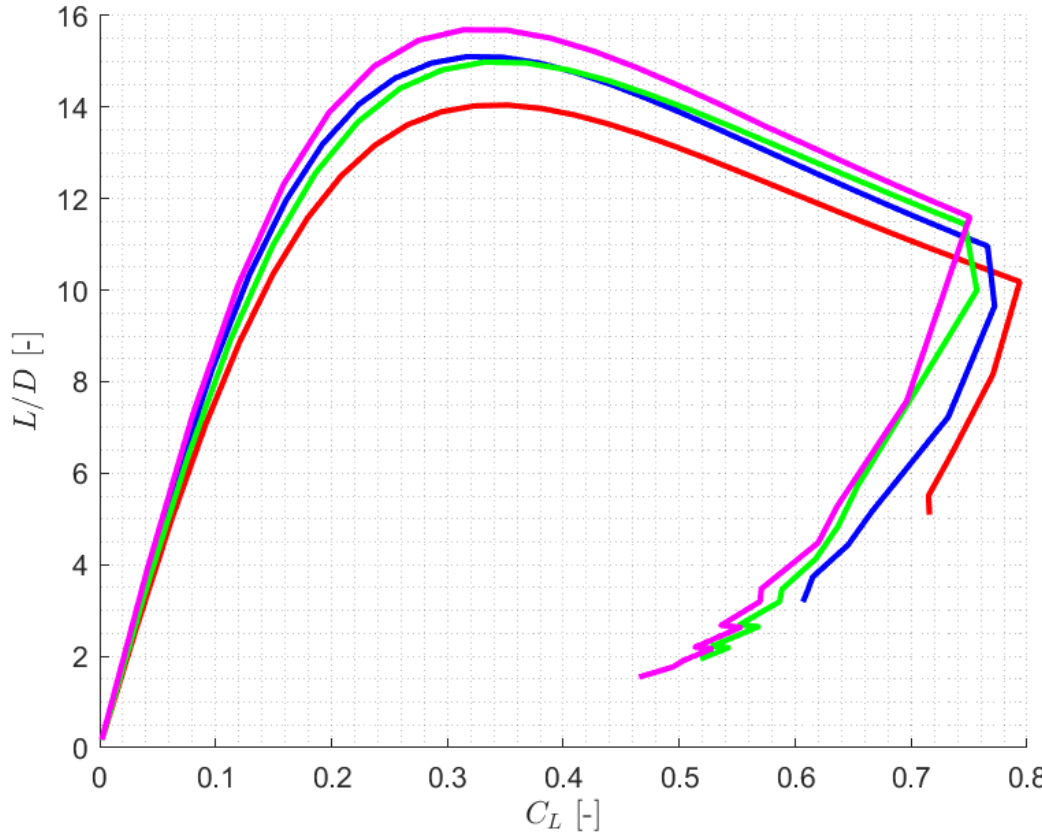
Temporary airfoils selected, airfoils chosen to optimize the planform.  
Simplified fuselage model included in OpenVSP.



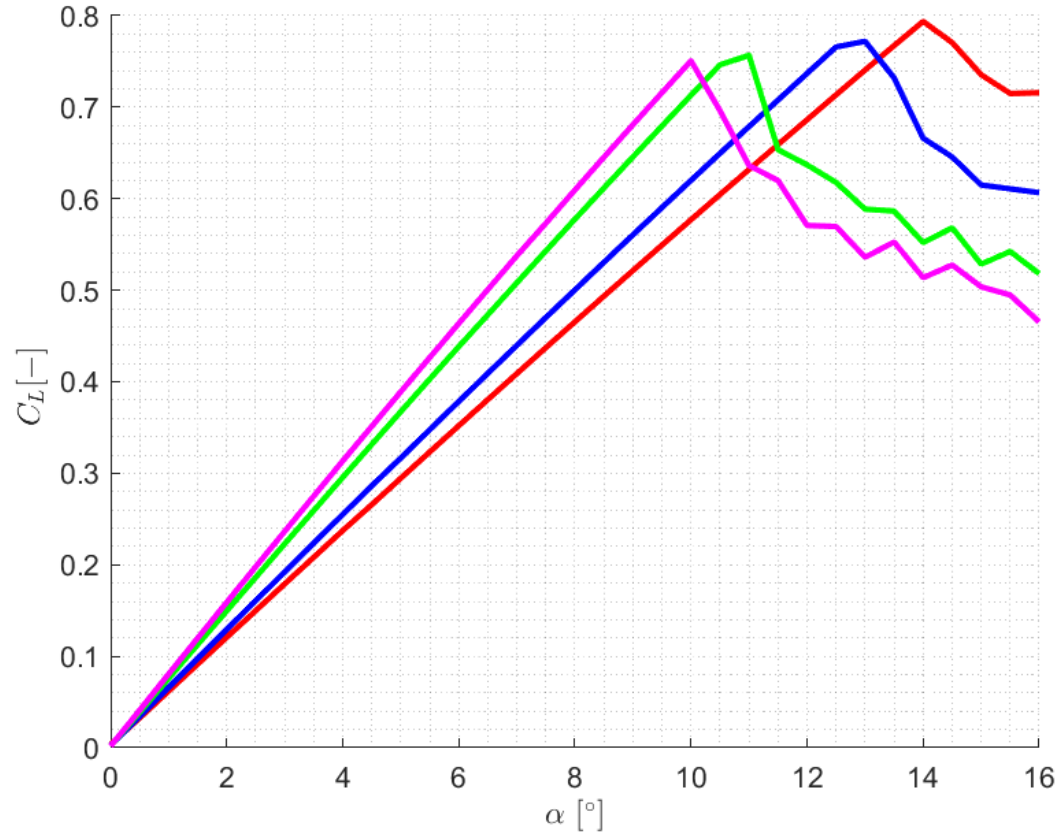
|                     | Root Section | Tip Section |
|---------------------|--------------|-------------|
| Leading edge sweep  | 40°          | 40°         |
| Trailing edge sweep | -35°         | 35°         |
| Section span        | 2.58 m       | 2.70 m      |
| Root chord          | 5.61 m       | 1.64 m      |
| Tip chord           | 1.64 m       | 1.26 m      |
| Taper ratio         | 0.292        | 0.771       |
| Twist               | 0°           | -4°         |

| Airfoil     | Section position [m] | $t/c$ [-] | Chord [m] |
|-------------|----------------------|-----------|-----------|
| NACA 64A010 | 1.10                 | 0.10      | 3.92      |
| NACA 64A008 | 2.58                 | 0.08      | 1.64      |
| NACA 64A208 | 3.88                 | 0.06      | 1.46      |
| NACA 64A206 | 5.28                 | 0.06      | 1.26      |

# Wing Planform Design: OpenVSP Results



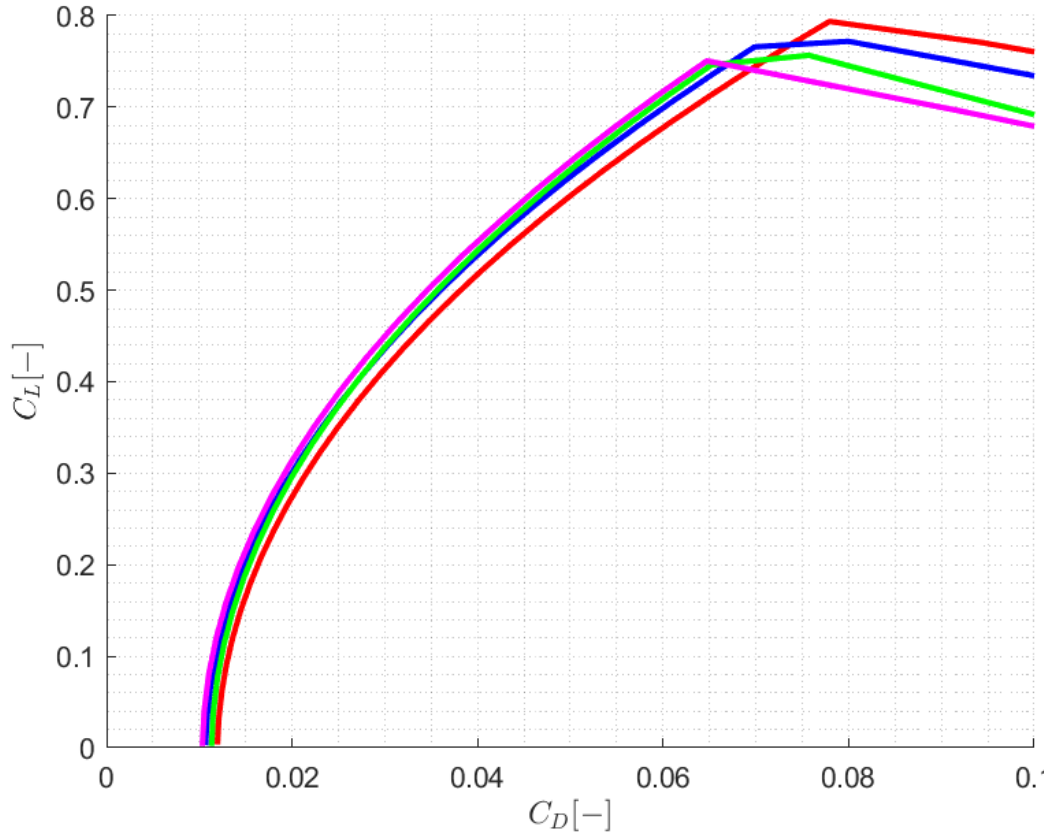
|                          |       |                           |
|--------------------------|-------|---------------------------|
| $L/D$                    | 14.80 | $M_a = 0.50$ at 15,000 ft |
| $\alpha_{Stall}^{Clean}$ | 14°   | $M_a = 0.20$ in H&H       |
| $C_{LMax}^{Clean}$       | 0.77  | $M_a = 0.20$ in H&H       |



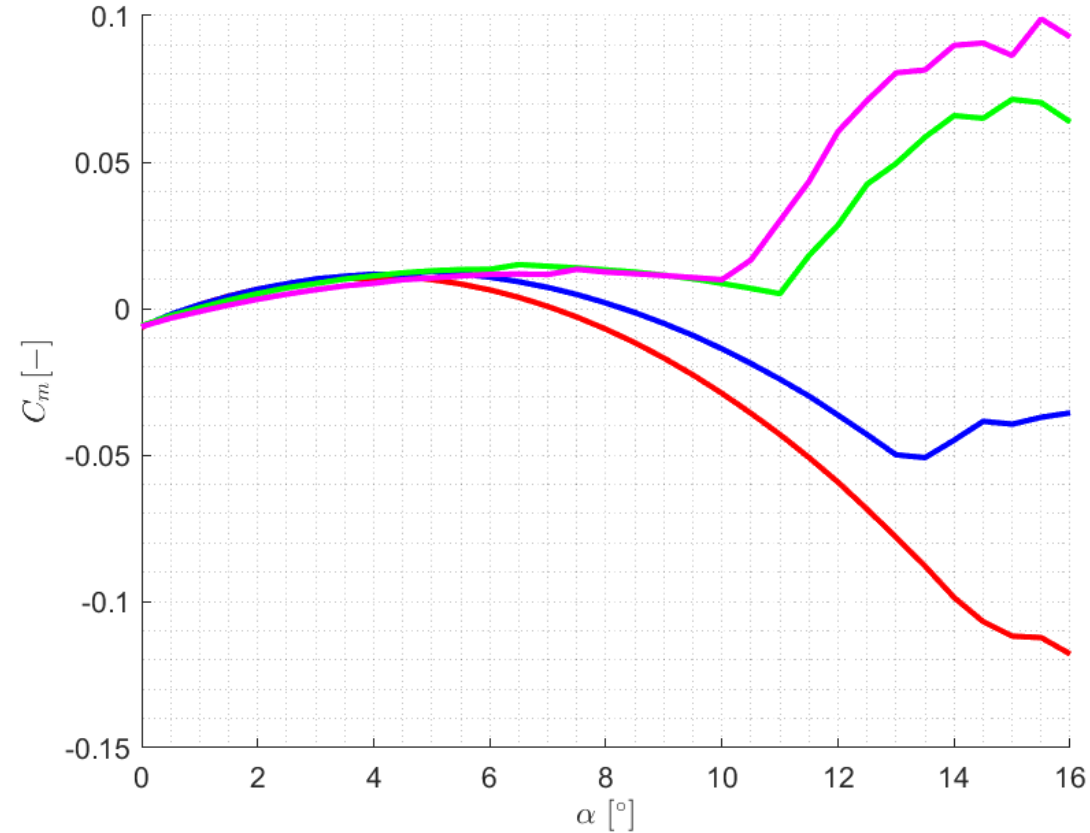
- $M_a = 0.20$  and H&H
- $M_a = 0.50$  and 15k ft
- $M_a = 0.75$  and 30k ft
- $M_a = 0.85$  and 15k ft



# Wing Planform Design: OpenVSP Results



|                          |       |                           |
|--------------------------|-------|---------------------------|
| $L/D$                    | 14.80 | $M_a = 0.50$ at 15,000 ft |
| $\alpha_{Stall}^{Clean}$ | 14°   | $M_a = 0.20$ in H&H       |
| $C_{LMax}^{Clean}$       | 0.77  | $M_a = 0.20$ in H&H       |



Note:  $C_m$  referred to 5.9 m from the nose

- $M_a = 0.20$  and H&H
- $M_a = 0.50$  and 15k ft
- $M_a = 0.75$  and 30k ft
- $M_a = 0.85$  and 15k ft



# Tail Sizing

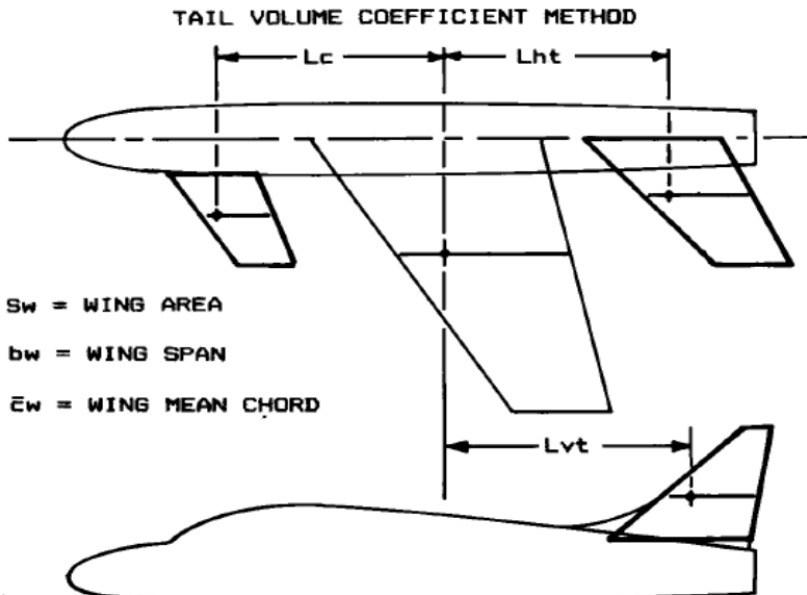


V-Tail sized by the Tail Volume Coefficients method:

$$\cancel{S_H^t = \frac{c_H^t S_{Ref} \bar{c}}{L_H^t}}$$

$$S_V^t = \frac{c_V^t S_{Ref} b_{Wing}}{L_V^t} \rightarrow S^t = \frac{S_V^t}{\sin(\gamma)}$$

$$S_H^t = \frac{S_V^t}{\tan(\gamma)}$$



Where:

- $c_H^t = 0.40$  from Raymer
- $c_V^t = 0.08$  from Raymer
- $L_V^t = L_H^t = 4 \text{ m}$  compromise between fuselage length and  $S^t$

| Surface                                 | [ $m^2$ ] |
|---|-----------|
| $S_V^t$ (from Tail Volume Method)       | 5.61      |
| $S_H^t$ (from Tail Volume Method)       | 7.04      |
| $S^t$ (Actual Tail Surface)             | 6.48      |
| $S_V^t$ (Equivalent Vertical Surface)   | 5.61      |
| $S_H^t$ (Equivalent Horizontal Surface) | 3.24      |

Source - Aircraft Design: A Conceptual Approach, D. P. Raymer



# Tail Sizing

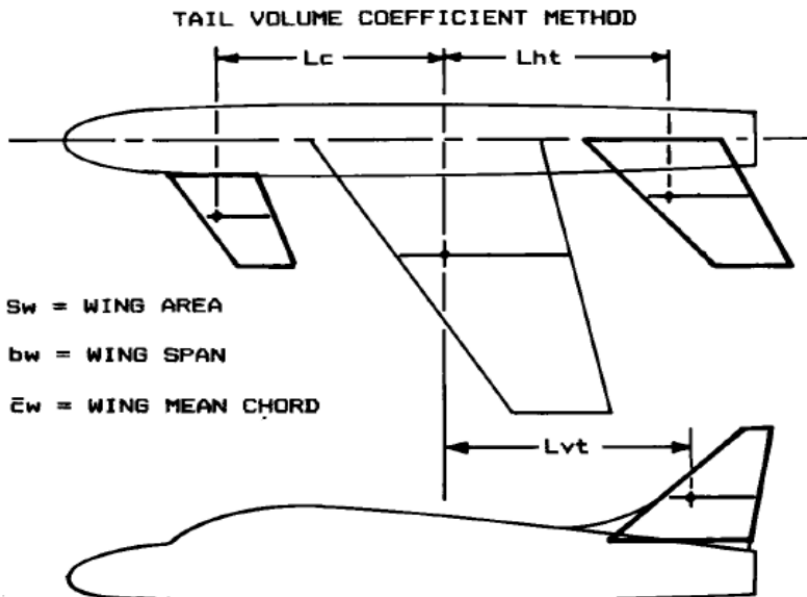


V-Tail sized by the Tail Volume Coefficients method:

$$\cancel{S_H^t = \frac{c_H^t S_{Ref} \bar{c}}{L_H^t}}$$

$$S_V^t = \frac{c_V^t S_{Ref} b_{Wing}}{L_V^t} \rightarrow S^t = \frac{S_V^t}{\sin(\gamma)}$$

$$S_H^t = \frac{S_V^t}{\tan(\gamma)}$$



Source - Aircraft Design: A Conceptual Approach, D. P. Raymer

Where:

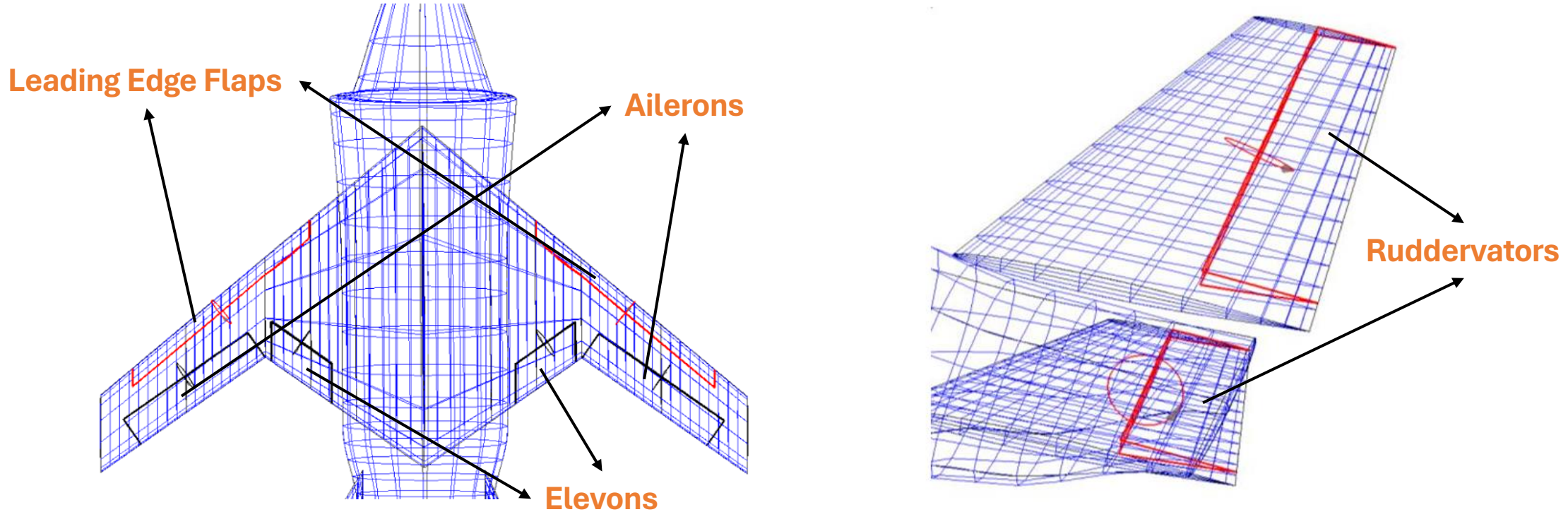
- $c_H^t = 0.40$  from Raymer
- $c_V^t = 0.08$  from Raymer
- $L_V^t = L_H^t = 4 \text{ m}$  compromise between fuselage length and  $S^t$

| Tail Parameters                 | Value |               |
|---------------------------------|-------|---------------|
| Longitudinal Position [m]       | 8.93  | → Fixed       |
| Tail Surface [ $m^2$ ]          | 6.48  | → From Raymer |
| Mean Chord [m]                  | 1.68  | → For RCS     |
| Root Chord [m]                  | 2.40  |               |
| Taper Ratio [-]                 | 0.400 |               |
| Leading Edge Sweep [ $^\circ$ ] | 40    |               |
| Dihedral Angle [ $^\circ$ ]     | 60    |               |
| Span [m]                        | 1.93  |               |
| Height [m]                      | 1.67  |               |

# High-Lift Devices Design: Approach



High-lift surfaces act also as control surfaces,  
Spoiler not included, FCS deflects control surfaces in high-drag mode.



|                        | $S_{Flapped} [m^2]$ | Chord [m] | Span [m] | $\Delta_{Hinge} [^\circ]$ |
|------------------------|---------------------|-----------|----------|---------------------------|
| $S_{Elevons}$          | 5.00                | 0.66      | 1.96     | -35                       |
| $S_{Ailerons}$         | 6.09                | 0.50      | 4.06     | 35                        |
| $S_{LE \text{ flaps}}$ | 11.80               | 0.30      | 5.81     | 40                        |

# High-Lift Devices Design: First Sizing

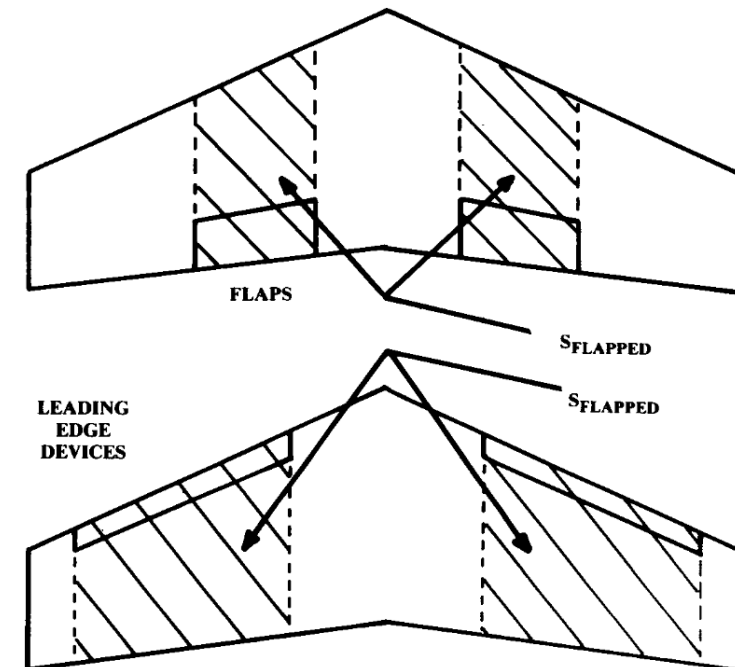


*First method based on typical values used for the sizing:*

- $C_{L_{Max}}^{Flap} = C_{L_{Max}} + \Delta C_{L_{Max}}$
- $\Delta C_{L_{max}} = 0.9 \sum_i \Delta C_{L_{max,i}} \frac{S_{flap_i}}{S} \cos(\Lambda_{Hinge}^i)$

*More accurate semiempirical method used afterwards for final increments of  $\Delta C_{L_{max}}$  and  $\Delta C_D$*

| High-lift device     | $\Delta C_{l_{max}}$ |
|----------------------|----------------------|
| Flaps                |                      |
| Plain and split      | 0.9                  |
| Slotted              | 1.3                  |
| Fowler               | 1.3 c' / c           |
| Double slotted       | 1.6 c' / c           |
| Triple slotted       | 1.9 c' / c           |
| Leading edge devices |                      |
| Fixed slot           | 0.2                  |
| Leading edge flap    | 0.3                  |
| Kruger flap          | 0.3                  |
| Slat                 | 0.4 c' / c           |



Source - Aircraft Design: A Conceptual Approach, D. P. Raymer

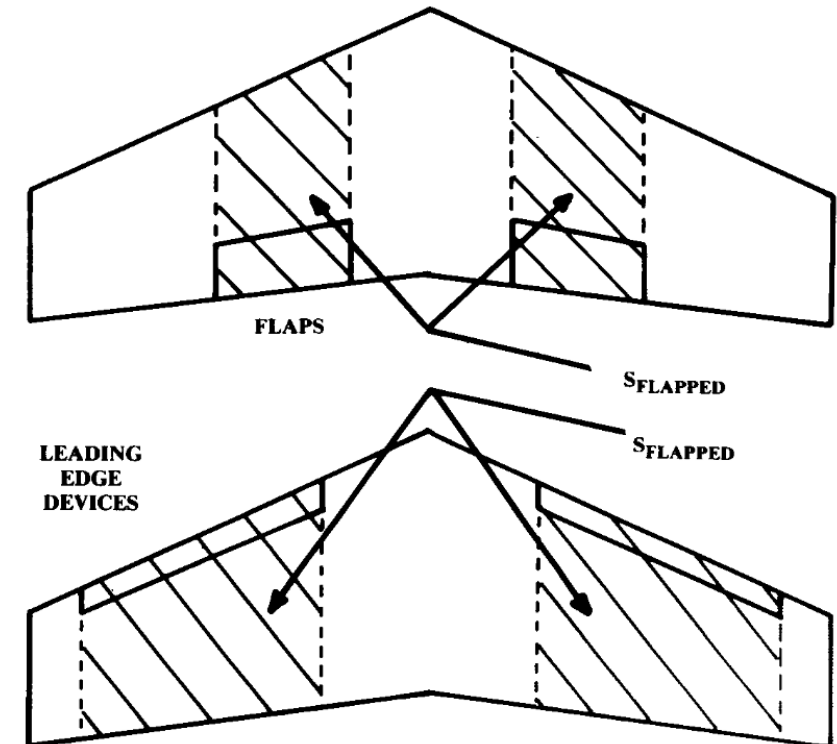
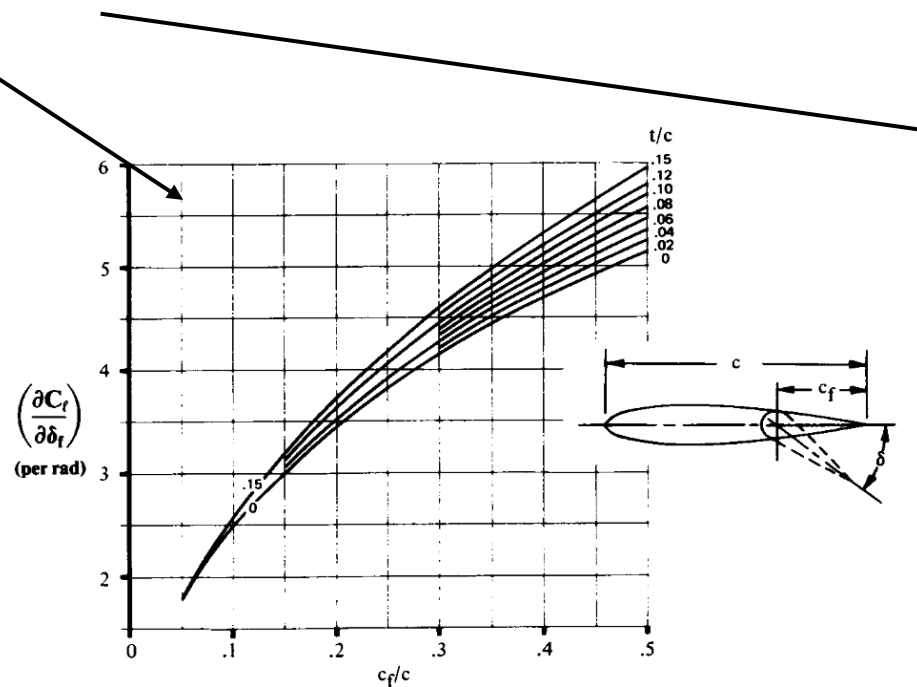
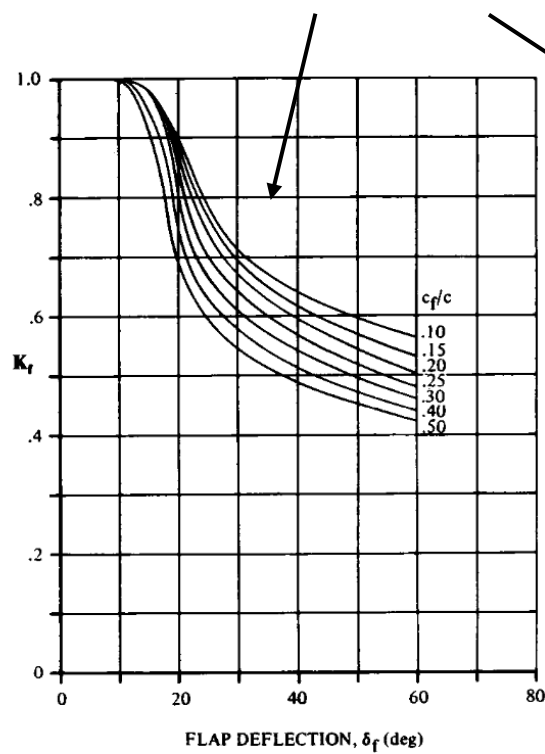


# High-Lift Devices Design: Plain Flap Method



Correction computed multiplying  $\delta_f$  to:

$$\left( \frac{\partial C_L}{\partial \delta_f} \right)_{TE} = 0.9 K_f \left( \frac{\partial C_l}{\partial \delta_f} \right)_{TE} \frac{S_{flapped}}{S_{ref}} \cos(\Lambda_{Hinge}^{local}) \quad \text{with: } \Lambda_{Hinge}^{local} = \pm 35^\circ \text{ for planform alignment (RCS)}$$



Source - Aircraft Design: A Conceptual Approach, D. P. Raymer

Note:  $c_f/c$  and  $t/c$  depends on the considered wing section



# High-Lift Devices Design: Leading Edge Flap Method

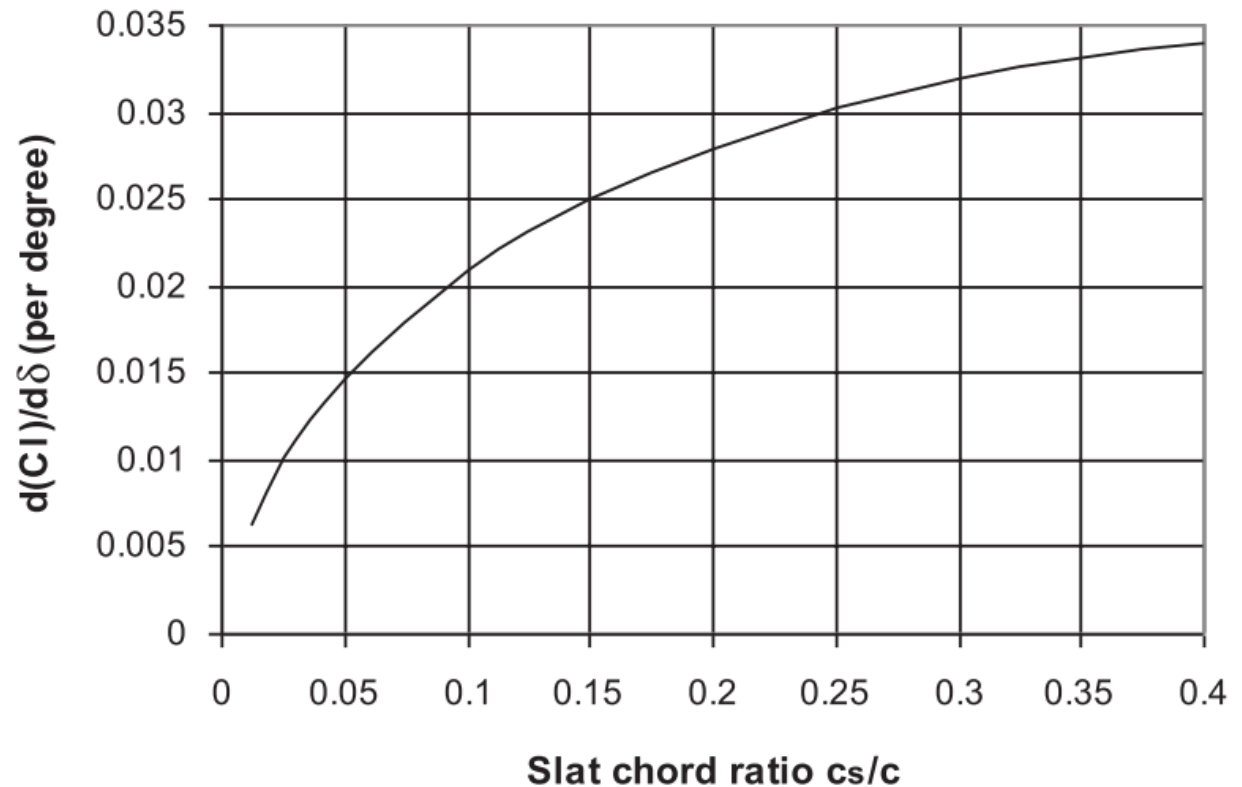


Correction computed multiplying  $\delta_f$  to:

$$\left( \frac{\partial C_L}{\partial \delta_f} \right)_{LE} = \left( \frac{\partial C_l}{\partial \delta_f} \right)_{LE} \frac{S_{flapped}}{S_{ref}} K_A$$

Where:

- $K_A = (1 - 0.08 \cos^2 \Lambda_{Hinge}) \cos^{3/4} \Lambda_{Hinge}$
- $\Lambda_{Hinge} = 40^\circ$  for planform alignment (RCS)



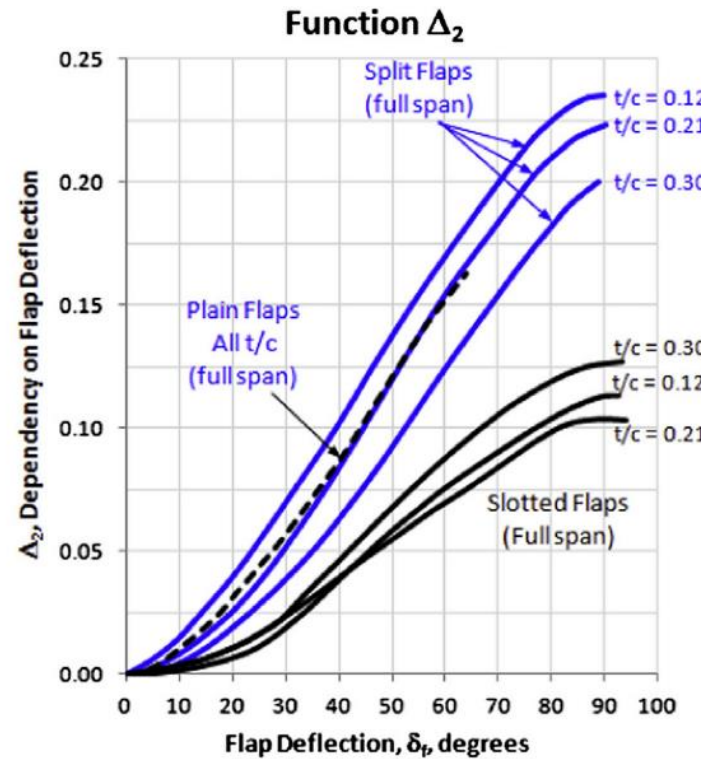
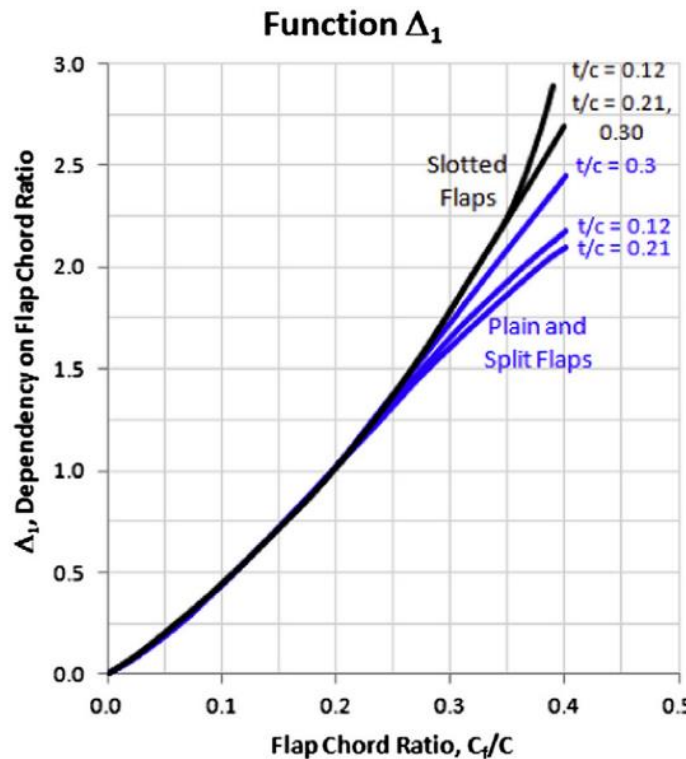
Source - Commercial Airplane Design Principles, P. M. Sforza.

# High-Lift Devices Design: Drag Increment



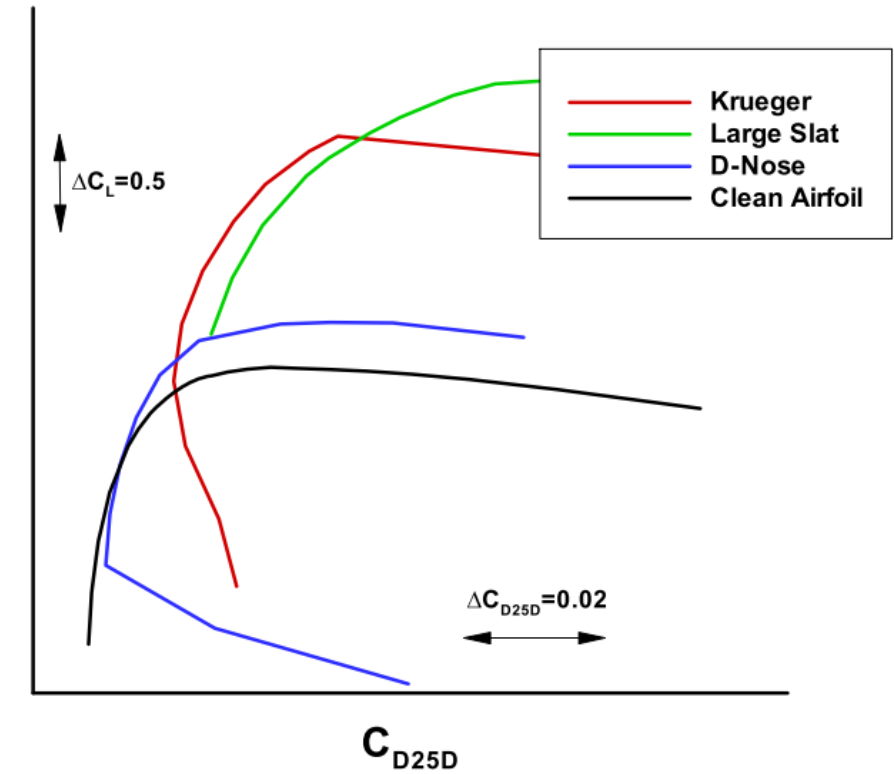
For TE surfaces (plain flaps):

$$\Delta C_D = \Delta_1 \left( \frac{C_f}{c} \right) \Delta_2(\delta_{Flap}) \frac{S_{flapped}}{S_{Ref}}$$



Source -General Aviation Aircraft Design - Applied Methods and Procedures, S. Gudmundsson

For LE flaps (D-nose) is negligible



Source - Design of a High-Lift System for a Laminar Wing,  
P. Iannelli, J. Wild, M. Minervino, H. Struber, F. Moens, A. Vervliet



# High-Lift Devices Design: Polars

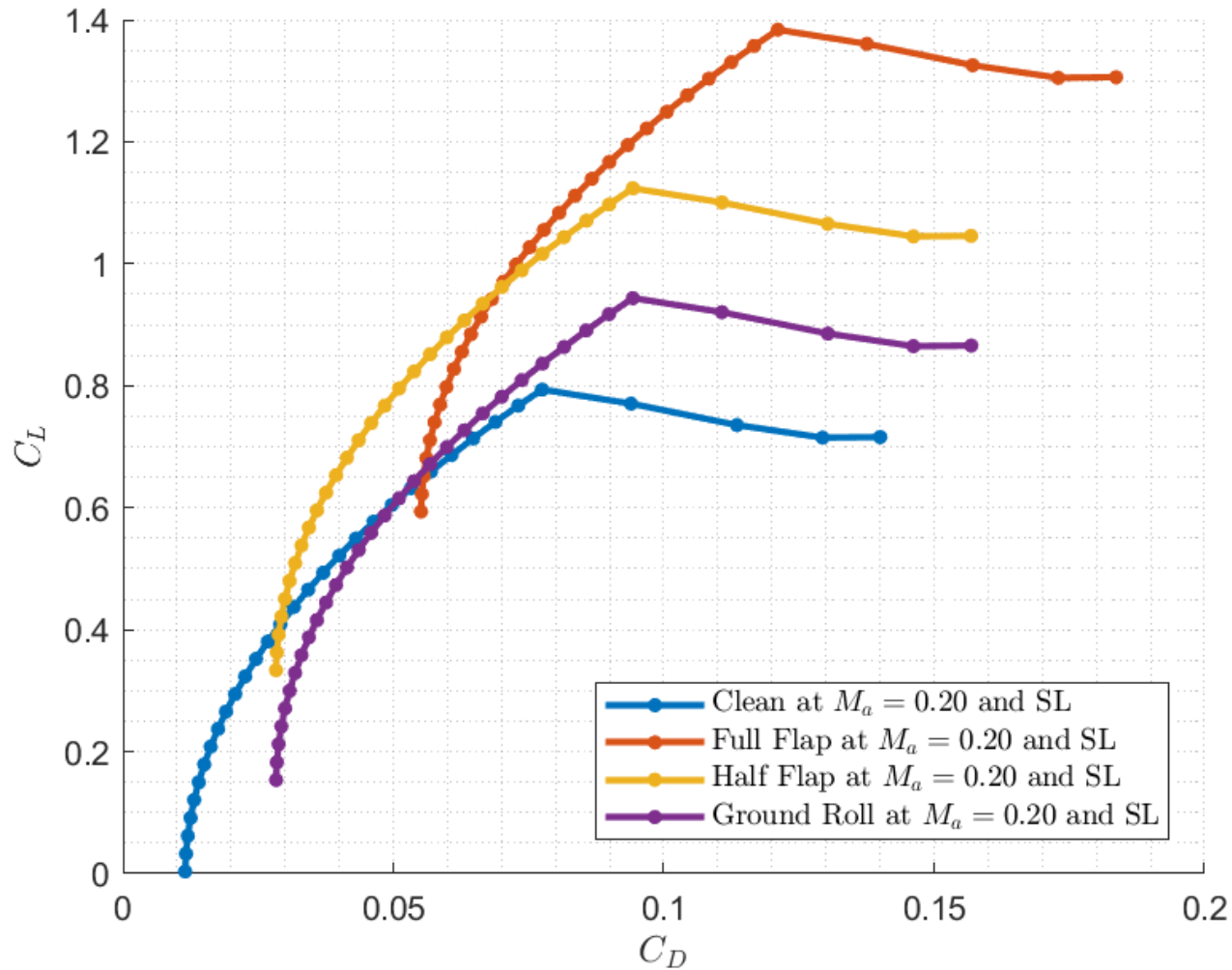


$\Delta C_L$  computed with semiempirical methods:

|             | $\Delta C_L^{LE}$ | $\Delta C_L^{Elevons}$ | $\Delta C_L^{Ailerons}$ | $C_{LMax}$  |
|-------------|-------------------|------------------------|-------------------------|-------------|
| Landing     | <b>0.18</b>       | <b>0.25</b>            | <b>0.16</b>             | <b>1.37</b> |
| Take-Off    | <b>0.18</b>       | <b>0.15</b>            | <b>0.00</b>             | <b>1.11</b> |
| Ground-Roll | <b>0.00</b>       | <b>0.15</b>            | <b>0.00</b>             | <b>0.93</b> |

$\Delta C_D$  also computed with semiempirical methods

|             | $\Delta C_D^{LE}$ | $\Delta C_D^{Elevons}$ | $\Delta C_D^{Ailerons}$ | $\Delta C_D^{Flap}$ |
|-------------|-------------------|------------------------|-------------------------|---------------------|
| Landing     | <b>0.0000</b>     | <b>0.0352</b>          | <b>0.0084</b>           | <b>0.0436</b>       |
| Take-Off    | <b>0.0000</b>     | <b>0.0168</b>          | <b>0.0000</b>           | <b>0.0168</b>       |
| Ground-Roll | <b>0.0000</b>     | <b>0.0168</b>          | <b>0.0000</b>           | <b>0.0168</b>       |



Note: the polar needs to add the landing gear drag  $\Delta C_D^{\text{Gear}} = 0.0190$

# Higher Order Methods Setup: Reasoning

---



Higher order CFD is used in the preliminary design as a mean to assess the effects that potential methods (like OpenVSP) are not able to capture:

- **Shockwaves**: it is fundamental to assess the wave drag in the sustained turn.
- **Leading Edge Extension's effects**: as the effect is interaction-driven, a higher order method is used to gain approximative results on the behavior.

Nevertheless, CFD is used in the industry since the conceptual design to gain knowledge on the aerodynamic choices made.

# Higher Order Methods Setup: Euler Analyses

---



For the first analyses, the solver employed is the compressible Euler solver in **SU2**, an inviscid solver where the viscous terms do not need to be solved.

It is a strong hypothesis but coherent with the fact that:

- This method is able to consider the presence of shock waves.
- The idea is to capture an estimate of the wave drag and the lift coefficient.
- The maximum angle of attack considered for these analyses is  $6^\circ$ .

Furthermore this method secures different advantages:

- Reduced computational time needed.
- Less costly mesh topology.
- Faster convergence when compared to a viscous flow simulation.

# Higher Order Methods Setup: Introduction to Meshing

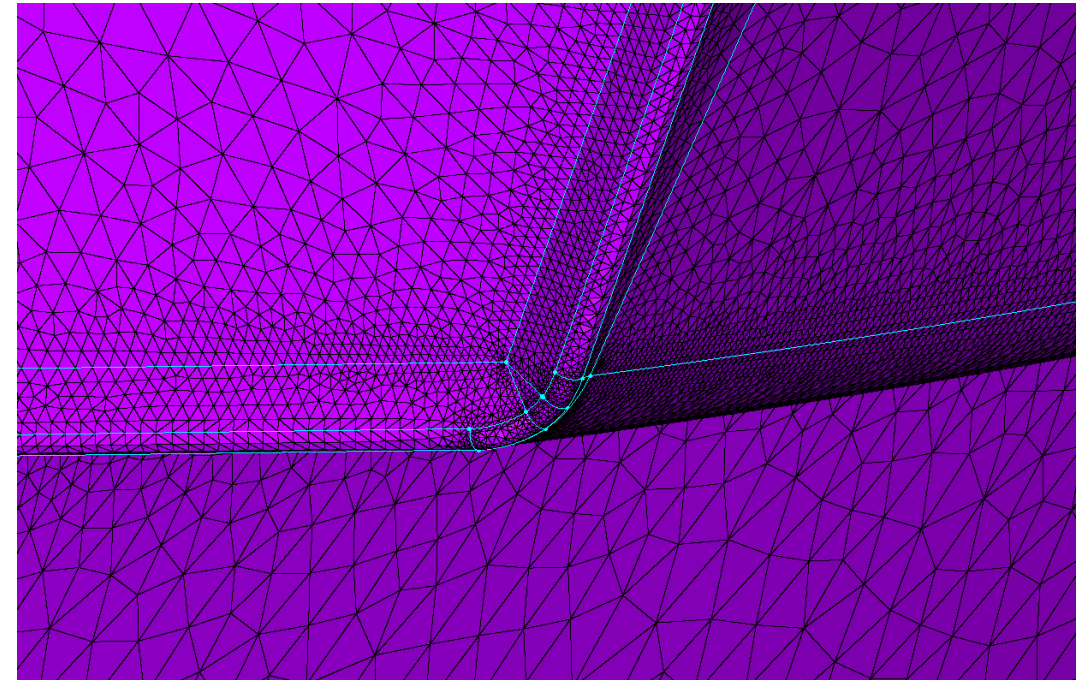


In order to obtain affordable and accurate results from the CFD analysis it is of fundamental importance to prepare the mesh carefully.

The real goal of this process is to find the right balance between elements concentrated where a more accurate solution is needed, and computational power available for the analysis.

Unstructured mesh which is:

- Easier to adapt to complex geometries.
- More flexible for local density changes.



Right Lower Edge of the Air Intake.

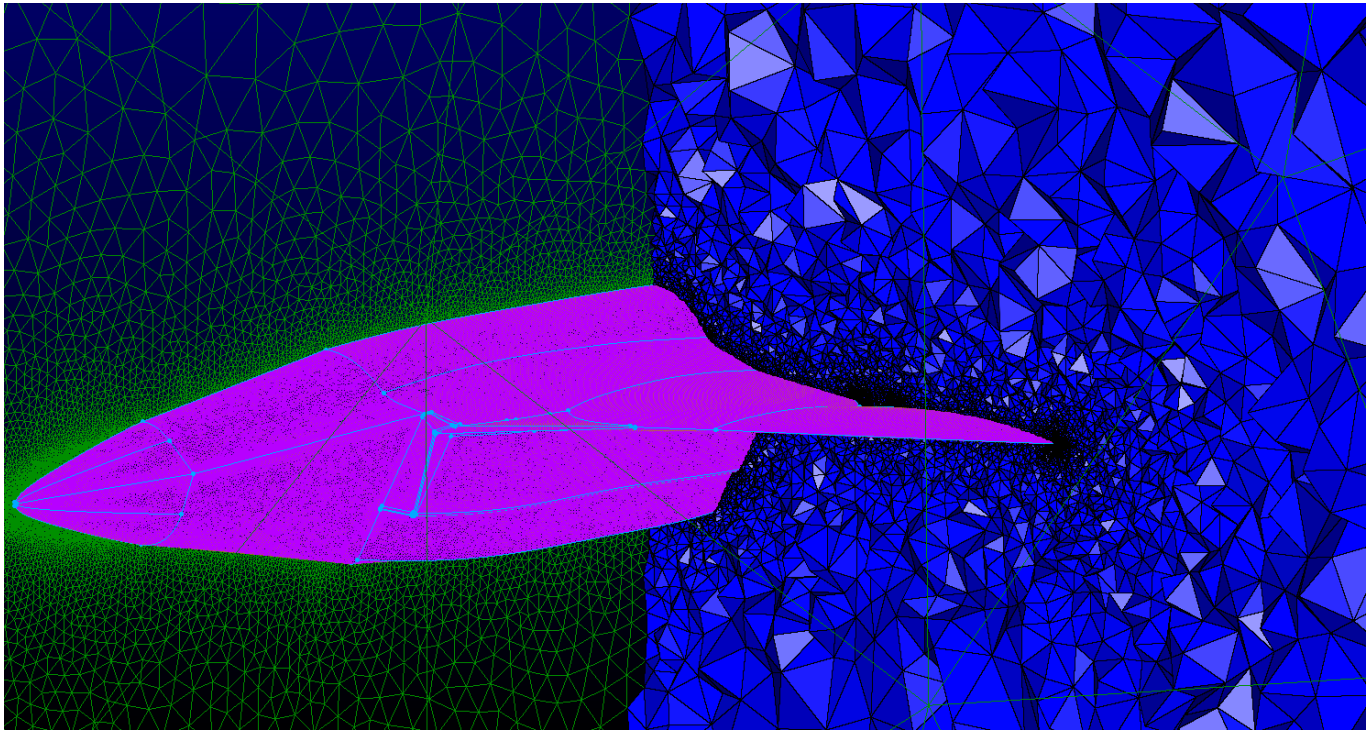
# Higher Order Methods Setup: Fullbody Grid Generation



Once the surface mesh has been created, an extension of the generation of elements to the farfield can be done with a box of 100x80x100 meters.

Different parameters are available to monitor the mesh quality:

- Intersections.
- Aspect ratio.
- Skewness.



Section of the Volume Mesh.

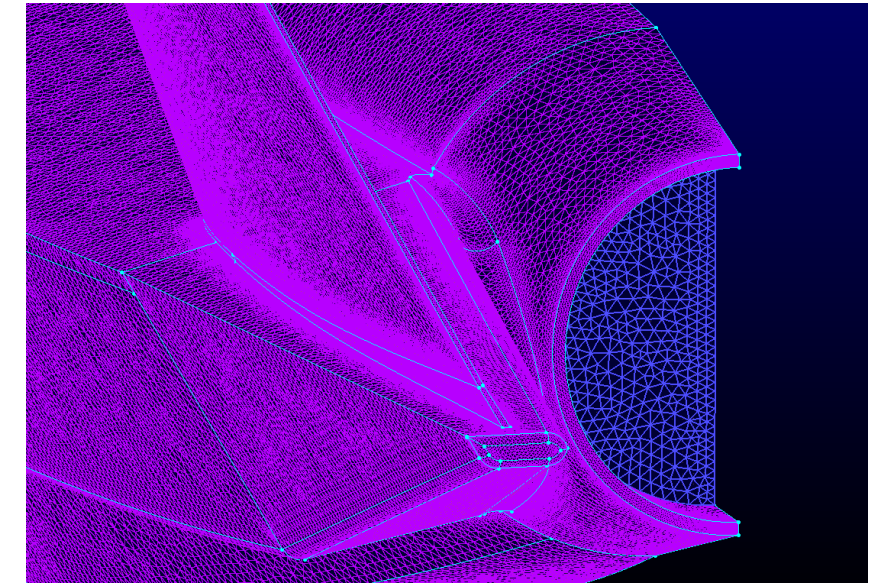
# Higher Order Methods Setup: Fullbody Grid Generation



The last stage where the mesh software generator is needed is the setting of the boundary conditions.

- **SYMMETRY**
- **FARFIELD**
- **MARKER\_WALL** for the Euler analyses.
- **MARKER\_HEATFLUX** for RANS.

|           | Values imposed for inlet and outlet marker.   |                             |                                    |
|-----------|---|-----------------------------|------------------------------------|
|           | Air Density at the Inlet [kg/m <sup>3</sup> ] | Velocity at the Inlet [m/s] | Static Pressure at the Outlet [Pa] |
| Mach 0.50 | 0.5849  | 319.87                      | 57182                              |
| Mach 0.85 | 0.9589  | 282.33                      | 57182                              |

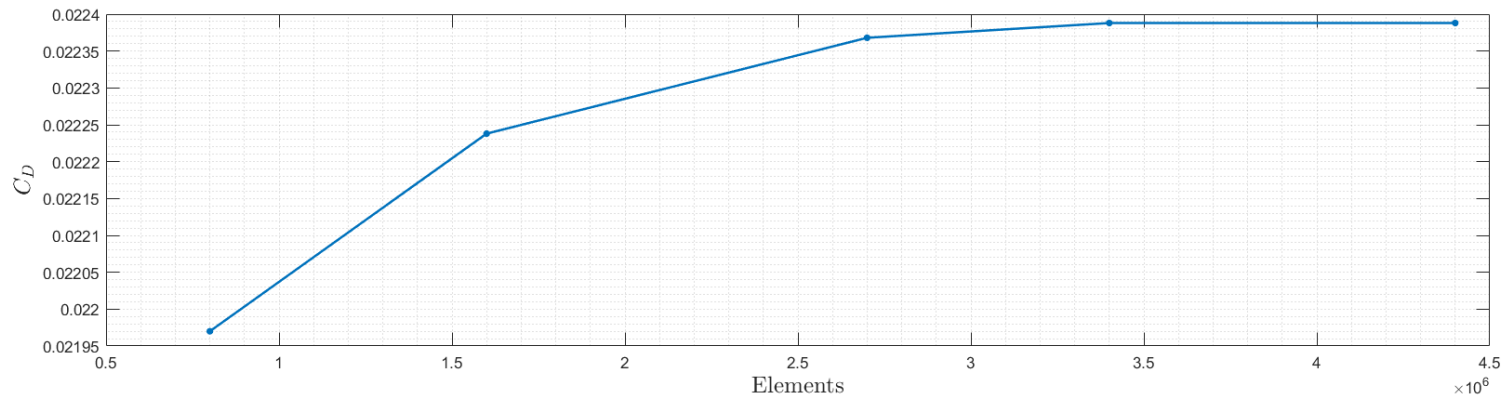
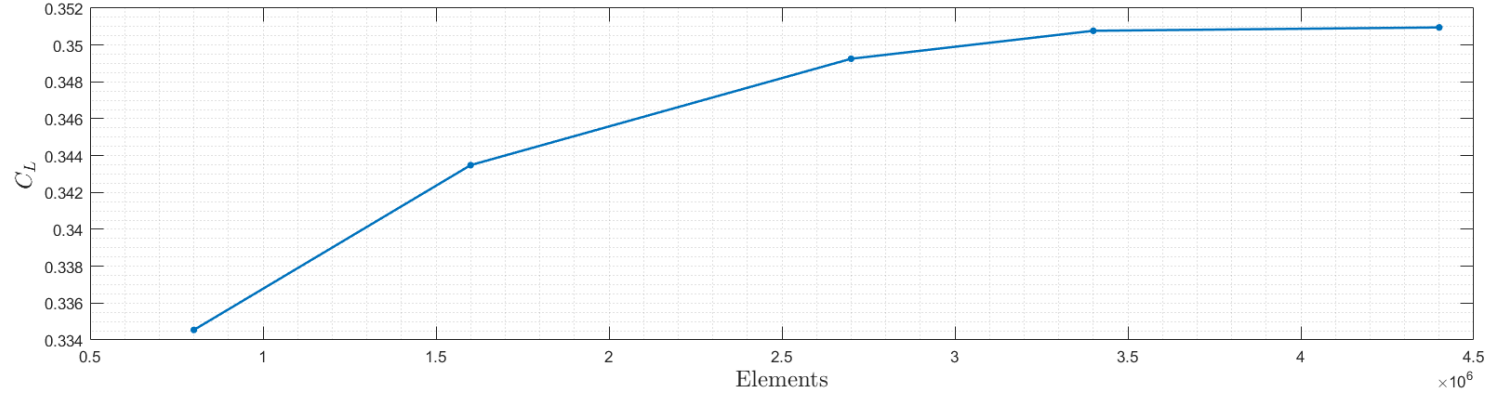


MARKER\_OUTLET at the nozzle.

# Higher Order Methods Setup: Grid Convergence



The grid convergence has been carried out for every analysis done.



Grid convergence results for the isolated wing for Euler.

# Higher Order Methods Setup: DUST



## What is DUST?

Open source mid fidelity aerodynamic solver

Developed in FORTRAN by Politecnico di Milano

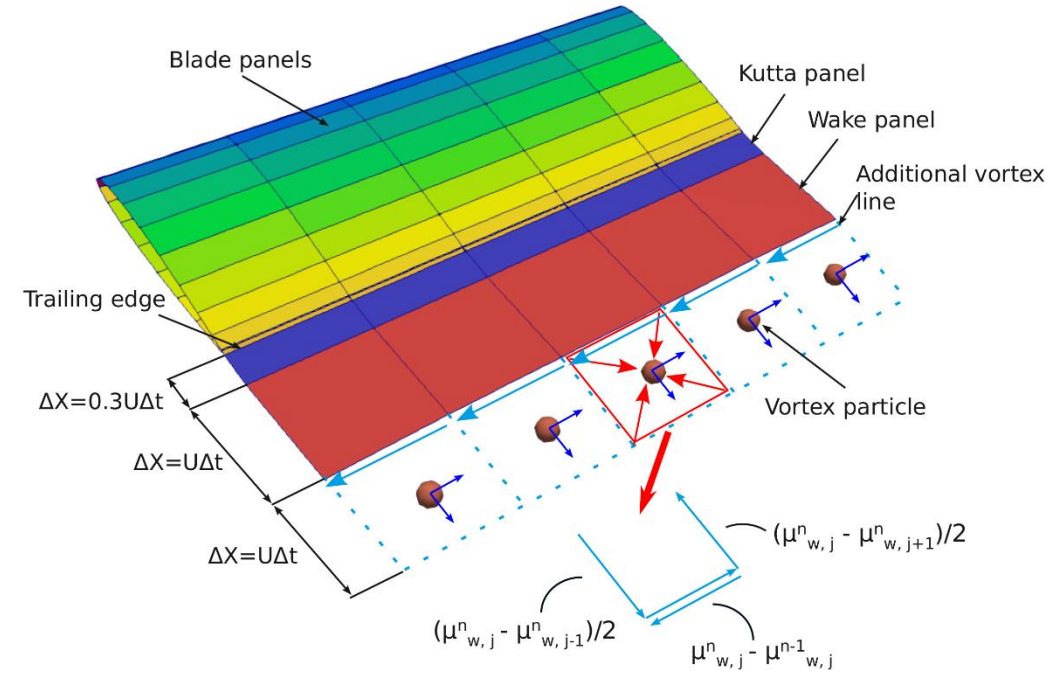
Released under MIT license

## Why DUST?

Vortex Particle method  $\Rightarrow$  Interactional aerodynamic

Hybrid 3D model  $\Rightarrow$  Different precision and cost

Incompressible potential flow



**DUST**

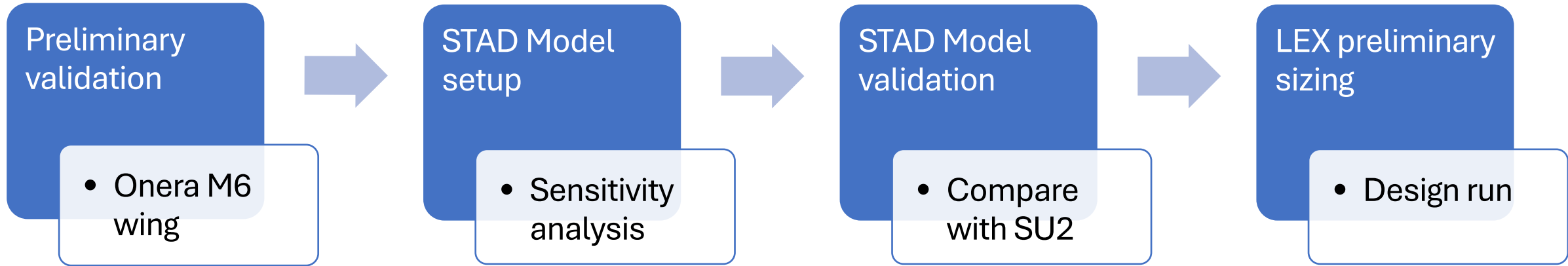
FLEXIBLE SOLUTION FOR  
AERODYNAMIC PROBLEMS



# Higher Order Methods Setup: DUST Analysis on STAD-1



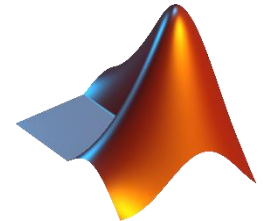
Roadmap of the DUST analysis done on STAD-1:



*Considering the big number of parametric analysis to perform and data to manage...*

*Details on how has been done in the appendix*

**DUST** interfaced with  
**MATLAB**

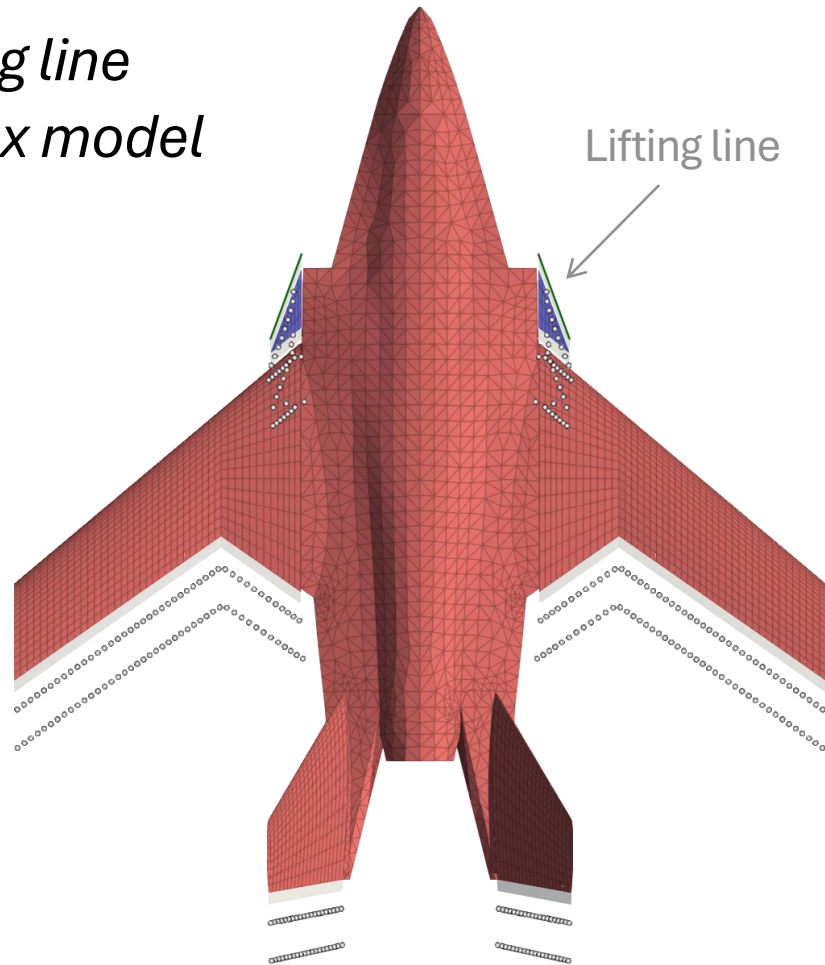


# Higher Order Methods Setup: STAD-1 model in DUST

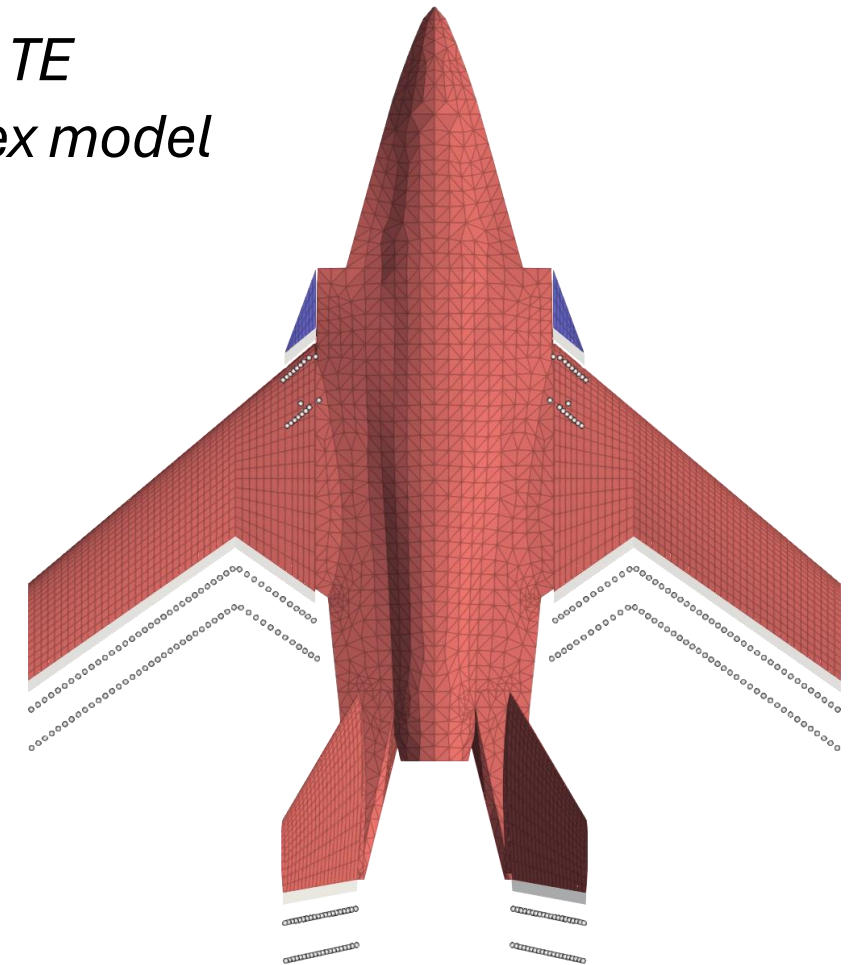


Two different modelizations have been developed:

*Lifting line  
vortex model*



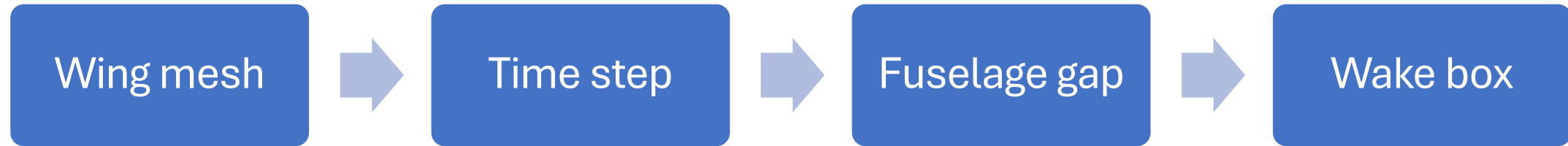
*VLM TE  
vortex model*



# Higher Order Methods Setup: DUST Sensitivity Analysis



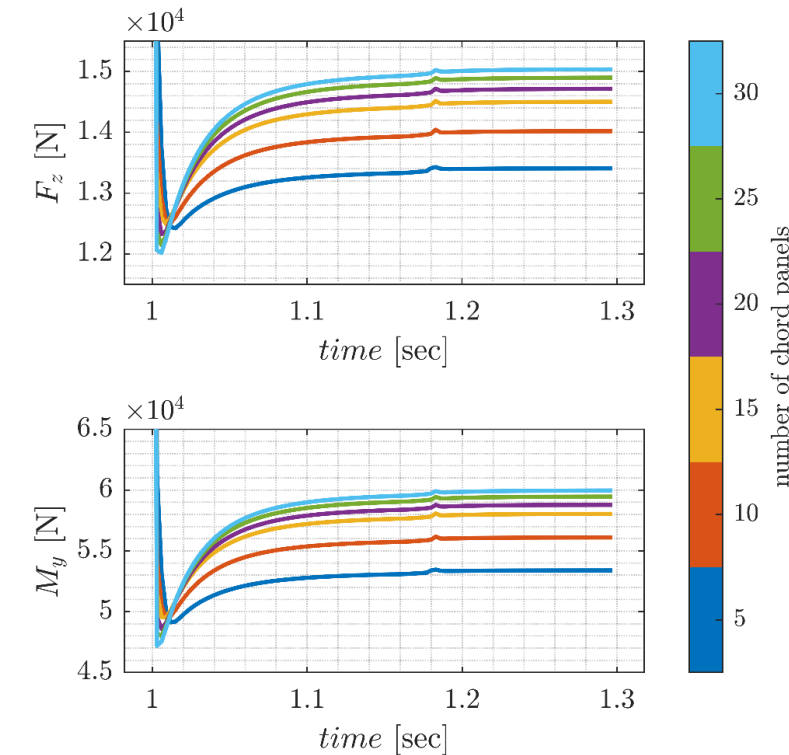
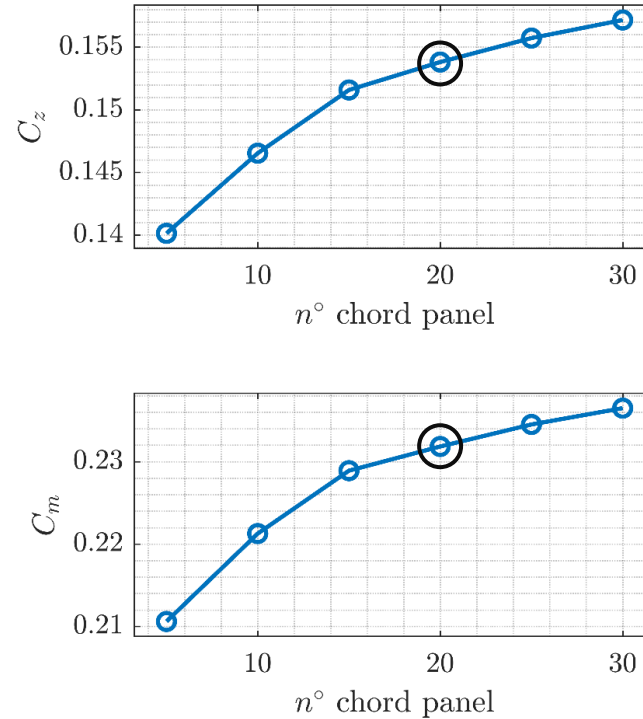
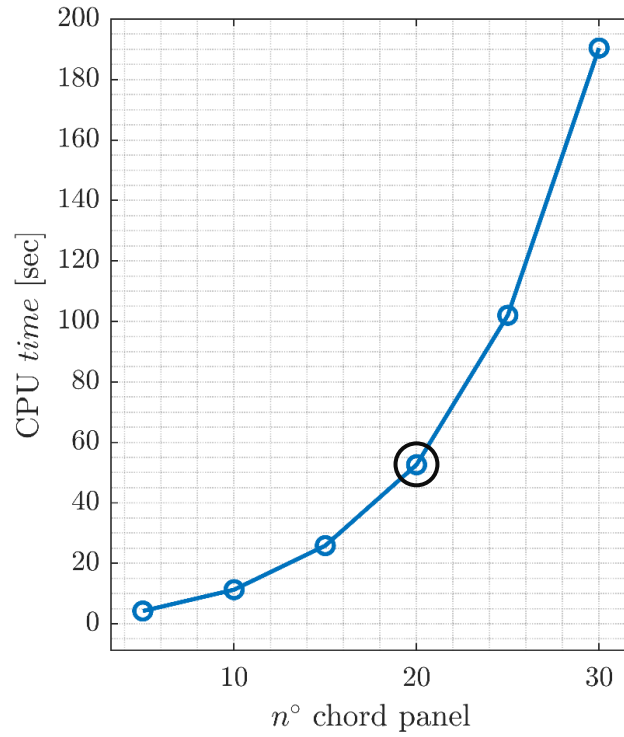
Sensitivity analysis to find **trade-off** between **precision** and **computational cost**



*Flow conditions considered during all the sensitivity analysis:*

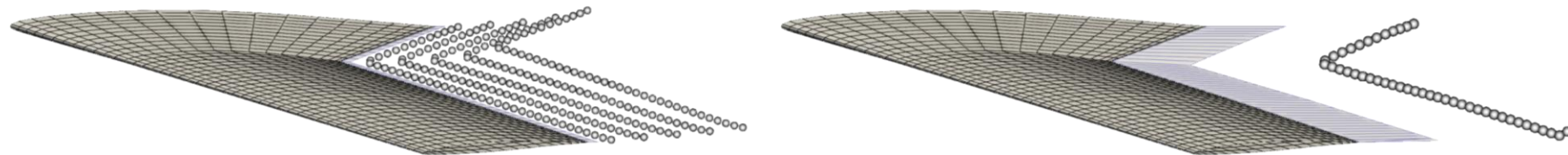
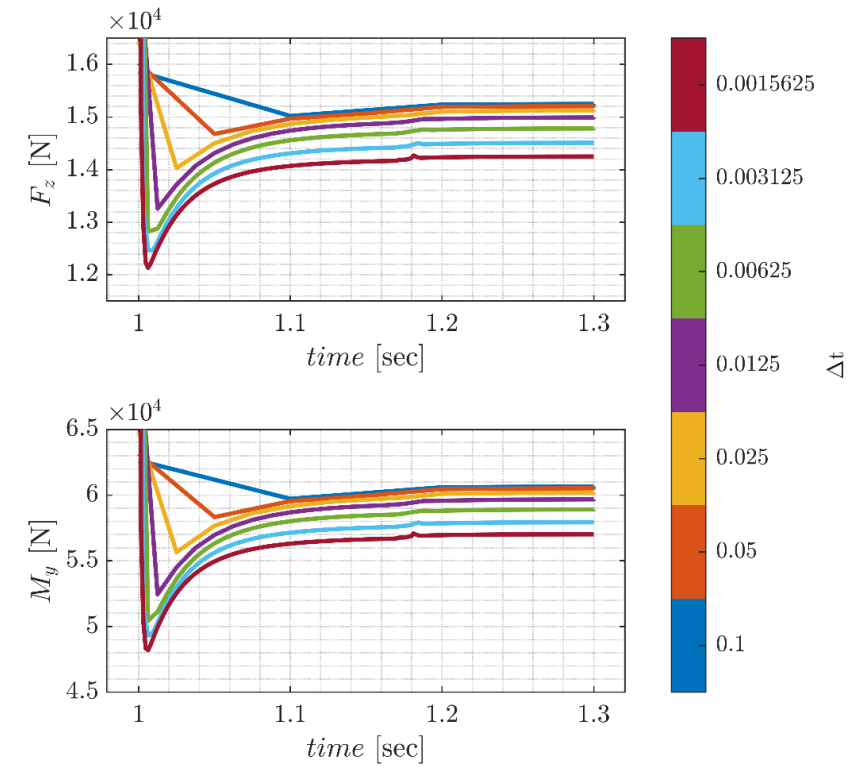
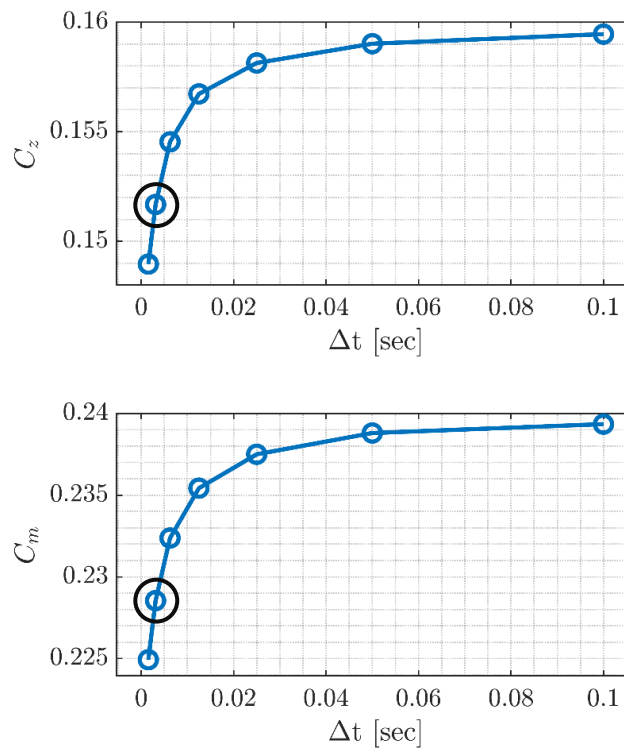
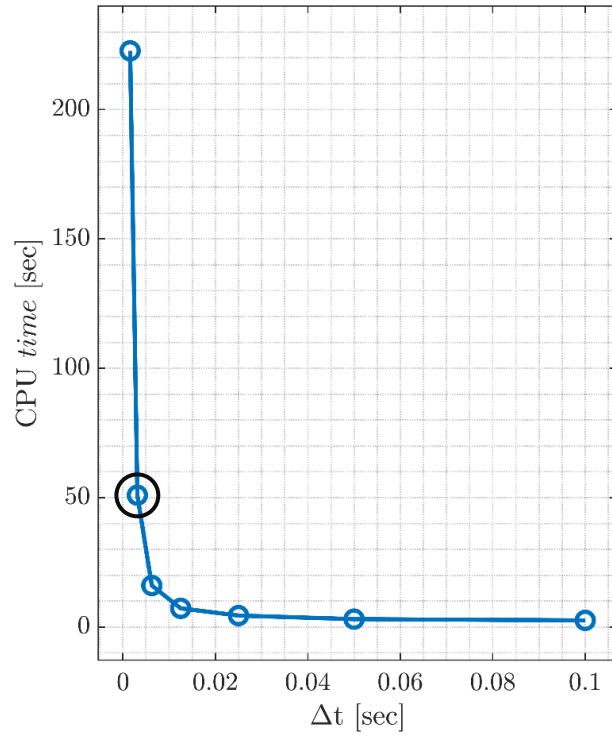
| Mach [-] | Static pressure [Pa] | Density [ $kg/m^3$ ] | Kinematic Viscosity [ $m^2/s$ ] | AOA [°] |
|----------|----------------------|----------------------|---------------------------------|---------|
| 0.30     | 57182                | 0.7708               | $1.642 \cdot 10^{-5}$           | 5       |

# Higher Order Methods Setup: DUST Mesh Sensitivity



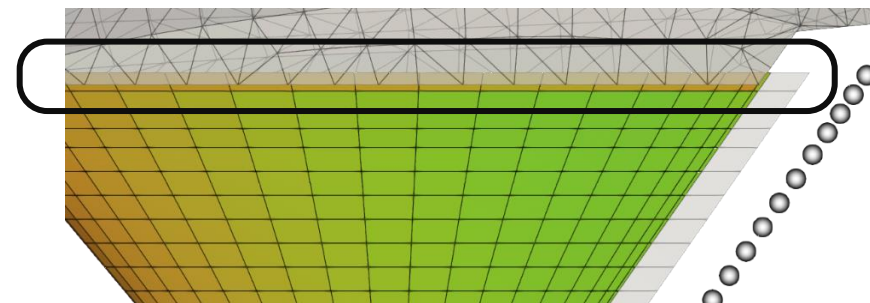
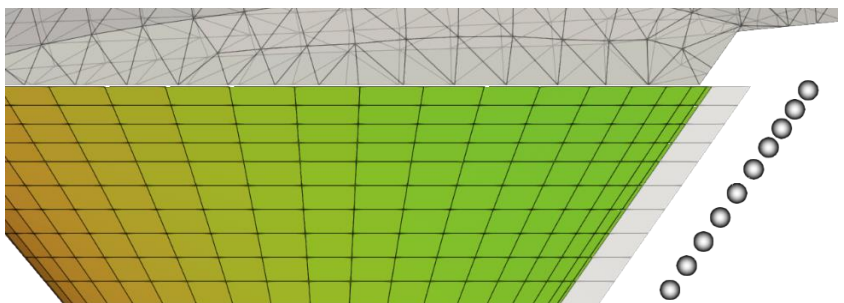
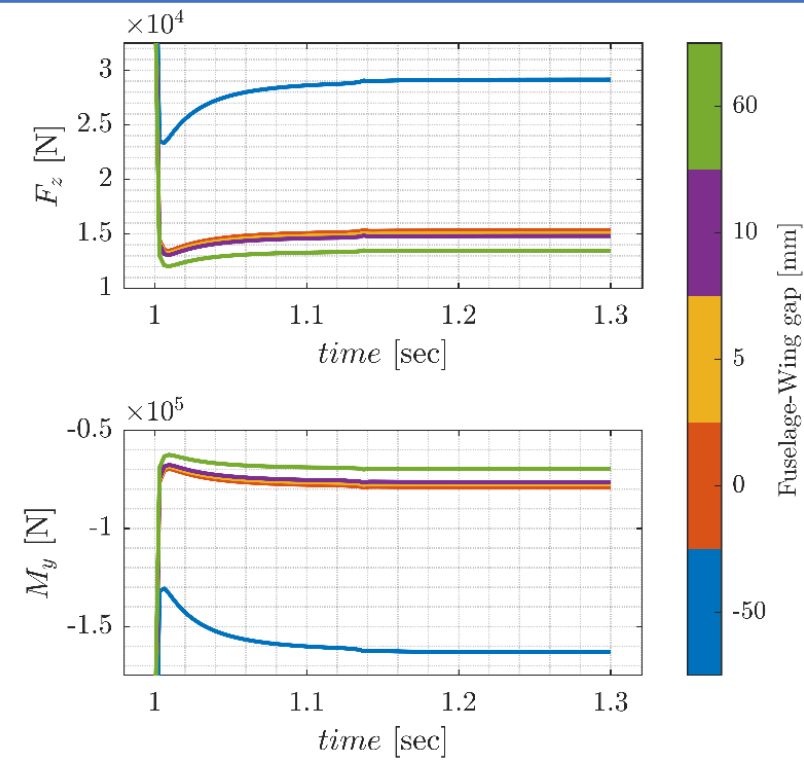
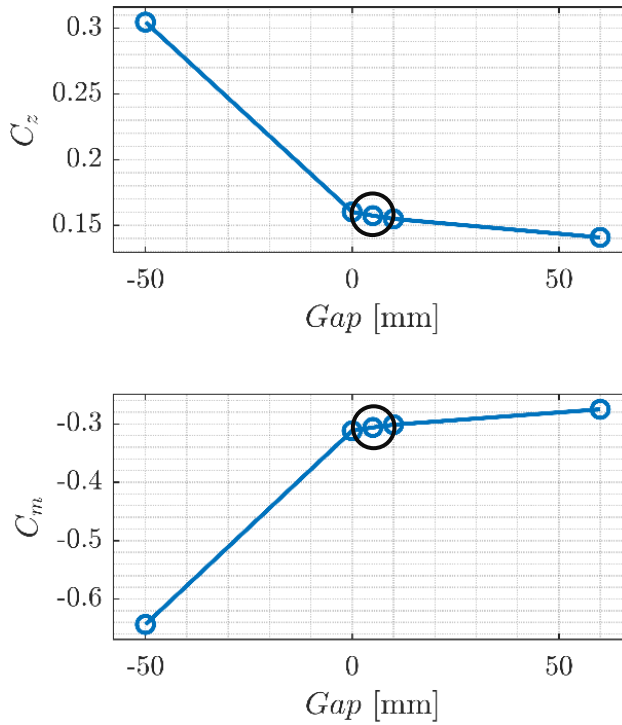
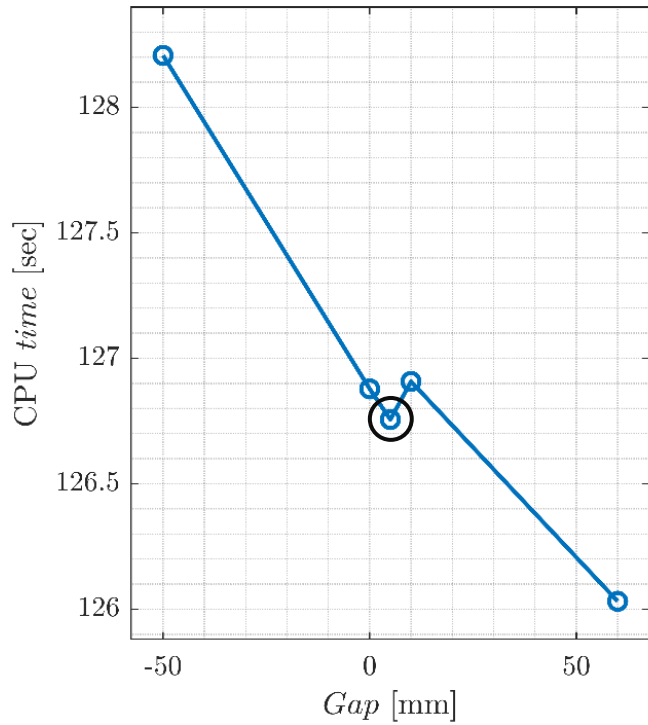
Free stream condition:  $M_a = 0.30$  and  $h = 15,000$  ft

# Higher Order Methods Setup: DUST Time Step Sensitivity



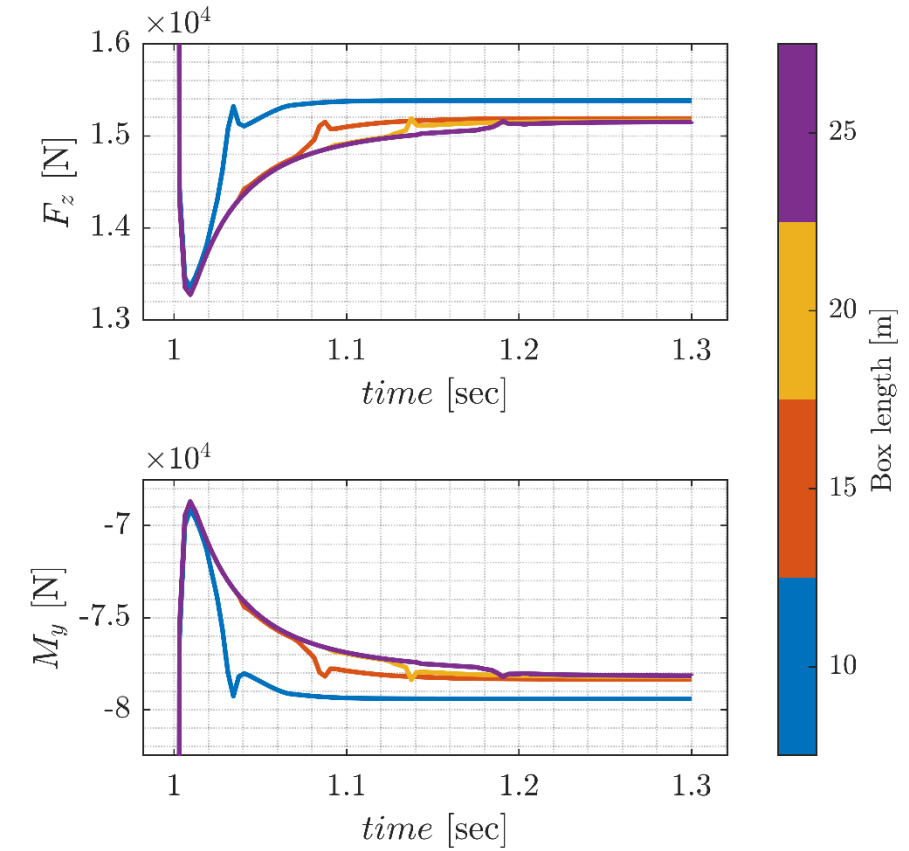
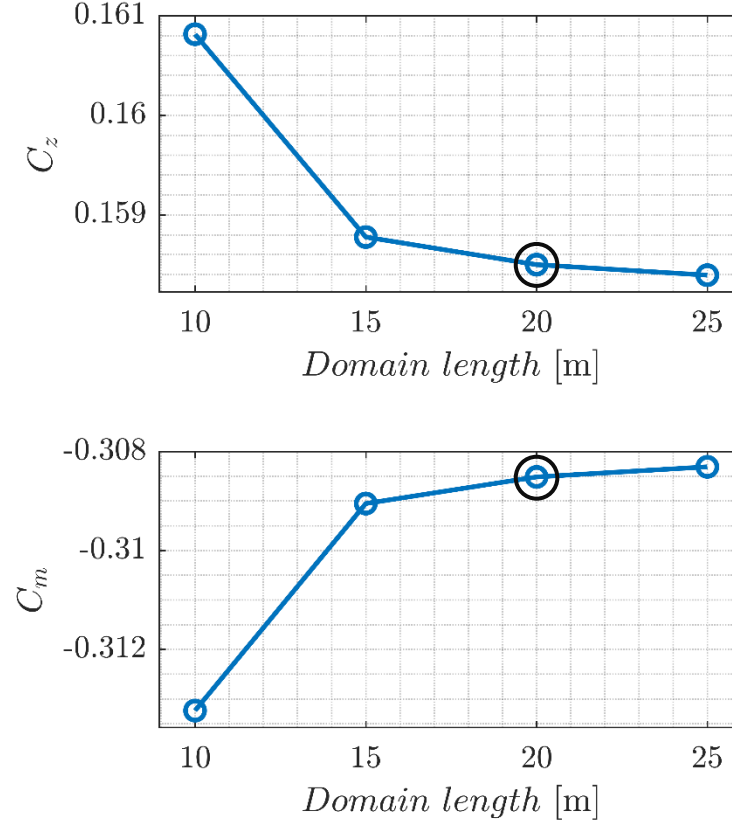
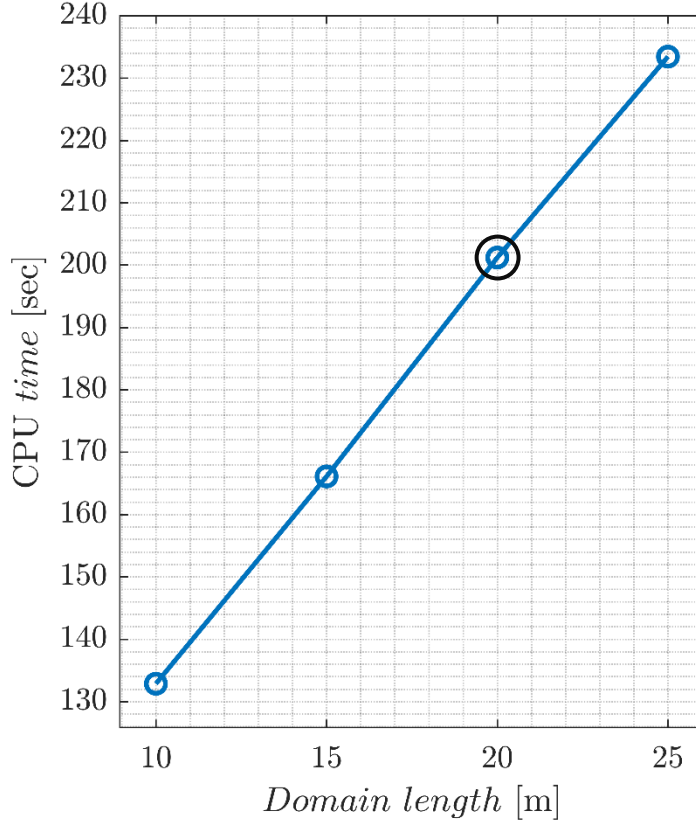
Free stream condition:  $M_a = 0.30$  and  $h = 15,000$  ft

# Higher Order Methods Setup: DUST Gap Sensitivity



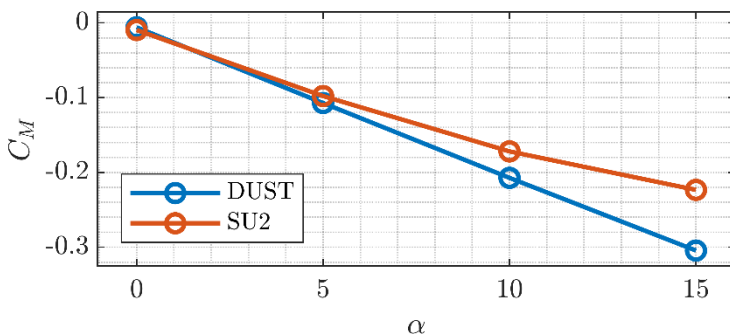
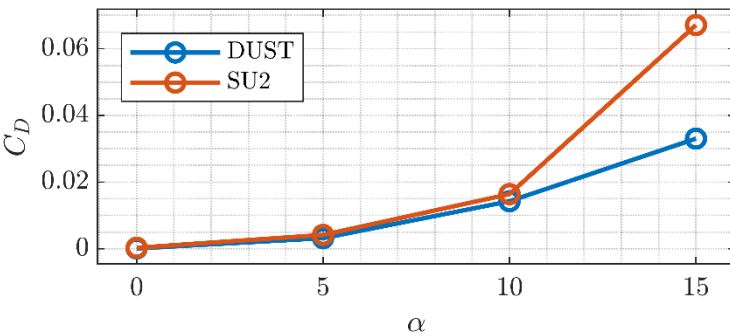
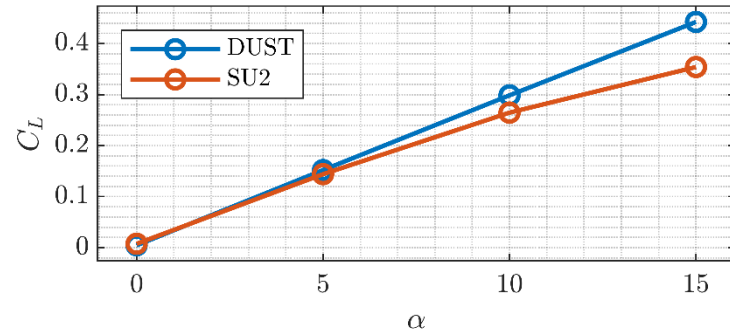
Free stream condition:  $M_a = 0.30$  and  $h = 15,000$  ft

# Higher Order Methods Setup: DUST Wake Box Sensitivity



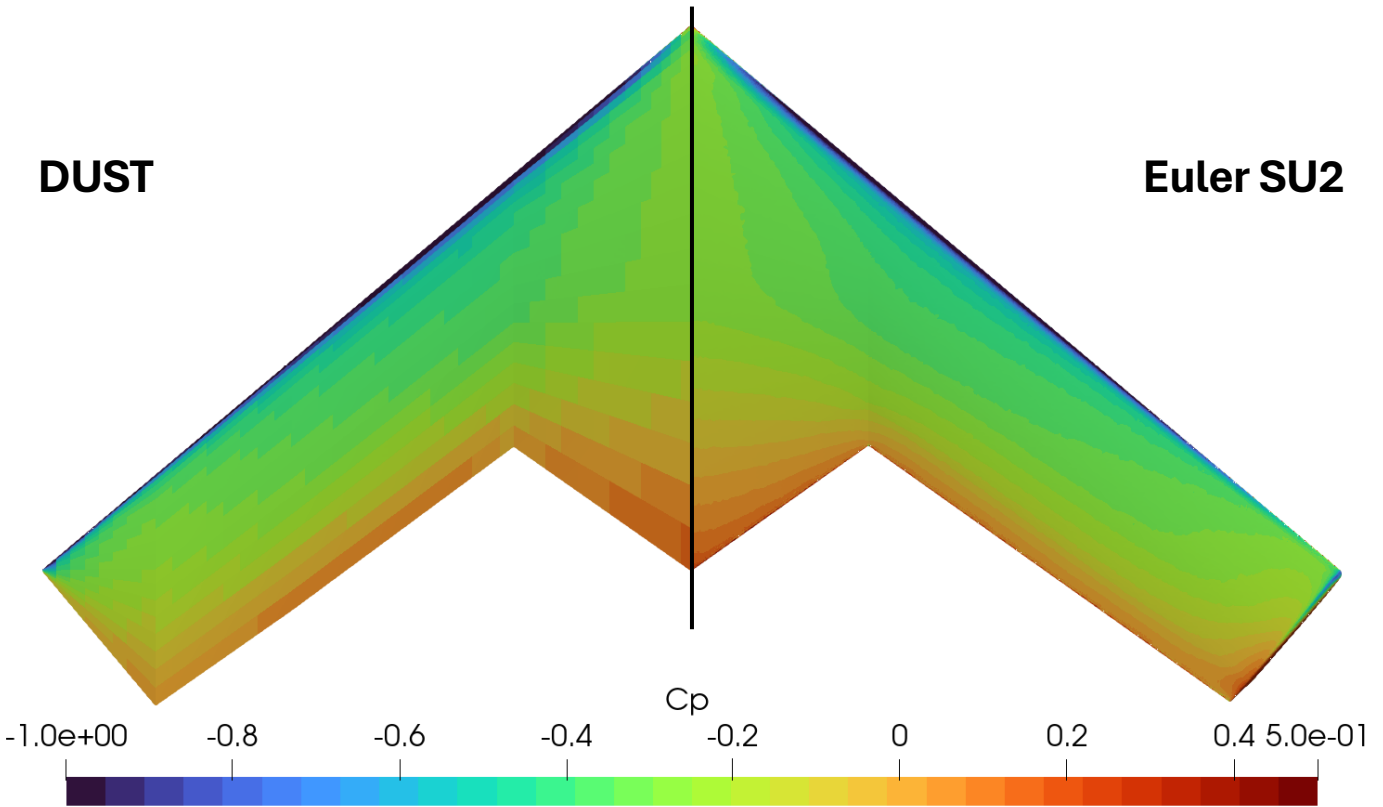
Free stream condition:  $M_a = 0.30$  and  $h = 15,000$  ft

# Higher Order Methods Setup: DUST Isolated Wing Comparison

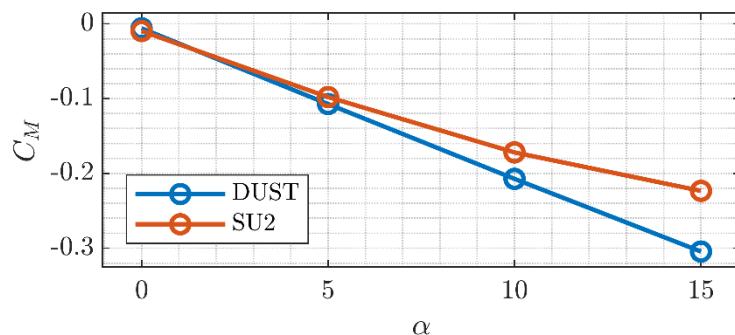
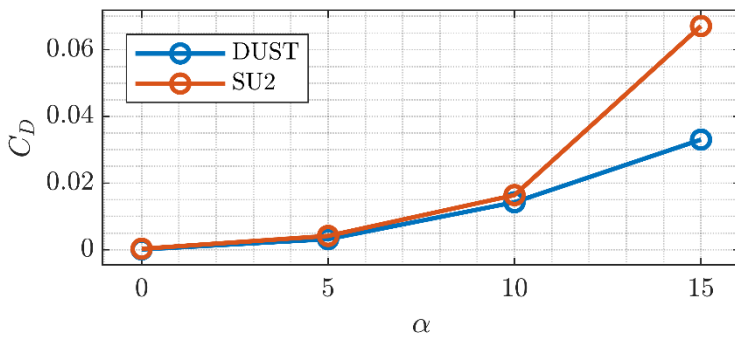
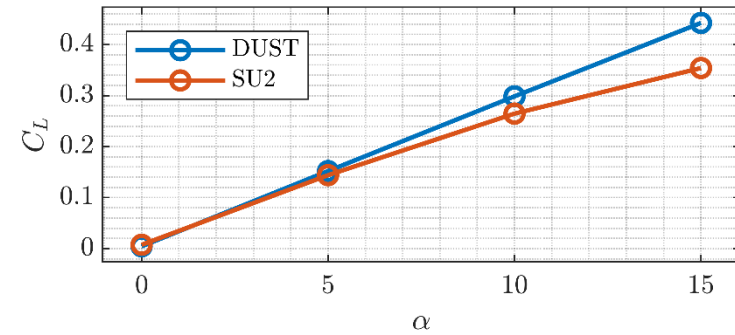


Isolated STAD-1 lambda wing surface pressure distribution

Free stream condition:  $M_a = 0.30$ ,  $h = 15000ft$ ,  $\alpha = 5^\circ$

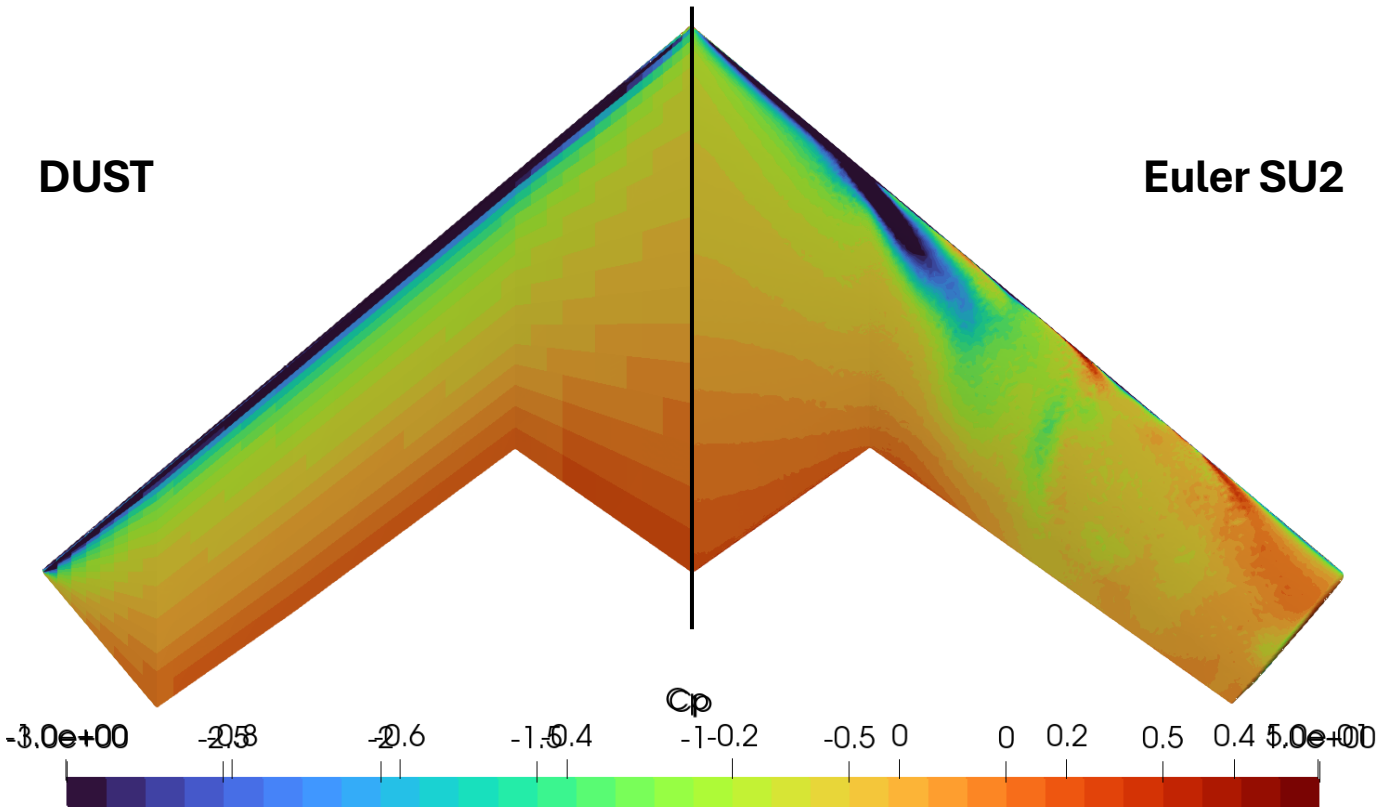


# Higher Order Methods Setup: DUST Isolated Wing Comparison

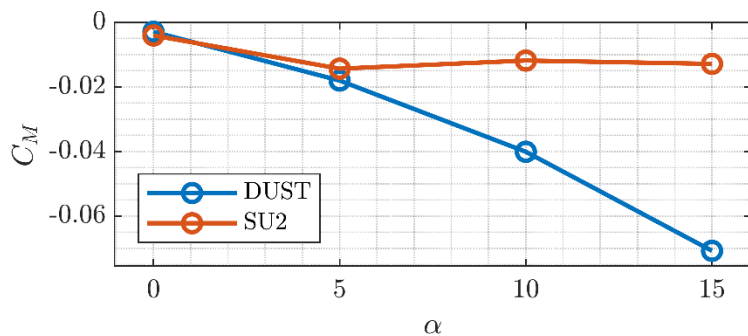
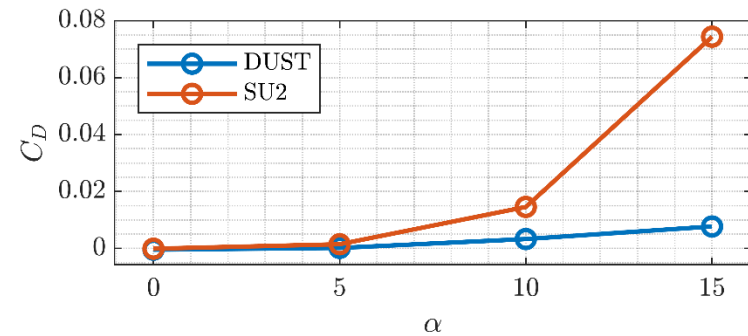
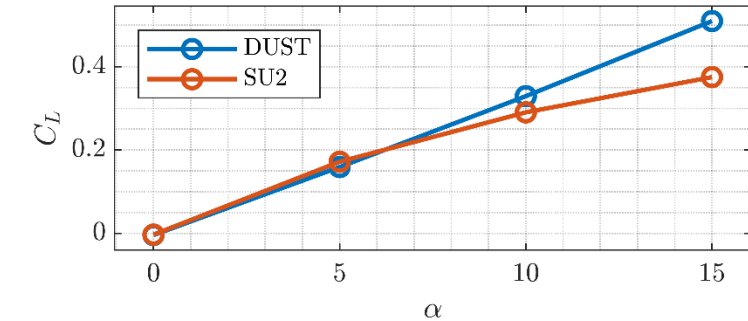


Isolated STAD-1 lambda wing surface pressure distribution

Free stream condition:  $M_a = 0.30$ ,  $h = 15000ft$ ,  $\alpha = 15^\circ$



# Higher Order Methods Setup: DUST Aircraft Comparison



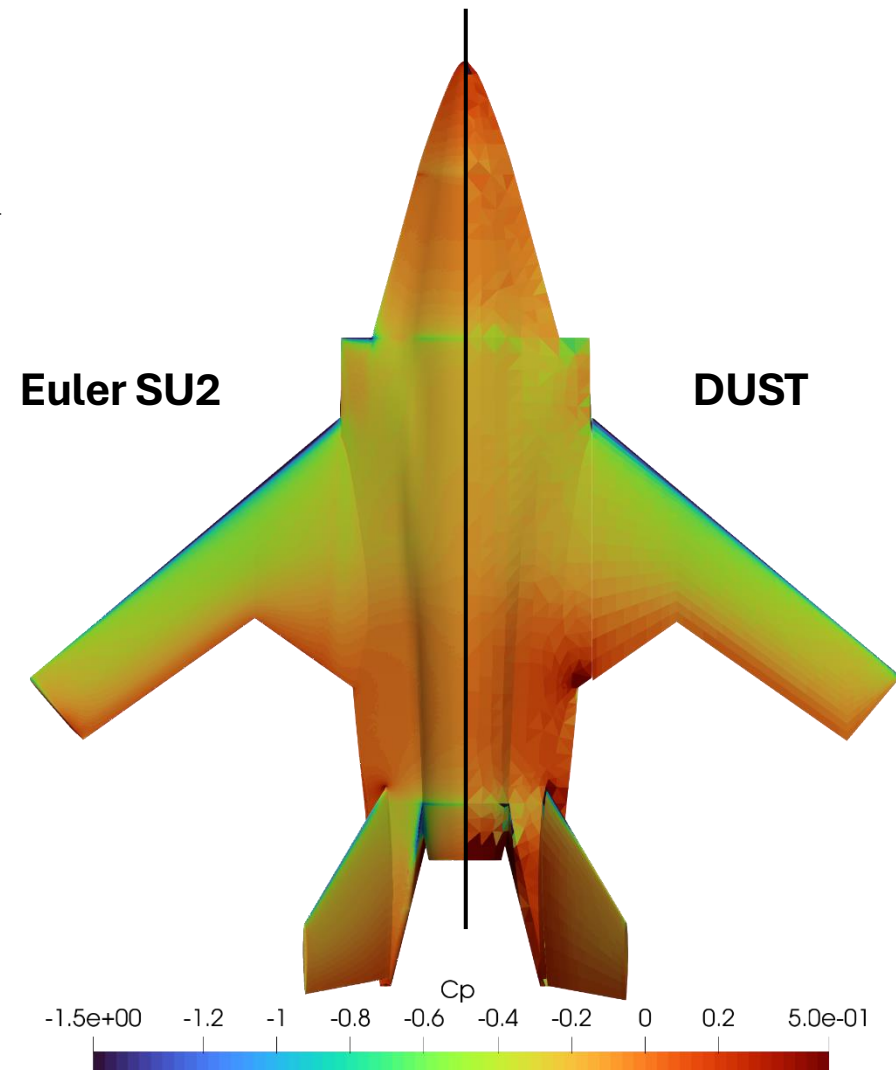
## STAD-1 Aircraft Pressure Distribution

Free stream condition:

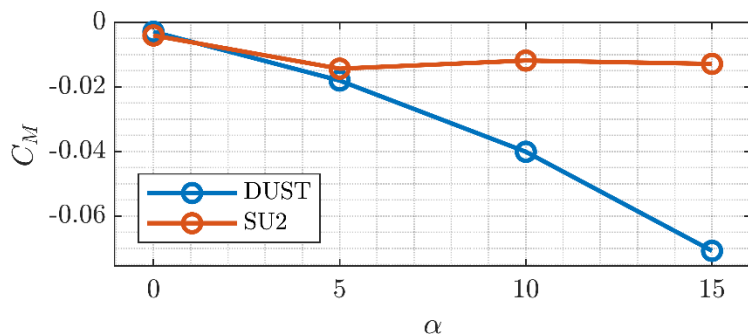
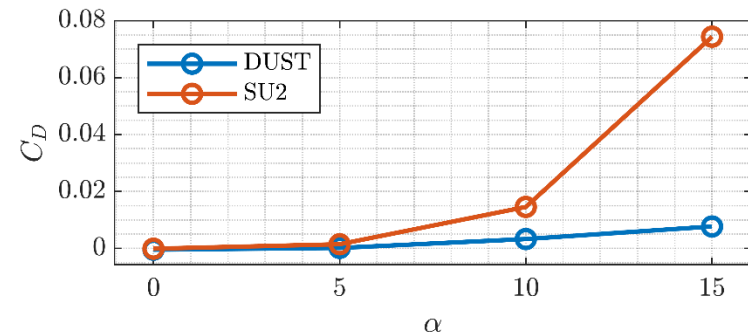
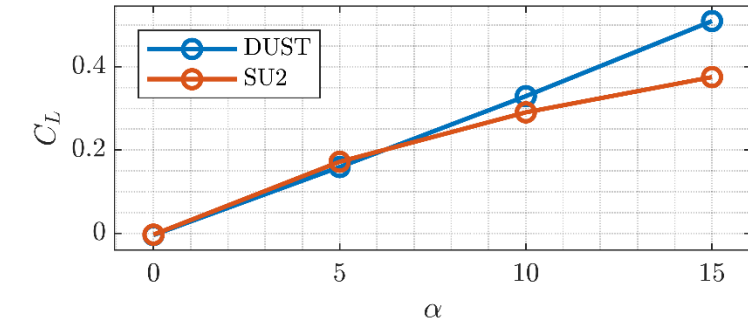
$$M_a = 0.30$$

$$h = 15,000 \text{ ft}$$

$$\alpha = 5^\circ$$



# Higher Order Methods Setup: DUST Aircraft Comparison



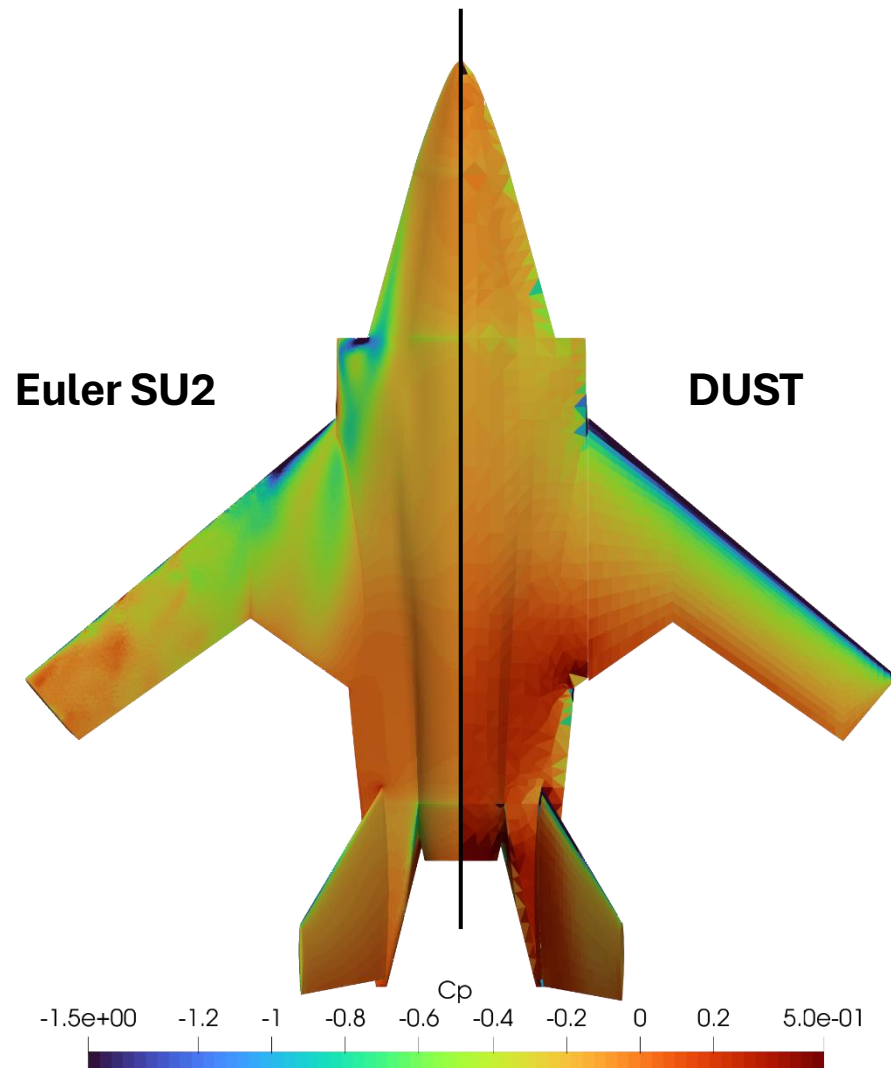
## STAD-1 Aircraft Pressure Distribution

*Free stream condition:*

$$M_a = 0.30$$

$$h = 15000\text{ft}$$

$$\alpha = 15^\circ$$



# Airfoil Choice: First Considerations



Airfoil choice is done after the planform design due to the 3D-driven planform. It is important to make preliminary considerations on airfoils to limit the possible configurations.

- **Curvature:** chosen between symmetric and airfoils with a 0.20 design  $C_L$  due to the planform considerations made and to have good performance in both directions.
- $t/c$ : chosen with the Korn equation.

$$(t/c)_{\max} = \left( K_a - \frac{C_L}{10 \cos(\Lambda_{LE})^2} - M_{a_{DD}} \right) \cos(\Lambda_{LE})$$

$$M_{a_{DD}} = 0.86 \text{ & } \Lambda_{LE} = 40^\circ$$

$M_{a_{DD}}$

$\Delta C_D = 0.002$

$\frac{dC_D}{dM_a} = 0.1$

Boeing

Douglas

| Airfoil       | $(t/c)_{\max}$ |
|---------------|----------------|
| NACA          | 0.11           |
| Supercritical | 0.18           |

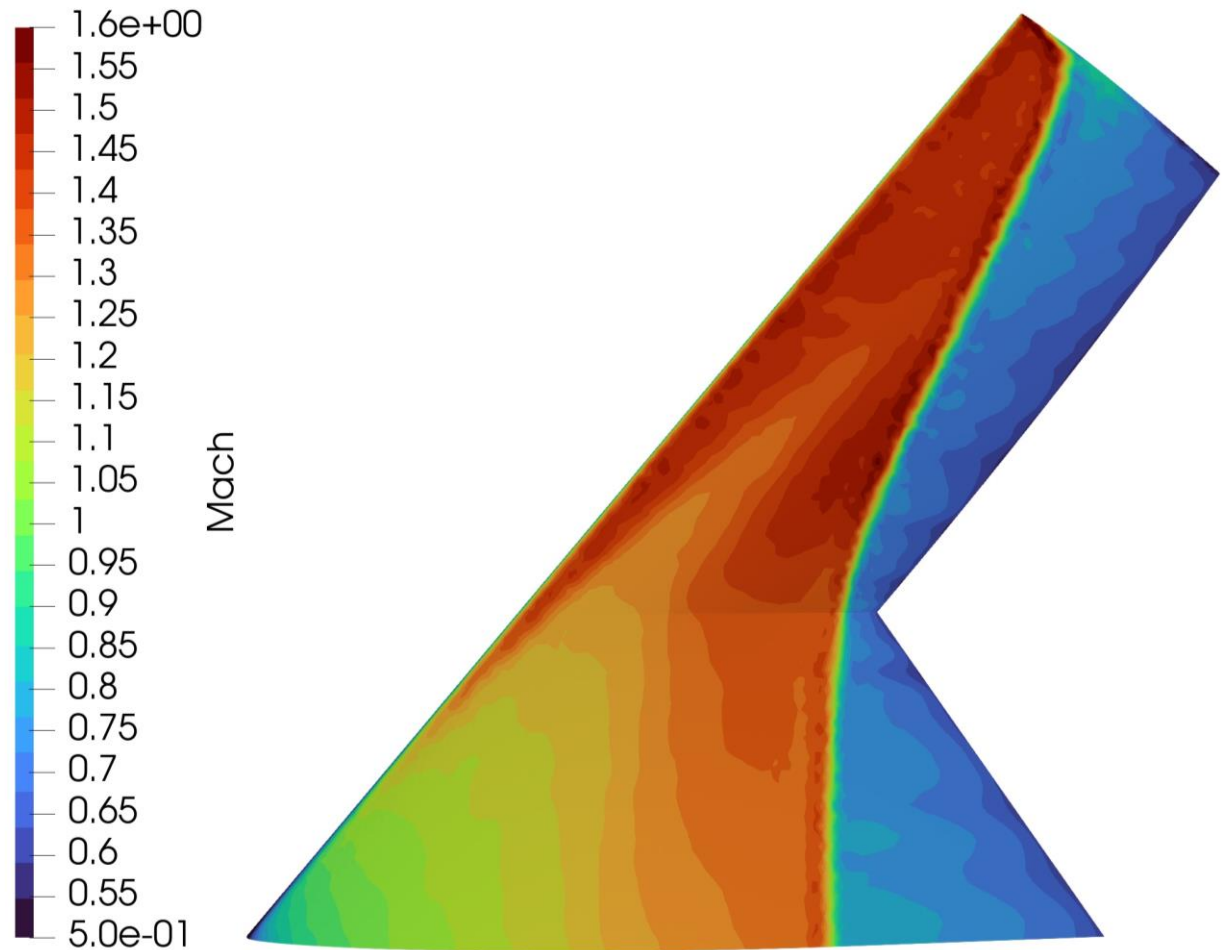
# Airfoil Choice: Initial Wing Euler Analysis



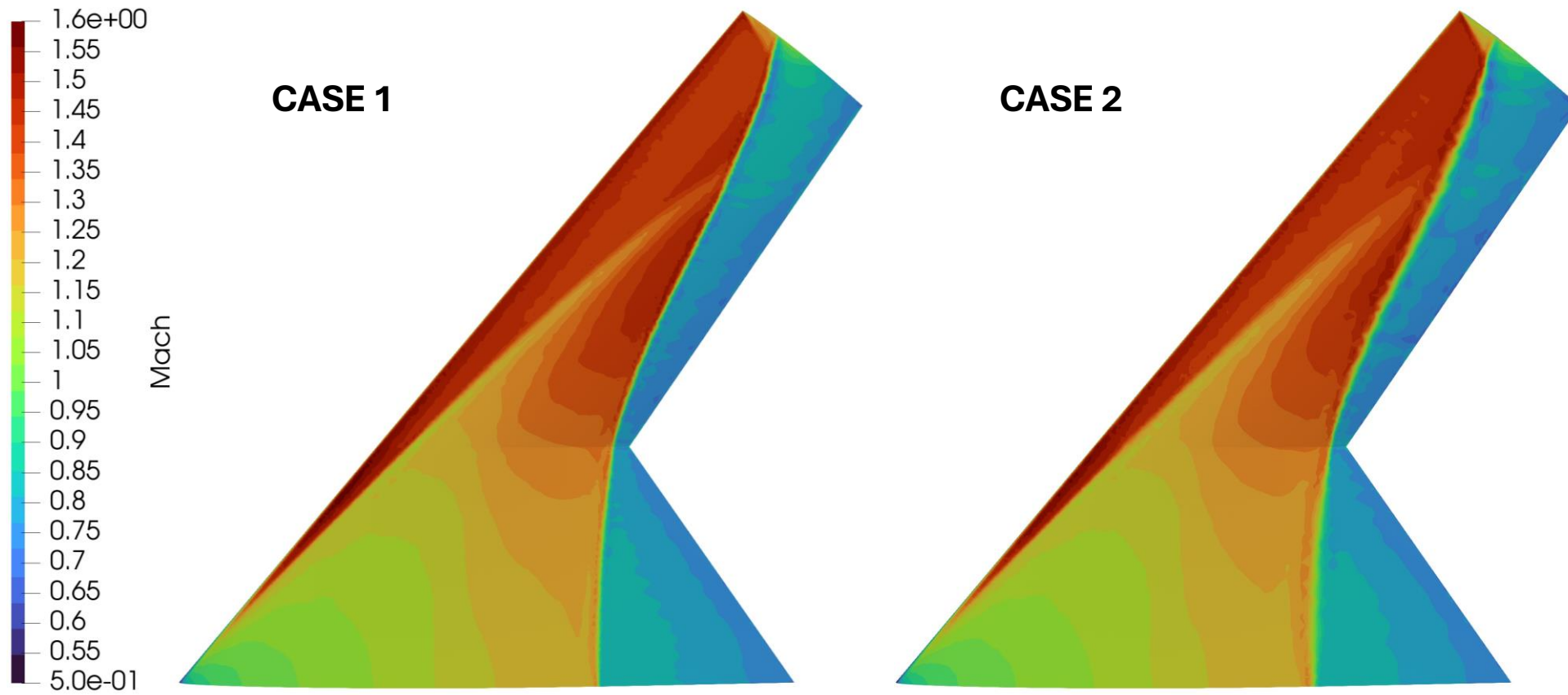
NACA 6 series airfoils and supercritical airfoils are evaluated. First, the initial wing configuration is tested to understand its performance and behavior.

| Flow Conditions      | $M_a = 0.50$ | $M_a = 0.85$ |
|----------------------|--------------|--------------|
| Pressure [Pa]        | 57182        | 57182        |
| Temperature [K]      | 258.65       | 258.65       |
| Density [ $kg/m^3$ ] | 0.7708       | 0.7708       |
| Angle of Attack [°]  | 4.5          | 6.0          |

| Wing Section | Final Configuration |
|--------------|---------------------|
| Root         | NACA 64A010         |
| Mid          | NACA 64A008         |
| Pre-Tip      | NACA 64A208         |
| Tip          | NACA 64A206         |



# Airfoil Choice: Case 1 and 2 Configurations

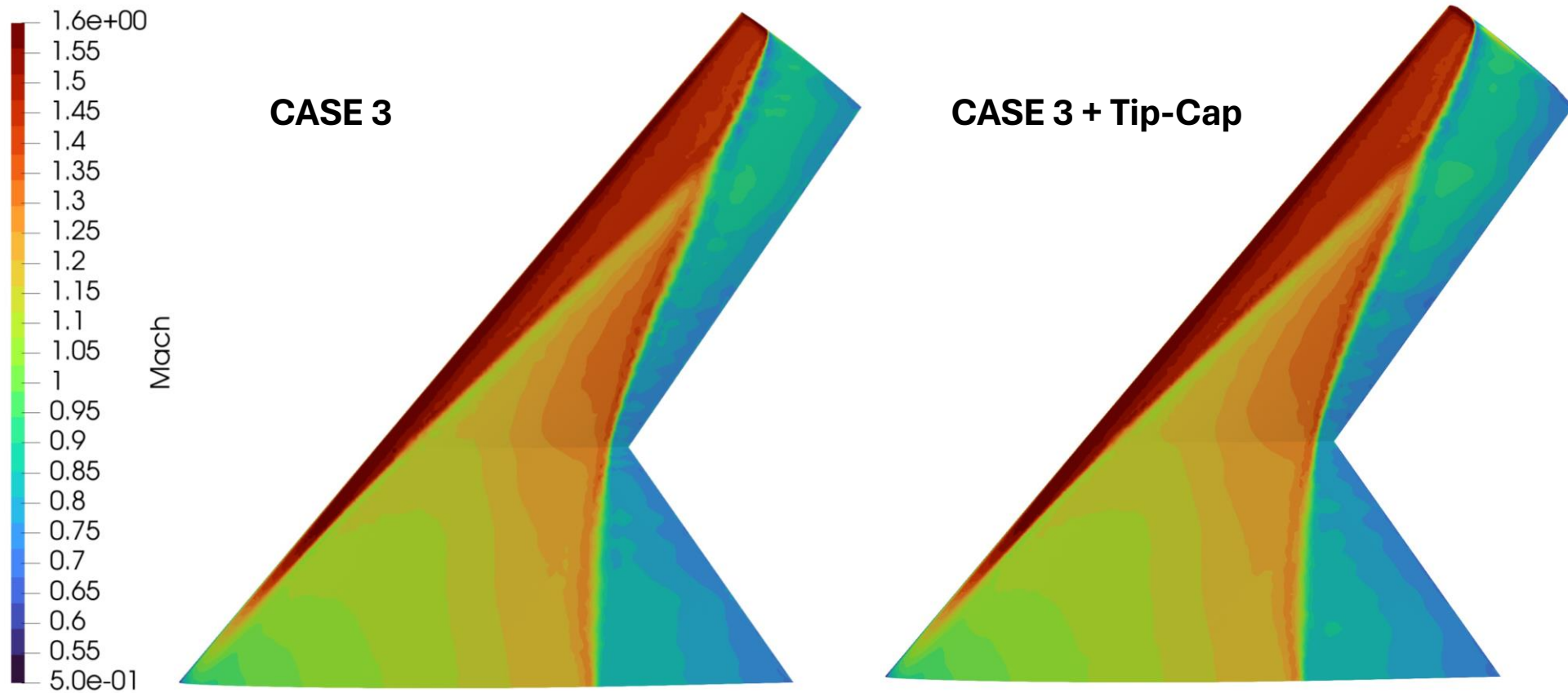


| Wing Section | Case 1      | Case 2      |
|--------------|-------------|-------------|
| Root         | NACA 64A008 | NACA 64A008 |
| Mid          | NACA 64A208 | NACA 64A208 |
| Pre-Tip      | NACA 64A206 | NACA 64A206 |
| Tip          | NACA 64A206 | NACA 64A204 |

|       | Initial Wing | Case 1  | Case 2  |
|-------|--------------|---------|---------|
| $C_L$ | 0.324        | 0.351   | 0.351   |
| $C_D$ | 0.02790      | 0.02239 | 0.02278 |
| $L/D$ | 11.61        | 15.68   | 15.41   |



# Airfoil Choice: Case 3 With and Without Tip-Cap



| Wing Section | Case 3      |
|--------------|-------------|
| Root         | NACA 65A008 |
| Mid          | NACA 65A206 |
| Pre-Tip      | NACA 65A206 |
| Tip          | NACA 65A204 |

| $M_a = 0.85$<br>$6.0^\circ \text{ AOA}$ | Without Tip Cap | With Tip Cap |
|---|-----------------|--------------|
| $C_L$                                   | 0.342           | 0.341        |
| $C_D$                                   | 0.01996         | 0.01946      |
| $L/D$                                   | 17.12           | 17.52        |

| $M_a = 0.50$<br>$4.5^\circ \text{ AOA}$ | Without Tip Cap | With Tip Cap |
|---|-----------------|--------------|
| $C_L$                                   | 0.179           | 0.174        |
| $C_D$                                   | 0.00512         | 0.00480      |
| $L/D$                                   | 34.94           | 36.18        |



# Airfoil Choice: Supercritical Airfoils



Supercritical airfoils have been tested as well, but they have been discarded due to their poor performance, possibly related to:

- Different design  $M_a$ .
- Medium Aspect Ratio effects.

Case 5 and 6 give a higher  $C_L$ , so they have been tested at a lower angle of attack too, but they output a lower  $L/D$  than case 3 anyway.

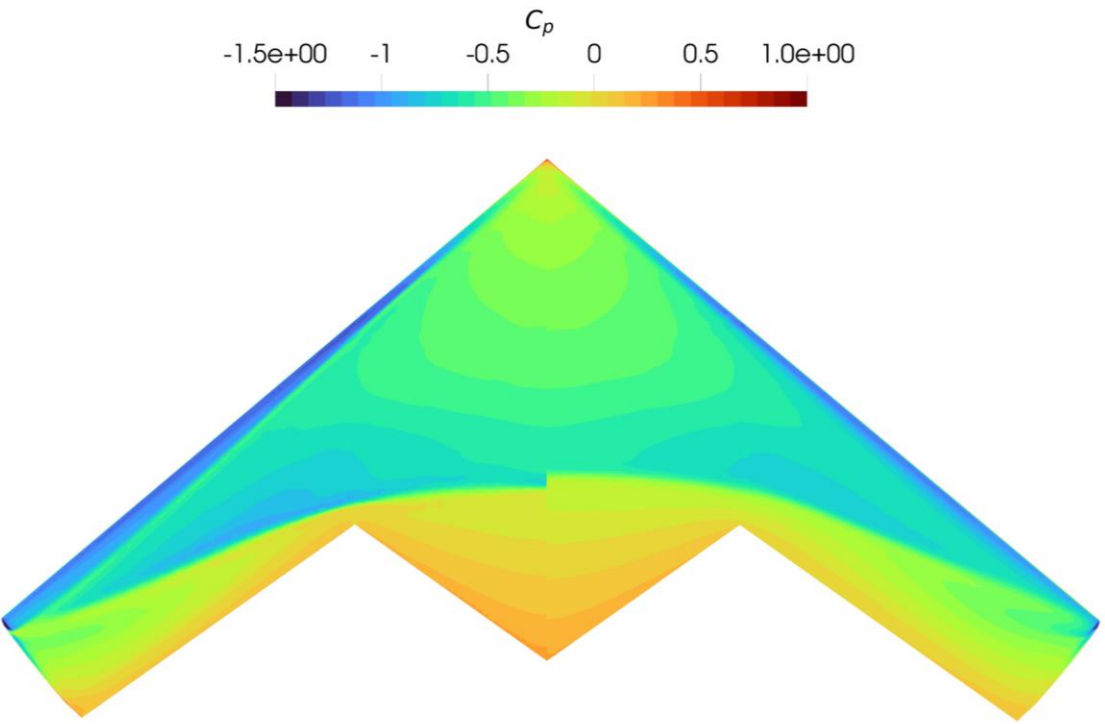
| Wing Section | Case 4          | Case 5          | Case 6    | Case 7          |
|--------------|-----------------|-----------------|-----------|-----------------|
| Root         | NACA SC(2)-0012 | KC-125-08       | Piaggio-1 | NACA SC(2)-0012 |
| Mid          | NACA SC(2)-0010 | NASA SC(2)-0706 | Piaggio-2 | NACA SC(2)-0010 |
| Pre-Tip      | NACA SC(2)-0010 | NASA SC(2)-0706 | Piaggio-3 | NACA SC(2)-0010 |
| Tip          | NACA SC(2)-0706 | NASA SC(2)-0404 | Piaggio-4 | NACA 65A206     |
| $C_L$        | 0.319           | 0.433           | 0.490     | 0.323           |
| $C_D$        | 0.0271          | 0.0391          | 0.0505    | 0.0266          |
| $L/D$        | 11.77           | 11.08           | 9.70      | 9.73            |



# Airfoil Choice: RANS Analysis



- Final configuration tested with a viscid formulation.
- RANS simulation carried on with the Spalart-Allmaras turbulence model.
- 4.5 Millions cells.
- $\alpha = 5^\circ$  has been considered, which is the one that will be used for the analysis of the complete aircraft



| $M_a = 0.85$<br>$AOA = 5^\circ$ | Euler  | Viscid |
|---------------------------------|--------|--------|
| $C_L$                           | 0.278  | 0.247  |
| $C_D$                           | 0.0121 | 0.0140 |
| $L/D$                           | 22.98  | 17.64  |

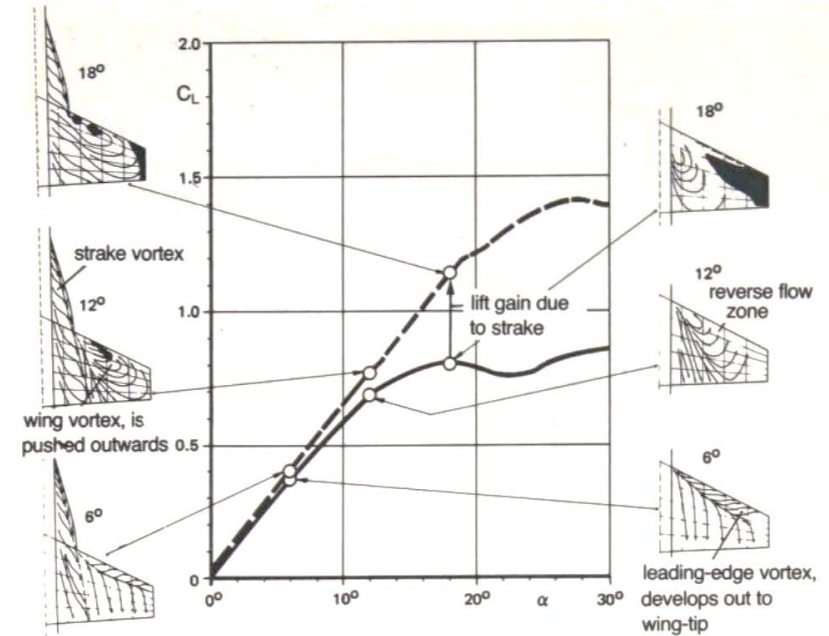
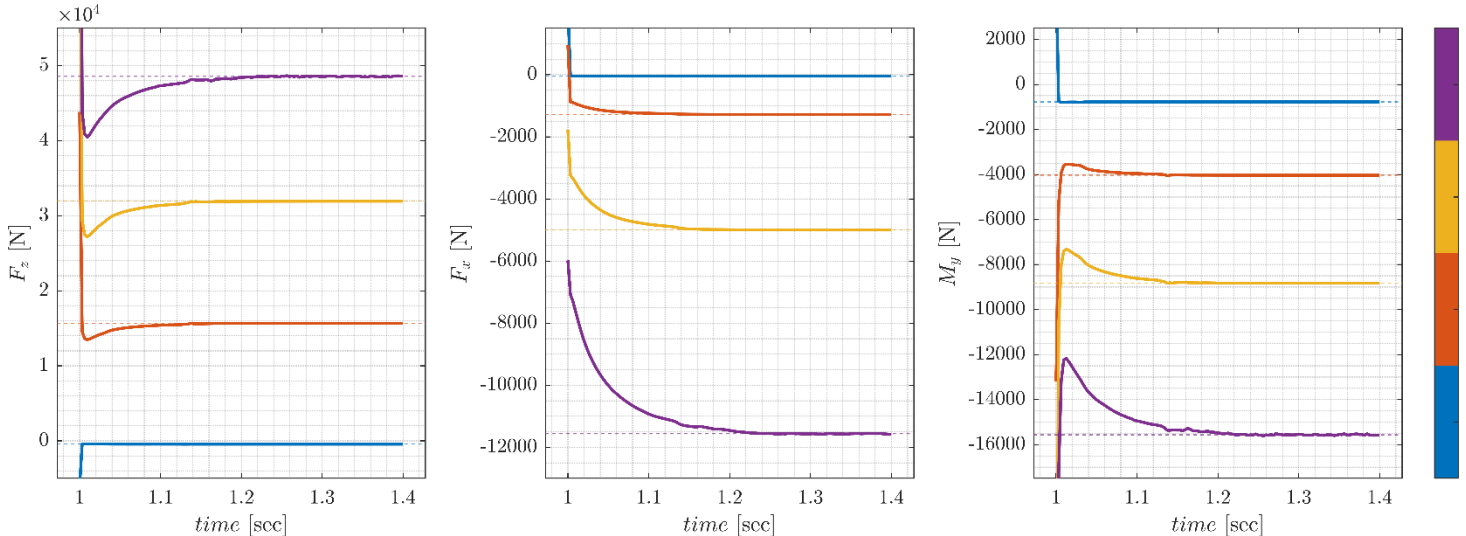
# LEX Design: Problem Setup



Exploiting the quickness and good reliability of DUST different configuration are tested:

- Different root chord length
- Different leading edge sweep angle

*Each simulation run until integral loads of aerodynamic surfaces converge*

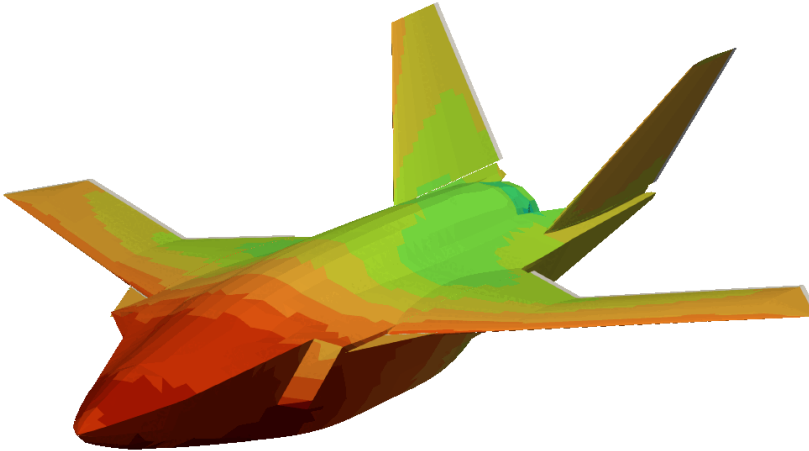
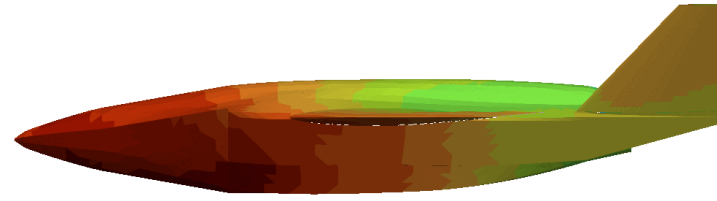


*Major limitation of used model  
⇒ Potential Lift vs Vortex Lift*

*Free stream condition:  $M_a = 0.30$  and  $h = 15,000ft$*

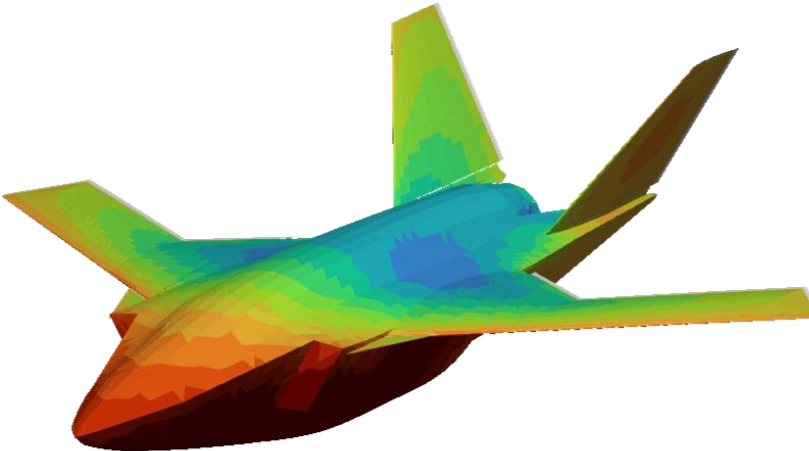
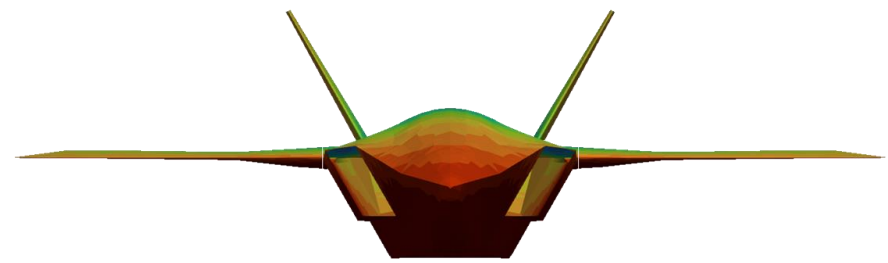
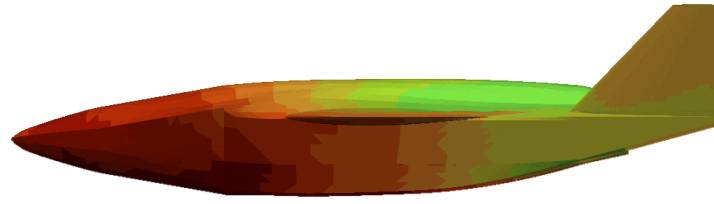


# LEX Design: Visual Output $\alpha = 5^\circ$



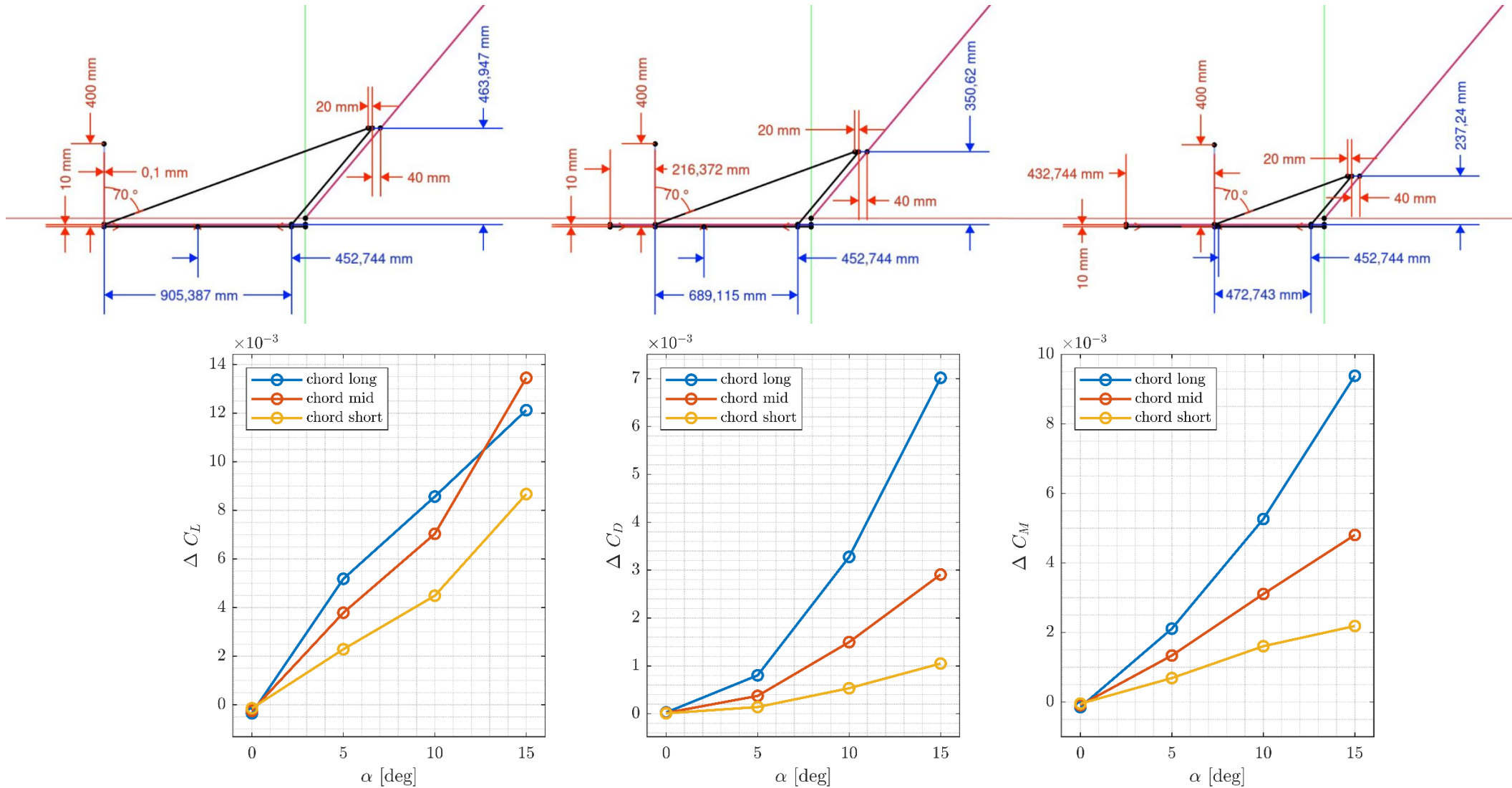
*Free stream condition:  $M_a = 0.30, h = 15,000 \text{ ft}, \alpha = 5^\circ$*

# LEX Design: Visual Output $\alpha = 15^\circ$

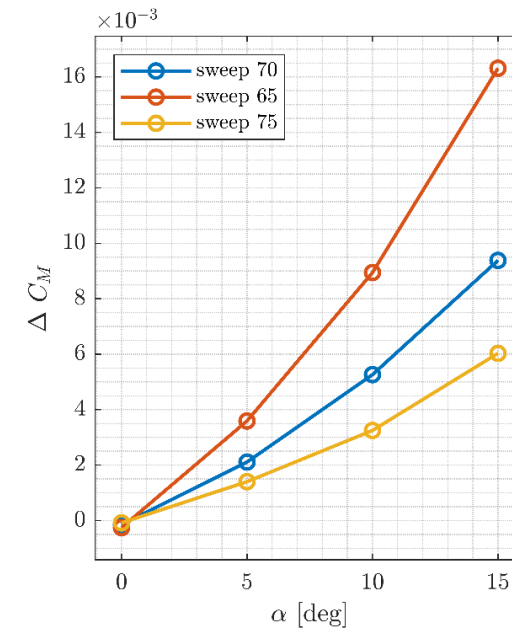
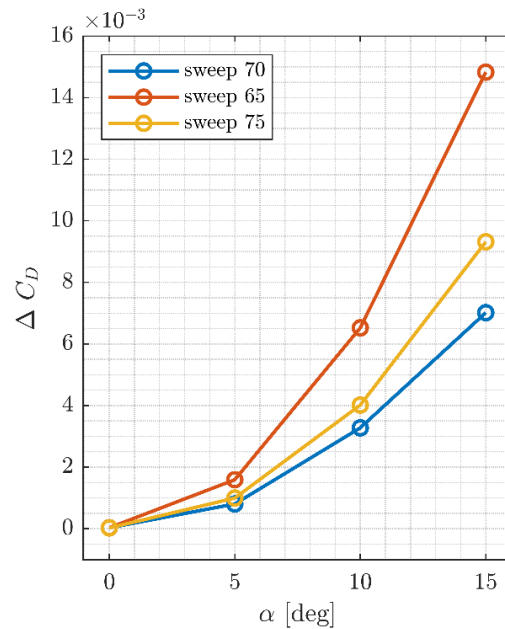
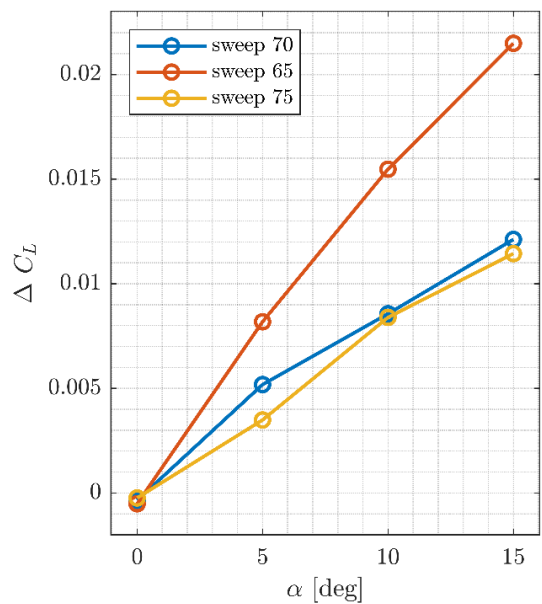
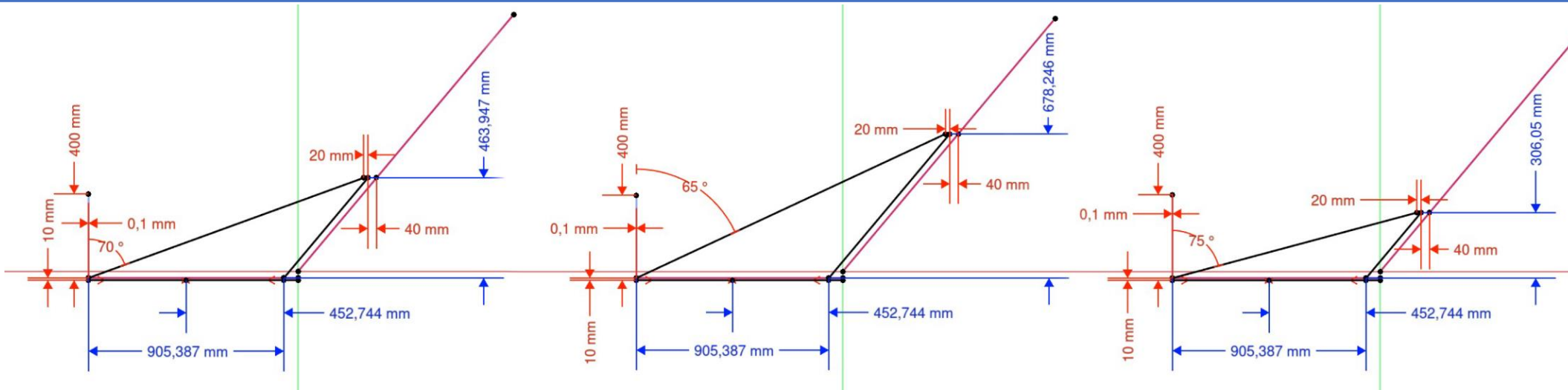


*Free stream condition:  $M_a = 0.30, h = 15,000 \text{ ft}, \alpha = 15^\circ$*

# LEX Design: Root Chord Analysis



# LEX Design: Leading Edge Sweep Analysis



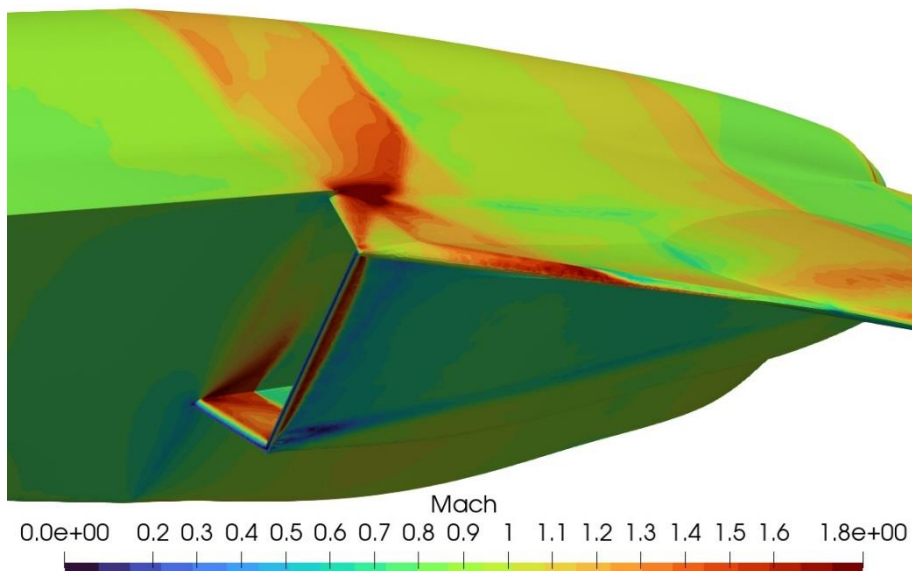
# LEX Design: Interaction with Air Intake



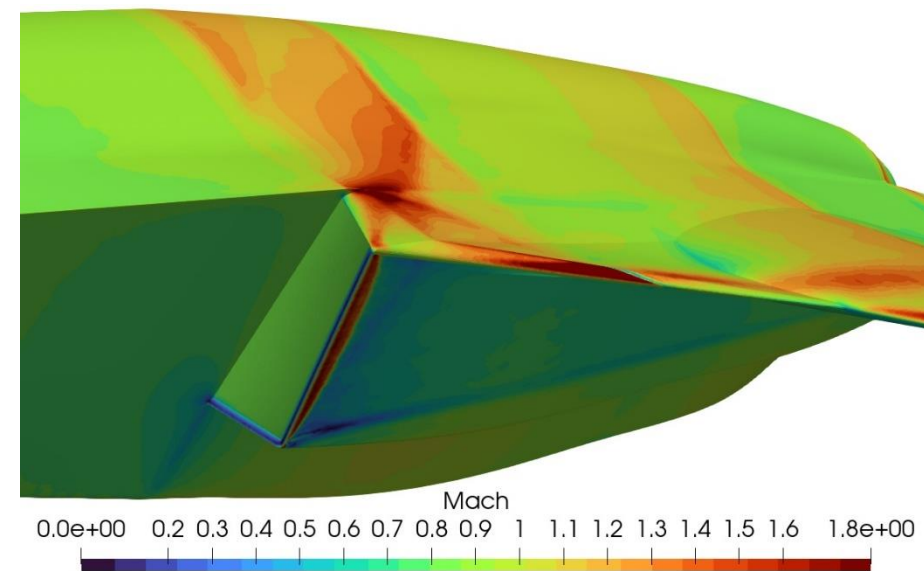
The correct geometry for these kind of analyses on a fighter aircraft requires the entire internal modelling from the intake to the compressor and from the turbine to the nozzle exit.

The 'closed' configuration was preferred due to:

- Computational limitations.
- Avoid complexities of shockwave management.



Open Configuration.



Closed Configuration.



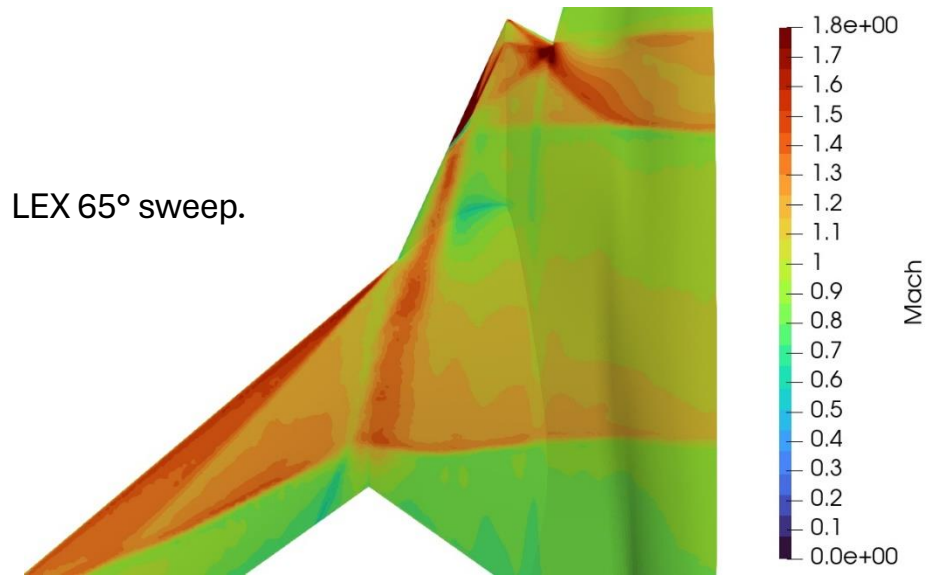
# LEX Design: Verification and Comparison



Advantages of the LEX designed at  $70^\circ$ :

- More lift is produced.
- The vortex is directed at the intersection between the trapezoidal and swept part of the wing.
- Less area covered and no need of resizing the LE flaps.

| Comparison between the two designs at $M_a = 0.85$ and $AOA = 5^\circ$ . |         |         |
|--|---------|---------|
|  | LEX 65° | LEX 70° |
| $C_L$  | 0.381   | 0.389   |
| $C_D$  | 0.02570 | 0.02702 |
| $L/D$  | 14.82   | 14.40   |



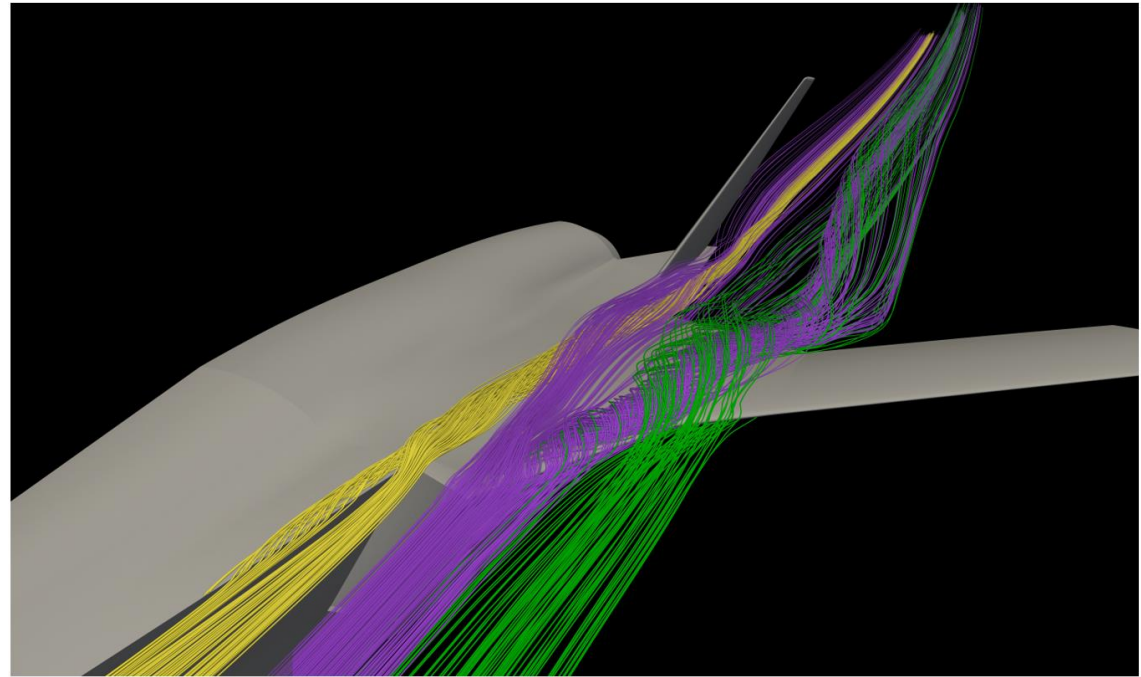
# LEX Design: Verification and Comparison



The presented streamlines provide an idea of the flow's behaviour, which is characterized by three “Eulerian” Vortices generated by:

- The nose partially acting as a strake as well as the air intake.
- The LEX itself.
- The zone of intersection between the LEX and the wing.

The two vortices on the right interact with each other to create a more intense single vortex.

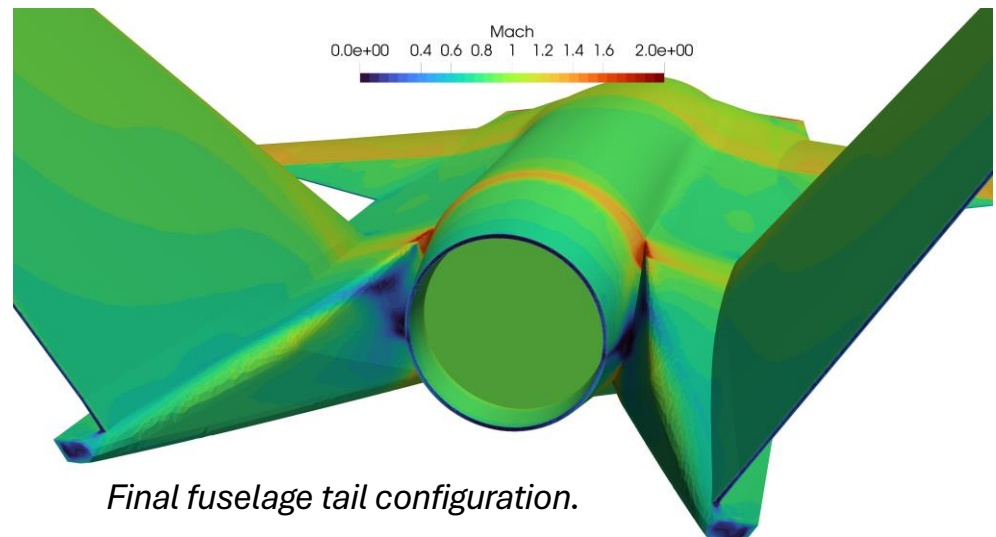
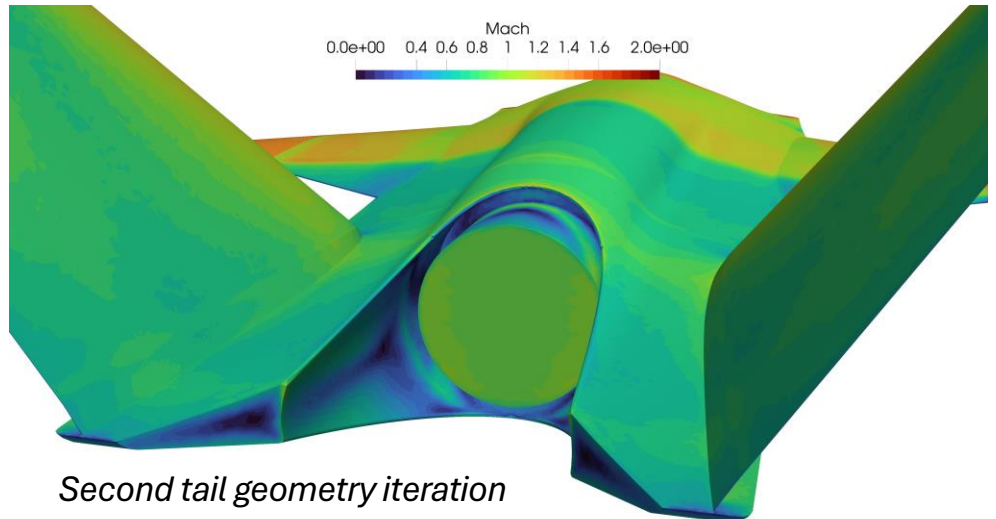
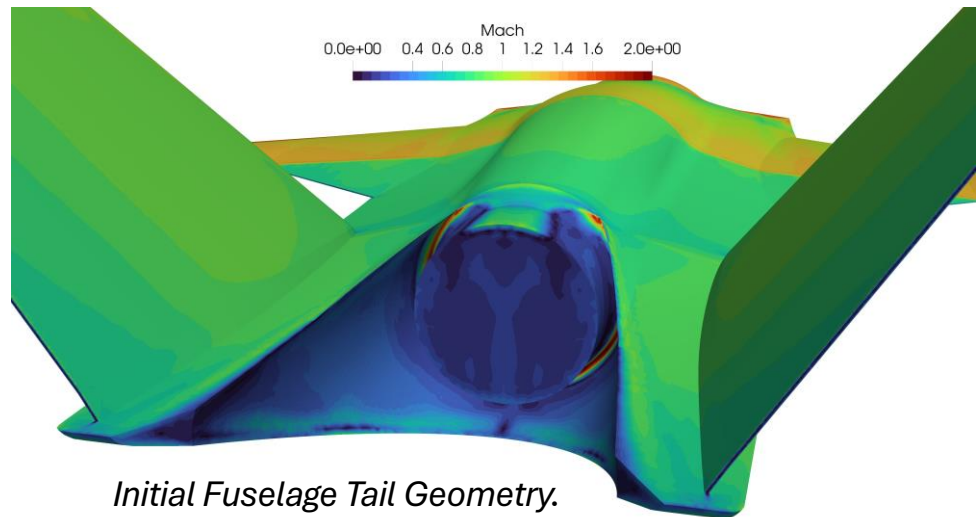


Flow Streamlines close to the LEX for  $\alpha = 5^\circ$ .

# Complete Aircraft Analysis: Fuselage Tail



The analyses of the complete aircraft also allow to notices problems that require a redesign of certain components. One of these cases is the **fuselage tail redesign**.

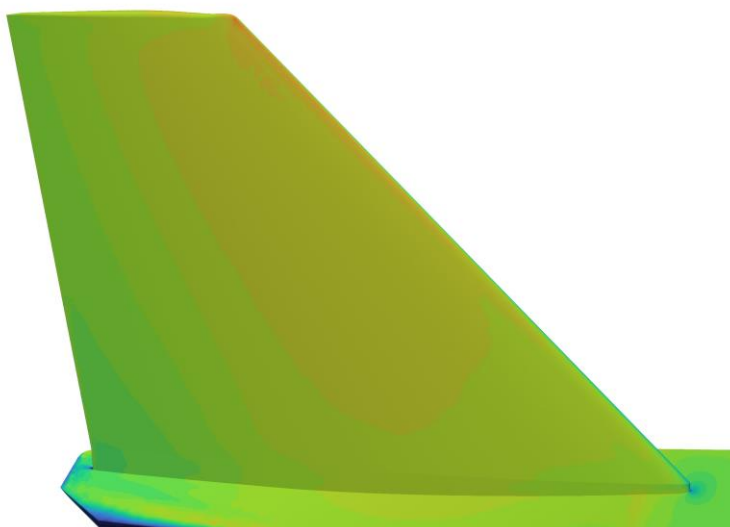
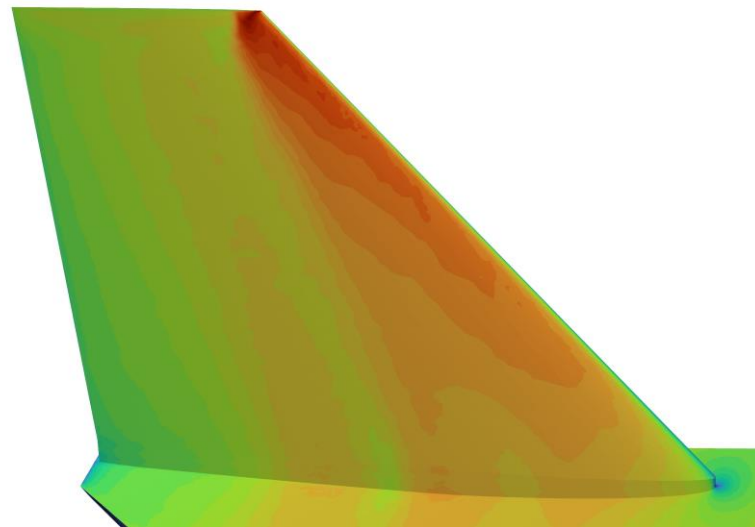
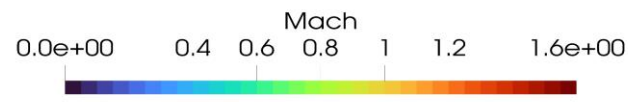


# Complete Aircraft Analysis: Tail Airfoil



A refinement of the airfoil selection of the tail has been possible as well.

*Initial (left) vs Final (right) tail airfoil configuration.*



# Complete Aircraft Analysis: Global Results



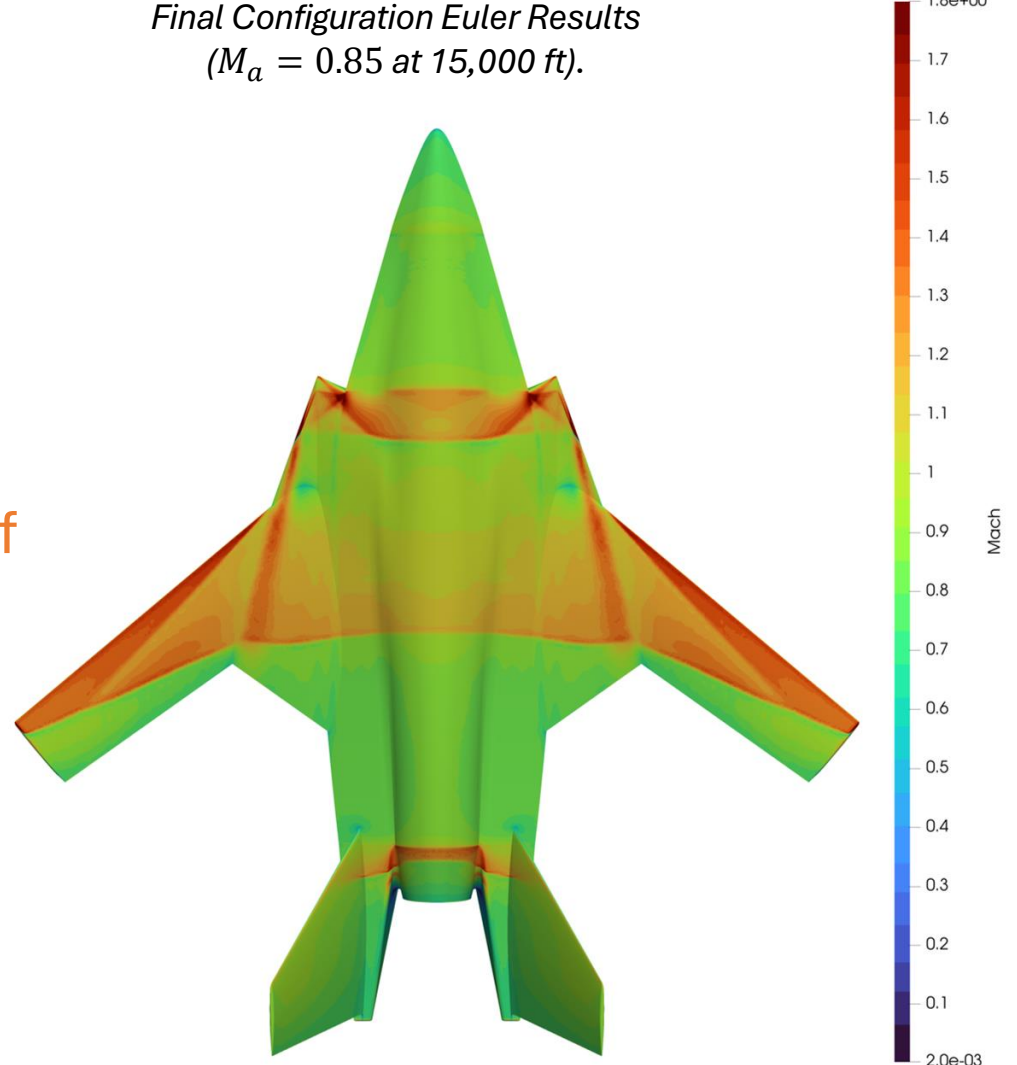
Final runs with the generated geometry are made to evaluate the global effects in sustained turn flying condition.

- Interaction between fuselage, wing, tail and LEX.
- Shockwaves' position.

The results, in terms of benefits gained from the introduction of the LEX, report an efficiency increase of 6% for the fuselage and 16% for the wing.

The fuselage is responsible for 25% of the lift produced.

*Final Configuration Euler Results  
( $M_a = 0.85$  at 15,000 ft).*



# Complete Aircraft Analysis: RANS Analysis

---



A **RANS analysis** was performed in order to verify the previous conclusion about the effectiveness of the LEX.

The following considerations must be kept in mind:

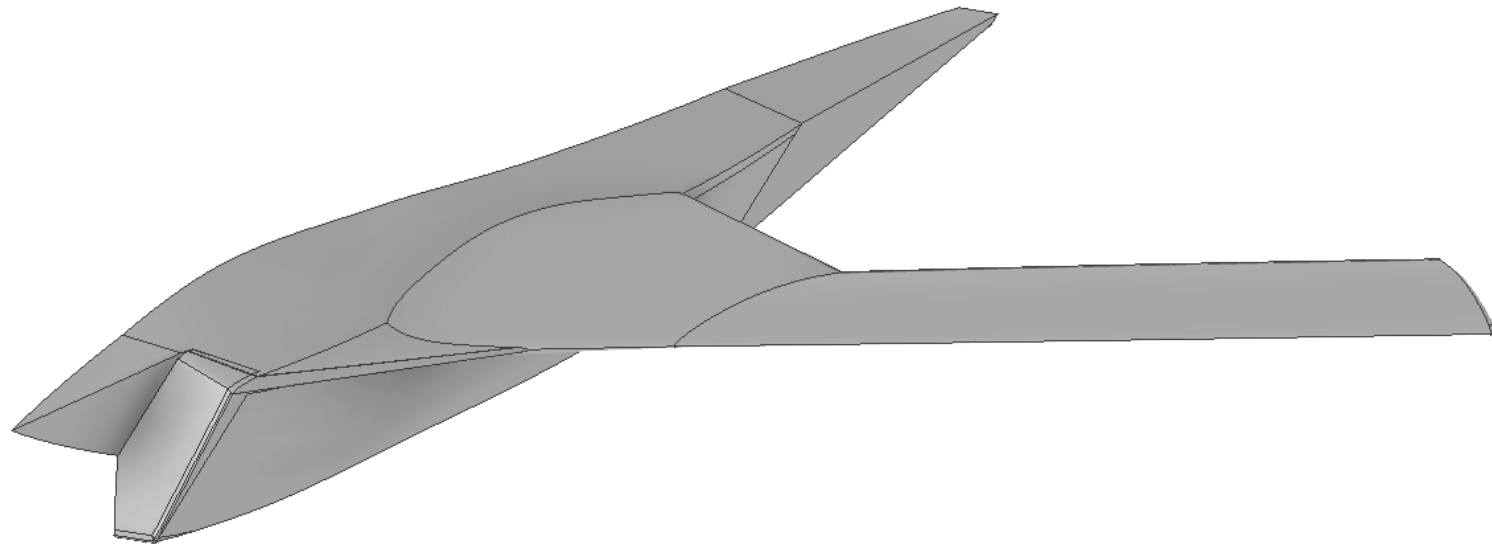
- The simulation was performed at **10° of angle of attack**, thus most of the model is already stalled;
- **Strong flow interaction** of the intake with the wing must be considered, thus a section of the fuselage was included in the domain;
- The symmetry constraint does not completely represent the physics, but it was evaluated as the best compromise;
- The mesh should be very fine, due to the **large separation regions**, but the wake was not refined due to limited computational resources.

Since the **goal** is to analyze the **impact of the LEX on the wing**, the simplifications are expected to be valid.

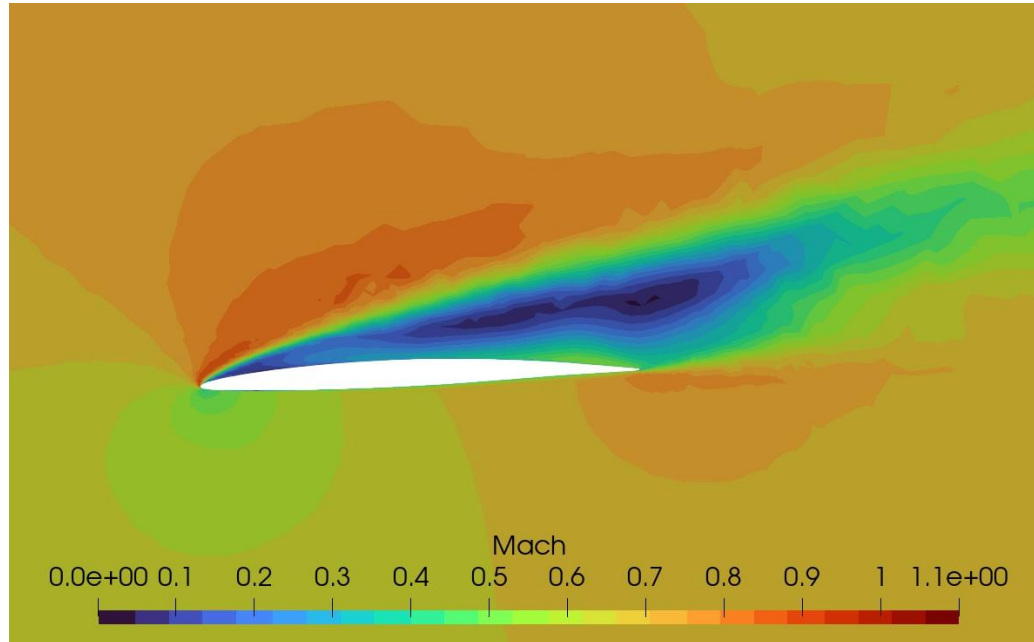


# Complete Aircraft Analysis: RANS Geometry

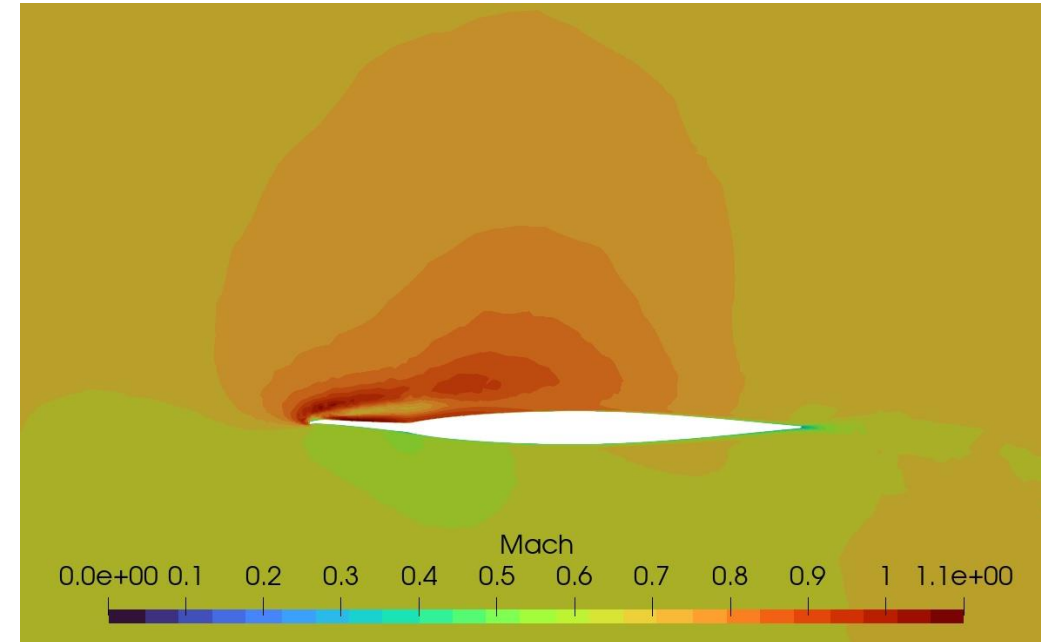
---



# Complete Aircraft Analysis: RANS Analysis



*Section of the wing near the tip.*



*Section of the LEX and the wing.*

# Adjoint Optimization: SU2 Implementation

---



Shape optimization techniques are particularly relevant in transonic conditions, because of the high sensitivity of the coefficients on the wing shape.

The adjoint method is a gradient-based optimization technique useful in CFD problems due to its efficiency in the gradient computation.

The optimization chain of the discrete adjoint formulation is performed in SU2 by means of the following C++ modules:

- SU2\_DEF (Mesh Deformation Code)
- SU2\_GEO (Geometry Definition Code)
- SU2\_CFD (Computational Fluid Dynamics Code)
- SU2\_DOT (Gradient Projection Analysis)

# Adjoint Optimization: Parametrization



The STAD-1 wing is parametrized with 2 FFD and 216 control boxes to capture the complex shape.

The following constraints are imposed:

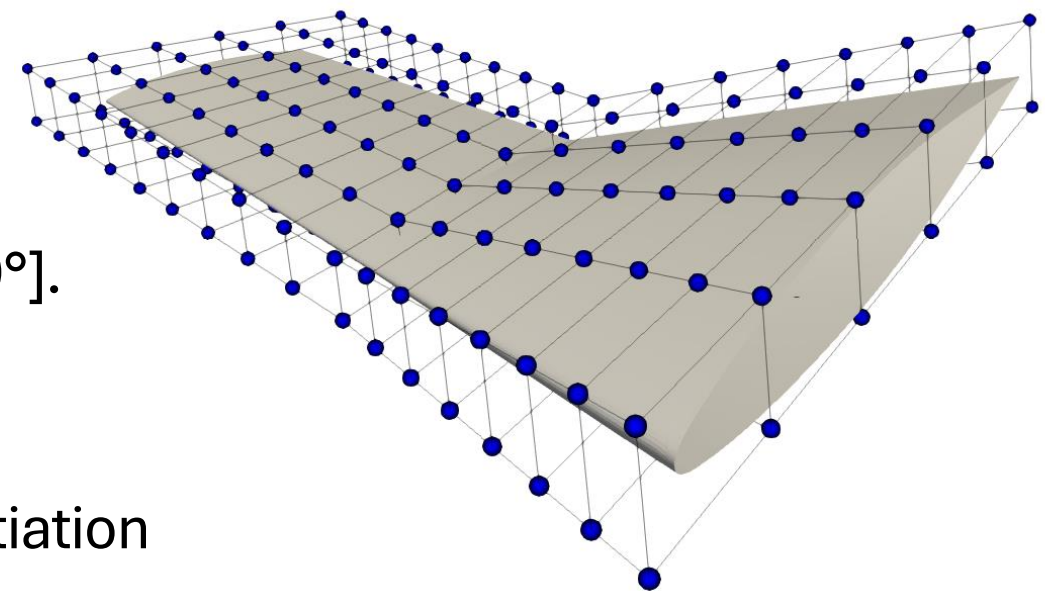
- Displacement only on z-direction.
- Fixed position of leading and trailing edge.
- Thickness constraints of 5 spanwise locations.

The  $C_L$  is fixed and the AOA is free to change in  $[2^\circ : 9^\circ]$ .

**Objective function:**  $C_D$  minimization

**Solver:** Euler

**Gradient computation method:** Automatic Differentiation



*Control box for the optimization problem.*

# Adjoint Optimization: Results

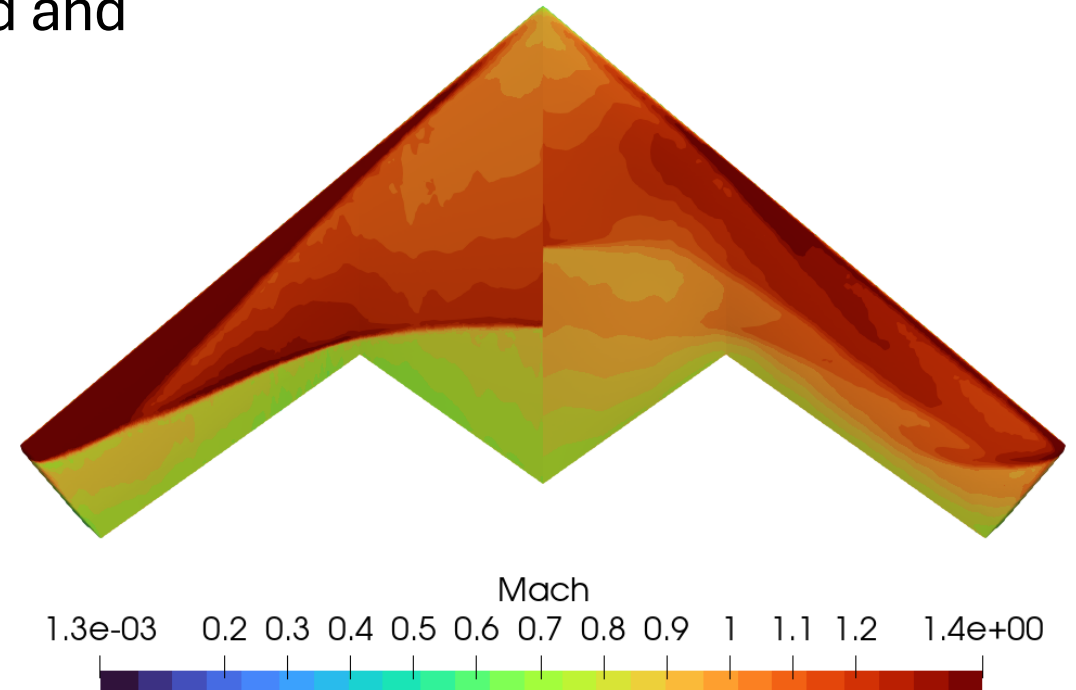


Reached convergence after 17 iterations, with a reduction of 39 drag counts, mainly because of the drop in the intensity of the shockwave.

Regions of high  $M_a$  near the leading edge are smoothed out and the distribution is more uniform.

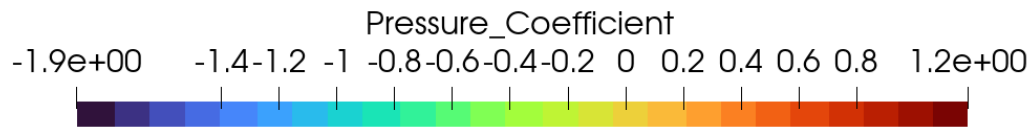
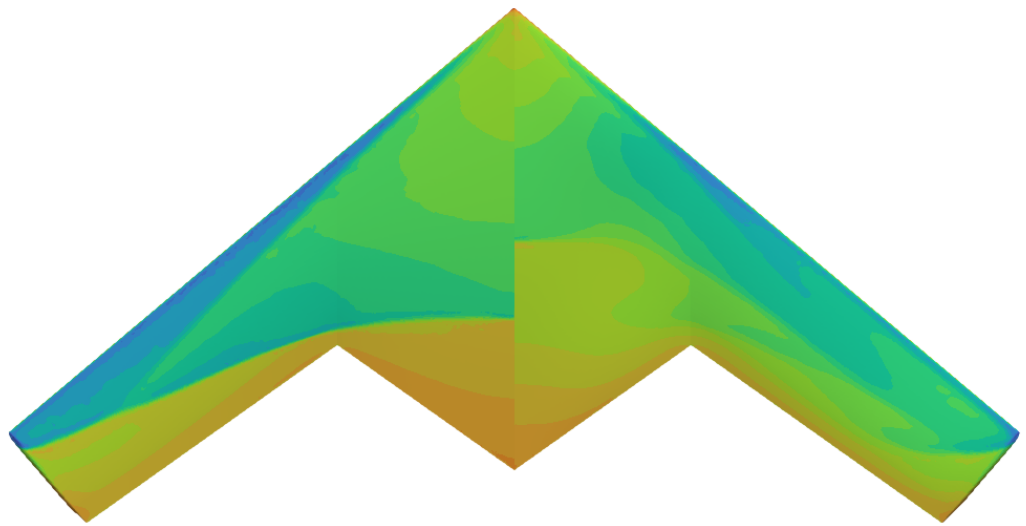
The extent of the shockwave at the root is reduced and the lambda shock pattern is no longer visible.

|                  | $C_L [-]$ | $C_D [-]$ | $\alpha [^\circ]$ |
|------------------|-----------|-----------|-------------------|
| <b>Baseline</b>  | 0.346     | 0.0212    | 6.00              |
| <b>Optimized</b> | 0.346     | 0.0173    | 5.73              |

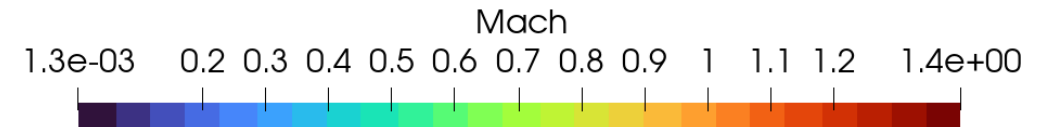
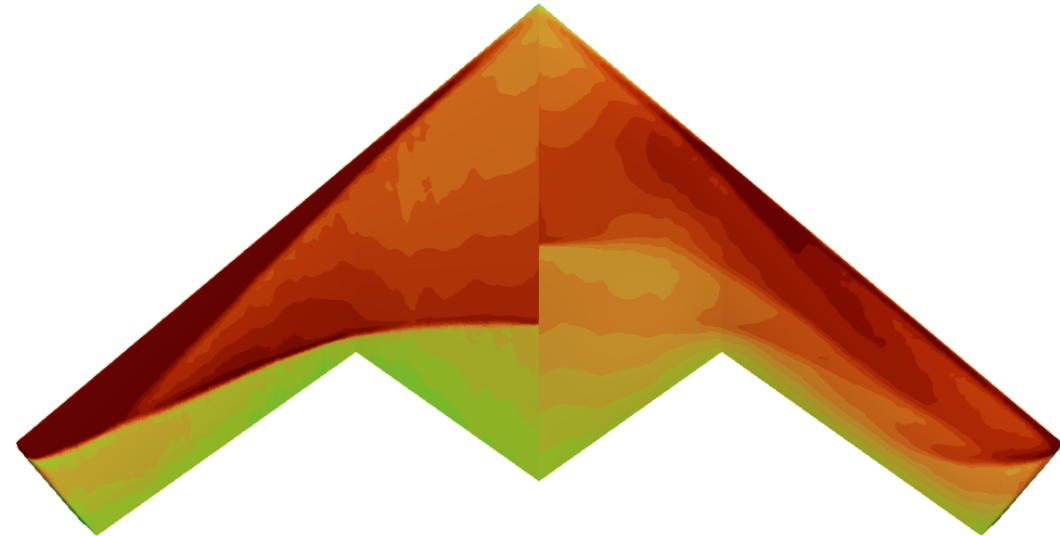


Mach number contours over the initial (left) and optimal (right) wing.

# Aerodynamics: Adjoint Optimization



Pressure coefficient over the initial (left) and optimal (right) wing.



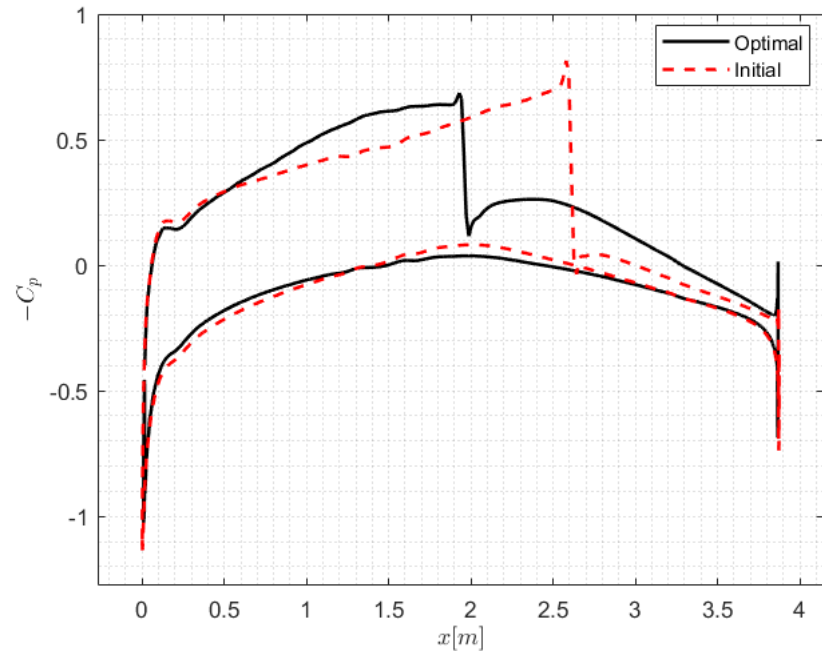
Mach number over the initial (left) and optimal (right) wing.

# Adjoint Optimization: Sections' Results

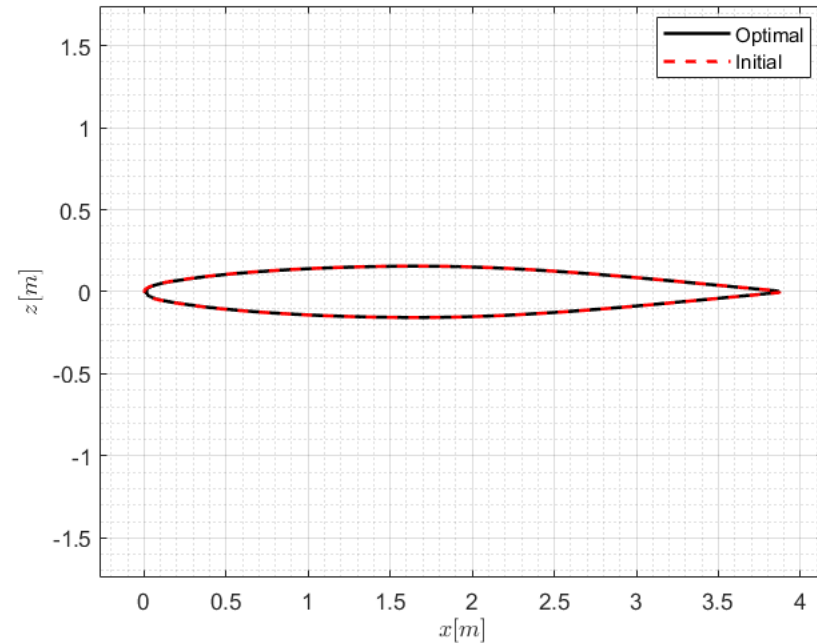


At the wing root the displacement of the control points is restricted, hence no change in shape is possible.

Reduction in the peak of the minimum value of the  $C_p$  and in the shock extent.



Pressure coefficient distribution at the wing root.



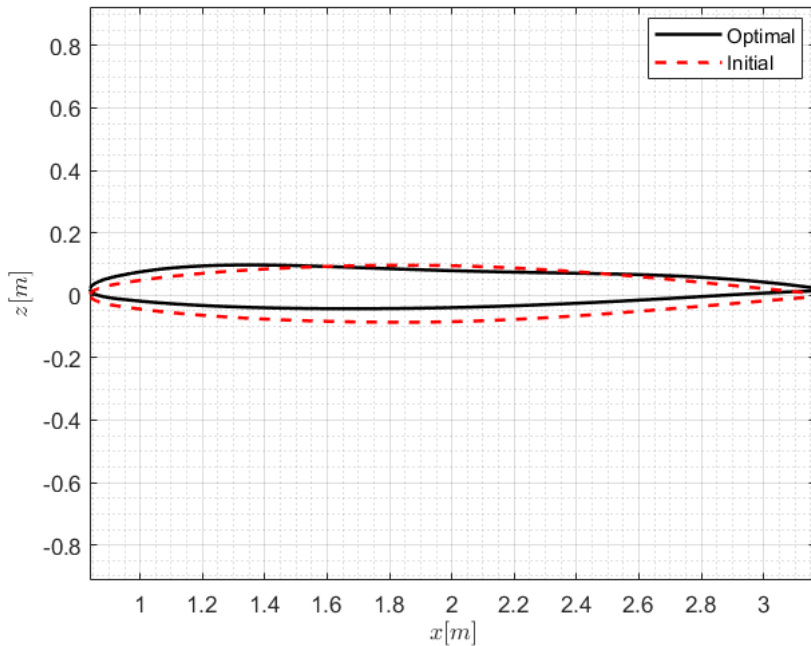
Airfoil shape at the wing root.

# Adjoint Optimization: Sections' Results

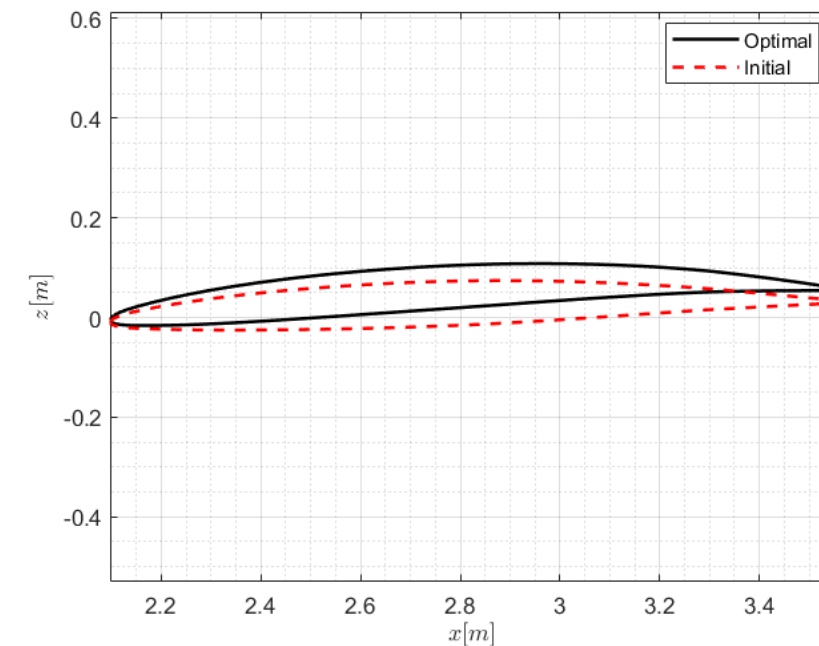


Moving further along the span, the optimization process led to:

- Thickness reduction
- Leading edge radius reduction
- Small variation in twist



*Airfoil shape at 23% of the wing span.*



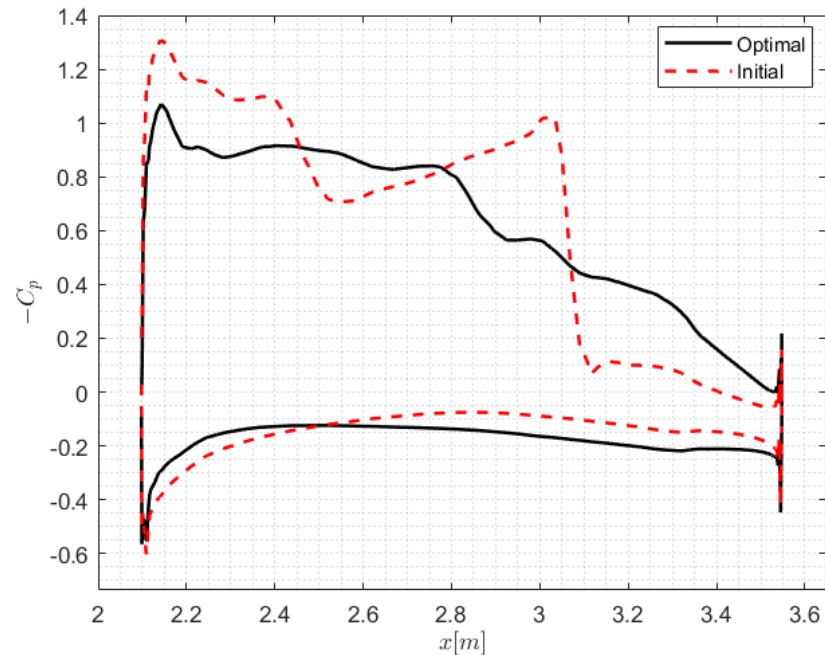
*Airfoil shape at 60% of the wing span.*

# Adjoint Optimization: Sections' Results

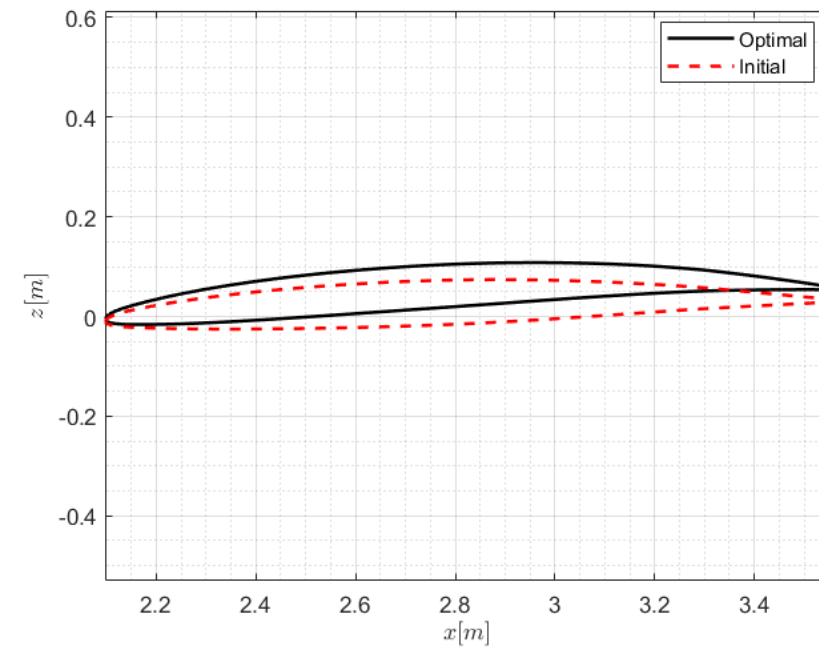


Moving further along the span, the optimization process led to:

- Thickness reduction
- Leading edge radius reduction
- Small variation in twist



Pressure coefficient distribution at 60% of the span.



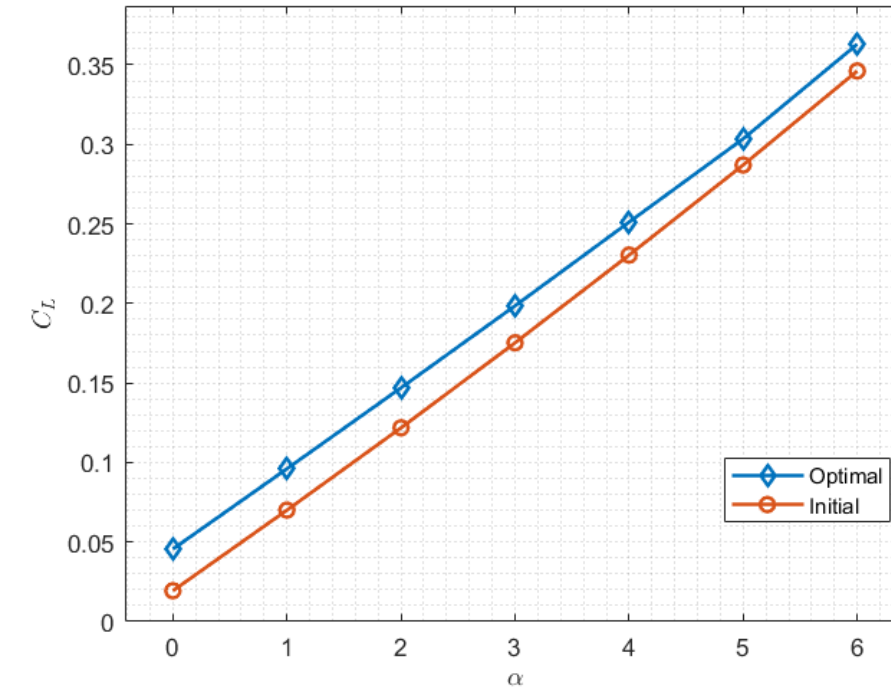
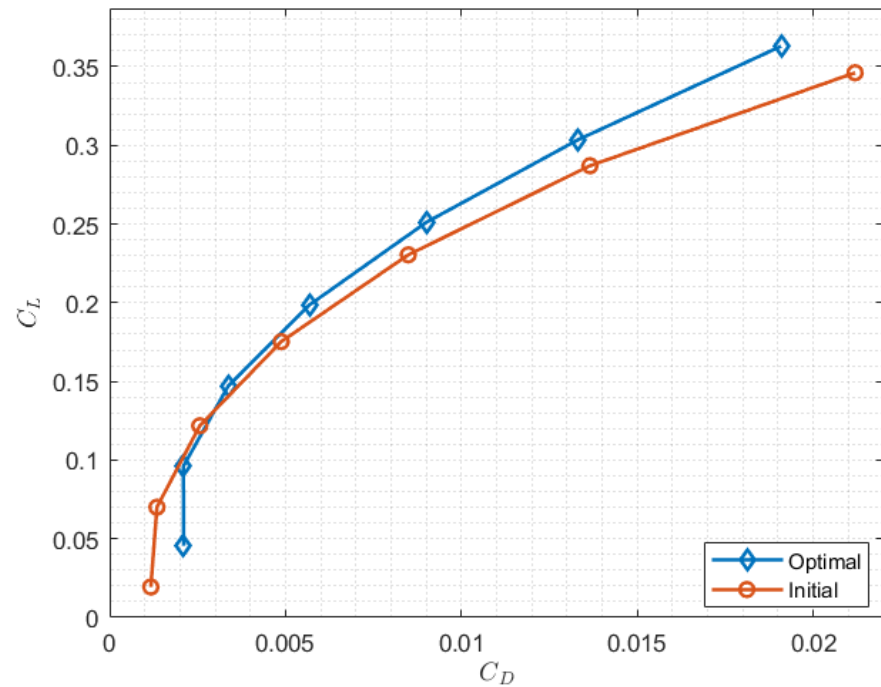
Airfoil shape at 60% of the wing span.

# Adjoint Optimization: Sections' Results



The polar curve shows an increase in the performances of the wing almost over the entire range tested.

The  $C_L - \alpha$  is shifted upwards after the adjoint optimization process.



# Conclusions and Open Points

---



In conclusion, it is possible to say that the use of different methods with different orders allows for a quick but fairly detailed preliminary design of the wing.

Nevertheless, more analysis should follow, considering:

- More precise viscous simulations with more flight conditions, especially higher angles of attack and/or sideslip conditions.
- Improved geometry design for the tail of the fuselage.
- More detailed design on the shape of the LEX.
- Full aircraft with the modelling of the internal ducts and deflected surfaces.



# Thank you for your attention



# Appendix



# Wing Planform Design: OpenVSP Validation

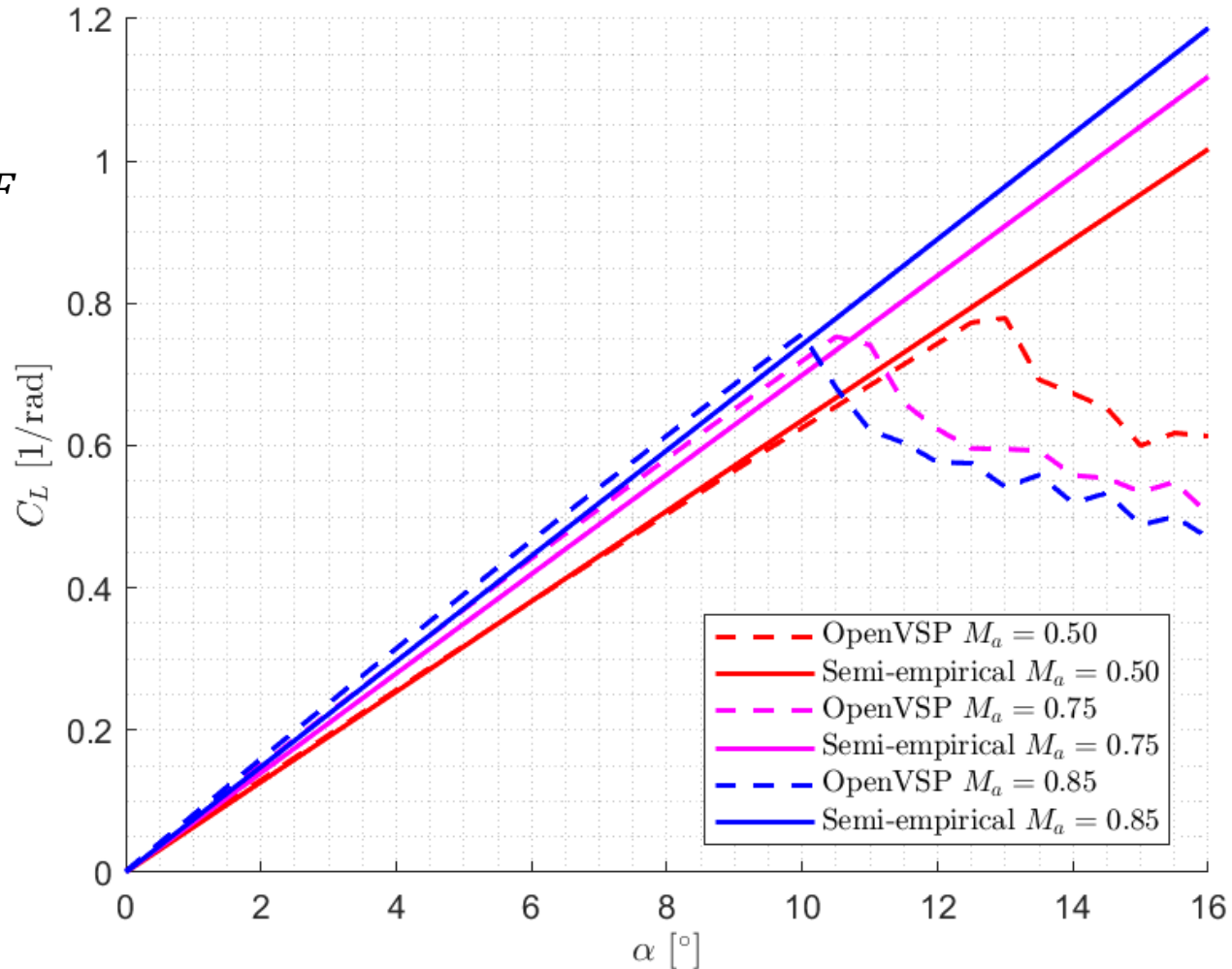


Method taken from Raymer:

$$C_{L\alpha} = \frac{2\pi AR}{2 + \sqrt{4 + \frac{AR^2\beta^2}{\eta^2} \left(1 + \frac{\tan^2 \Lambda_{maxt/c}}{\beta^2}\right)}} \frac{S_{exposed}}{S_{ref}} F$$

Where:

- $\beta^2 = 1 - M^2$
- $\eta = \frac{c_{l\alpha}}{2\pi/\beta}$
- $F = 1.07(1 + d/b)^2$



# DUST: Mathematical Formulation



Based on Helmholtz's decomposition applied to incompressible Newtonian fluid:

$$\begin{aligned} \left\{ \begin{array}{l} \nabla \cdot \mathbf{u} = 0 \\ \frac{\partial \mathbf{u}}{\partial t} + \mathbf{u} \cdot \nabla \mathbf{u} = -\frac{1}{\rho} \nabla p + \nu \nabla^2 \mathbf{u} \end{array} \right. & \quad \parallel \quad \begin{array}{l} \nabla \cdot \mathbf{u}_\phi = 0 \rightarrow \mathbf{u}_\phi = \nabla \phi \\ \nabla \cdot \mathbf{u}_\psi = 0 \rightarrow \mathbf{u}_\psi = \nabla \times \psi \end{array} \quad \Rightarrow \quad \begin{array}{l} \text{Lagrange equation} \\ \nabla \cdot \mathbf{u}_\phi = \nabla^2 \phi = 0 \\ \nabla \times \mathbf{u}_\psi = \mathbf{0} - \nabla^2 \psi = \boldsymbol{\omega} \end{array} \\ \mathbf{u}(\mathbf{r}, t) = \mathbf{u}_\phi(\mathbf{r}, t) + \mathbf{u}_\psi(\mathbf{r}, t) & \end{aligned}$$

Following Morino formulation differential problem rewrtiten as boundary element problem

Lagrange equation:

$$\begin{aligned} E(\mathbf{r})\varphi(\mathbf{r}, t) = & \oint_{S_s} \hat{\mathbf{n}}(\mathbf{r}_0, t) \cdot \nabla_0 G(\mathbf{r}_0, \mathbf{r}) \varphi(\mathbf{r}_0, t) dS(\mathbf{r}_0) \\ & + \oint_{\Omega_f \setminus S_s} \hat{\mathbf{n}}(\mathbf{r}_0, t) \cdot \nabla_0 G(\mathbf{r}_0, \mathbf{r}) \Delta \varphi(\mathbf{r}_0, t) dS(\mathbf{r}_0) \\ & - \oint_{S_s} G(\mathbf{r}_0, \mathbf{r}) \hat{\mathbf{n}}(\mathbf{r}_0, t) \cdot \nabla_0 \varphi(\mathbf{r}_0, t) dS(\mathbf{r}_0) \end{aligned}$$

Poisson equation:

$$\boldsymbol{\psi}(\mathbf{r}, t) = \int_{\Omega_f} G(\mathbf{r}, \mathbf{r}_0) \boldsymbol{\omega}(\mathbf{r}_0, t) dV(\mathbf{r}_0)$$





Lagrange equation is solved with a collocation method the problem si rewritten as:

$$\hat{\mathbf{n}} \cdot \mathbf{u}_\varphi = \hat{\mathbf{n}} \cdot (\mathbf{u}_b - \mathbf{U}_\infty - \mathbf{u}_\psi) =: \sigma$$

*Boudary condition*

$$\mu_{k_l} = f_{i_l}(\mu_{k_s}, \mu_{k_v}, \mu_{k_l}, \sigma_{k_s}, \mu_{k_w})$$

*... for Lifting line*

$$\begin{bmatrix} A_{ss} & A_{sv} \\ C_{vs} & C_{vv} \end{bmatrix} \begin{pmatrix} \mu_s \\ \mu_v \end{pmatrix} = - \begin{bmatrix} A_{sl} \\ C_{vl} \end{bmatrix} \boldsymbol{\mu}_l - \begin{bmatrix} B_{ss} & \emptyset_{sv} \\ D_{vs} & -I_{vv} \end{bmatrix} \boldsymbol{\sigma} - \begin{bmatrix} A_{sw} \\ C_{vw} \end{bmatrix} \boldsymbol{\mu}_w$$

*... for Surface Panel and Vortex lattice*

**BUT...**

To impose Kutta condition on Surface panels an implicit wake panel is needed

$$\mu_{w,i_{TE}} = \mu_{s^{up},i_{TE}} - \mu_{s^{low},i_{TE}} = T \mu_{s,i_{TE}}$$

$$\tilde{A}_{ss} = A_{ss} + A_{sw_{TE}} T$$

$$\tilde{C}_{ss} = C_{ss} + C_{sw_{TE}} T$$

$$\Rightarrow \begin{bmatrix} \tilde{A}_{ss} & A_{sv} \\ \tilde{C}_{vs} & C_{vv} \end{bmatrix} \begin{pmatrix} \mu_s \\ \mu_v \end{pmatrix} = - \begin{bmatrix} A_{sl} \\ C_{vl} \end{bmatrix} \boldsymbol{\mu}_l - \begin{bmatrix} B_{ss} & \emptyset_{sv} \\ D_{vs} & -I_{vv} \end{bmatrix} \boldsymbol{\sigma} - \begin{bmatrix} A_{s\tilde{w}} \\ C_{v\tilde{w}} \end{bmatrix} \boldsymbol{\mu}_{\tilde{w}}$$

# DUST: Mathematical Formulation



Poisson equation is solved with the Vortex Particle Method:

$$\mathbf{u}_\psi(\mathbf{r}, t) = \sum_{i_p=1}^{N_p} \mathbf{K}_\zeta(\mathbf{r}, \mathbf{r}_{i_p}(t)) \times \boldsymbol{\alpha}_{i_p}(t) \quad \text{where...}$$

$$\mathbf{K}_\zeta(\mathbf{x}, \mathbf{y}) = -\frac{1}{4\pi} \frac{\mathbf{x}-\mathbf{y}}{(|\mathbf{x}-\mathbf{y}|^2 + R_v^2)^{3/2}}$$

Vorticity evolution is described using Lagrangian discrete approximation:

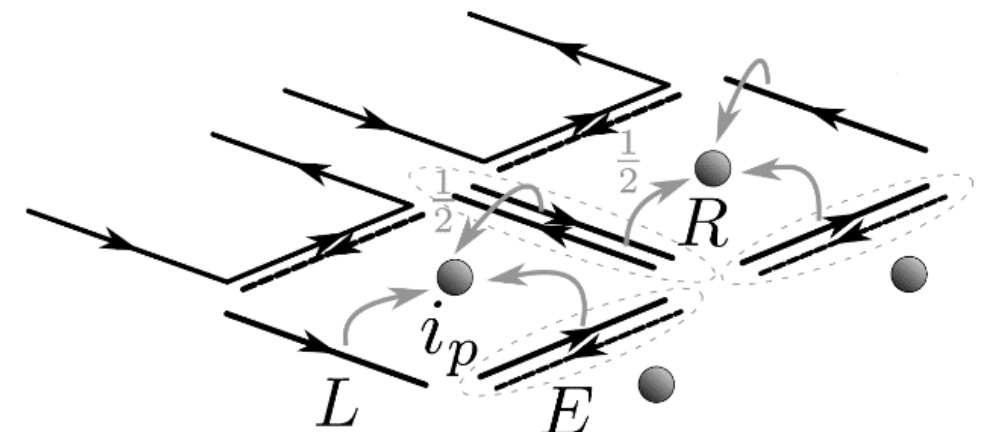
$$\frac{d\mathbf{r}_{i_p}}{dt} = \mathbf{u}(\mathbf{r}_{i_p}(t), t) \quad \frac{d\boldsymbol{\alpha}_{i_p}}{dt} = \nabla \mathbf{u}(\mathbf{r}_{i_p}(t), t) \cdot \boldsymbol{\alpha}_{i_p} + \nu " \Delta \boldsymbol{\alpha}_{i_p}"$$

---

Wake panel are converted into particle as follows:

$$\boldsymbol{\alpha}_{i_p} = J_L + J_R + J_E$$

where...  $J = \int_S (\mu_{w,i} - \mu_{w,j}) dl$

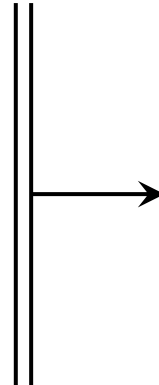


# DUST: Workflow



The final **dynamical system** obtained is solved as follows:

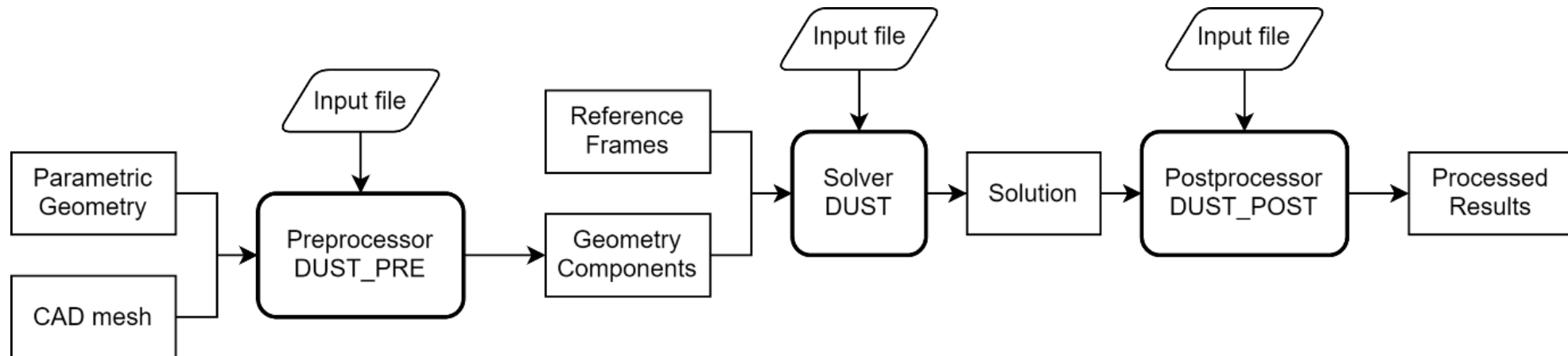
1. Boundary condition  $\sigma$  are computed
2. Potential-velocity problem solution
3. Nonlinear lifting line problem solution
4. Evolution of the wake



**Singularity** values ( $\sigma, \mu$ )  
known at each time step



Flow **velocity** known so...  
Can compute **loads** on the bodies



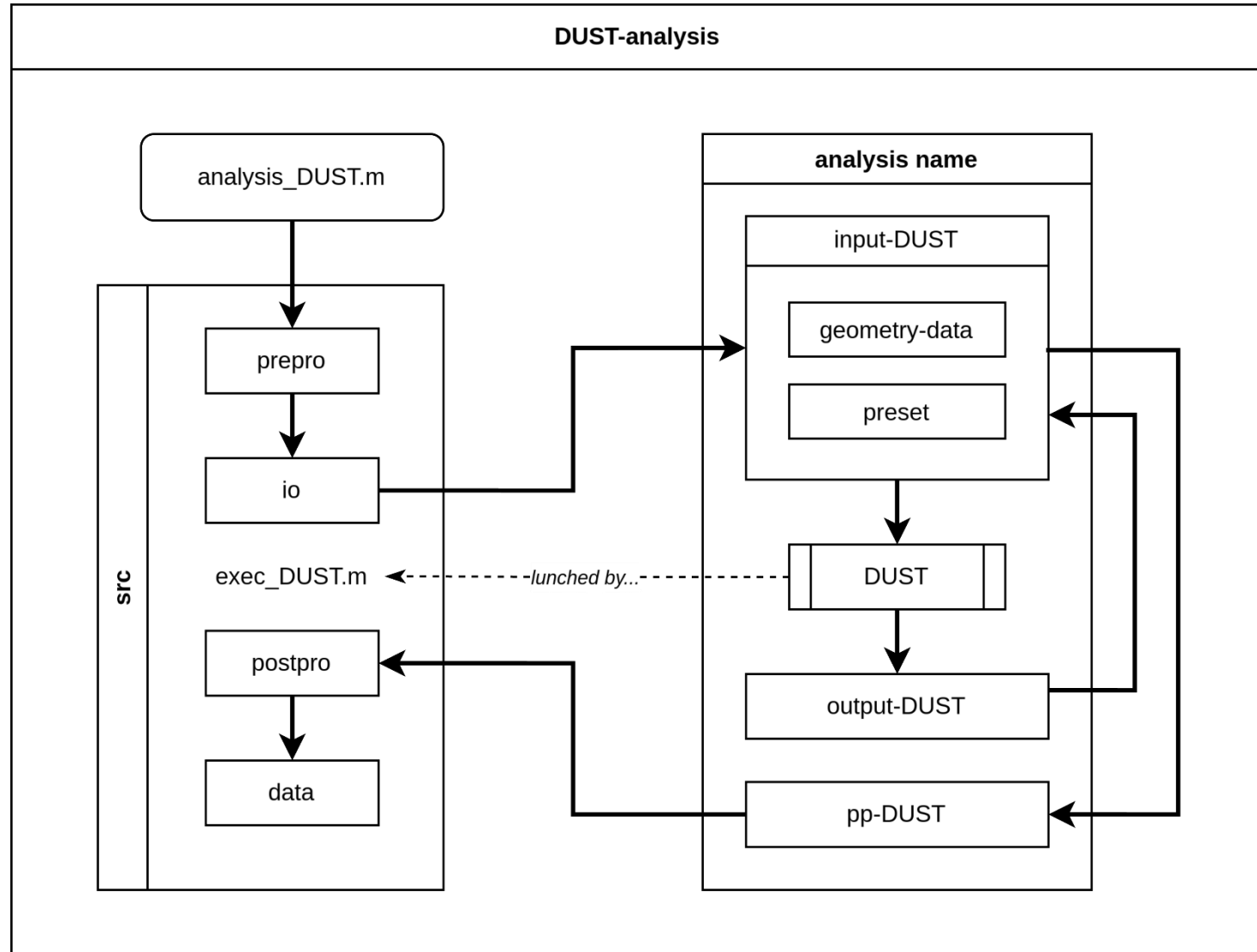
# DUST: MATLAB Interface Architecture



Interface written mainly in  
MATLAB language  
*With some minor script in Python*

System specifications:

- DUST release 0.8.2-b
- MATLAB 2023b
- Visual Studio Code
- Paraview 5.12.1
- Ubuntu 22.04.4 LTS
  - CPU: Ryzen 2700x
  - RAM: 16Gb
  - SSD: Samsung 860evo



# Onera M6: Test Case

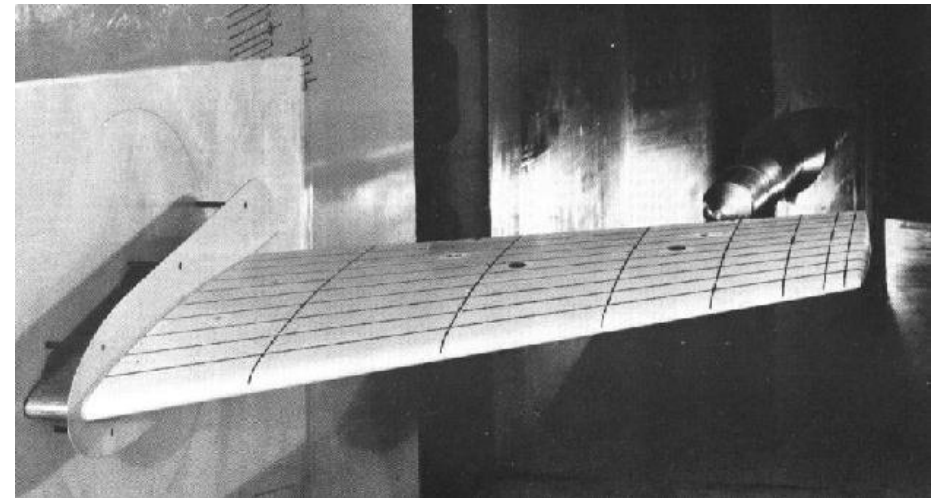


## **What is ONERA M6?**

Swept symmetrical semispan wing

Designed in 1972 by ONERA Aero Department

Experimental geometry for study 3D transonic flow



## **Why ONERA M6?**

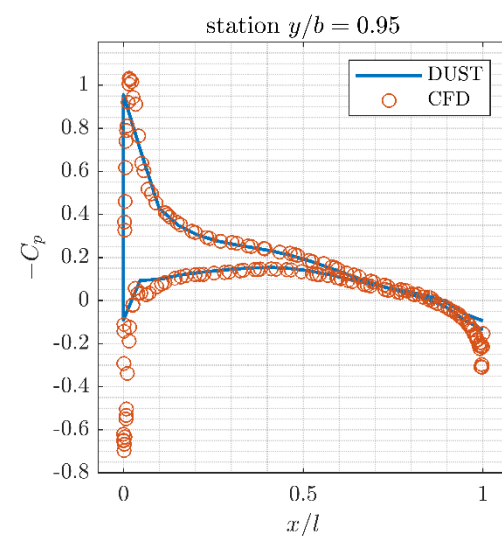
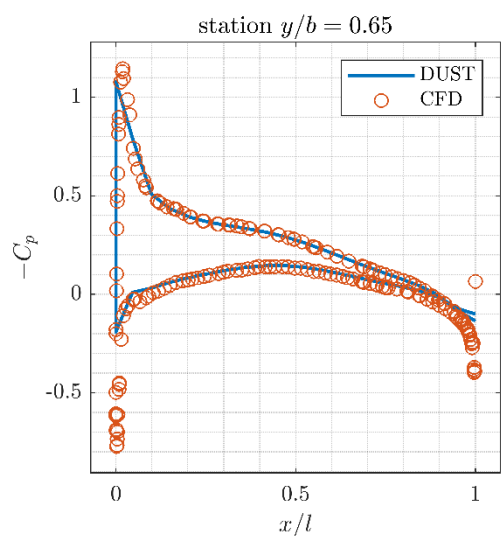
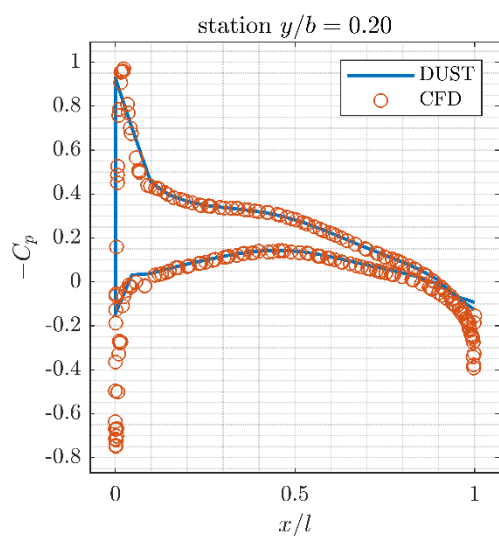
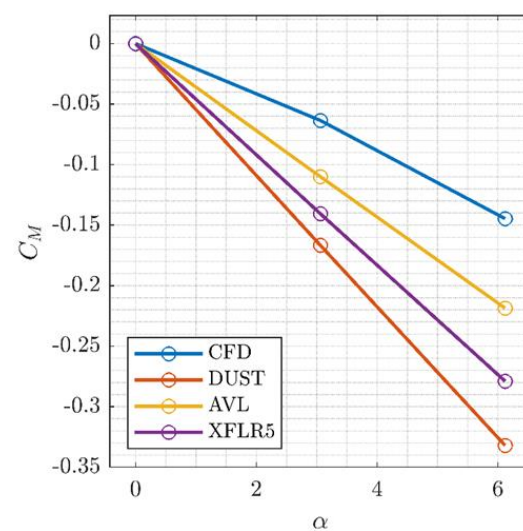
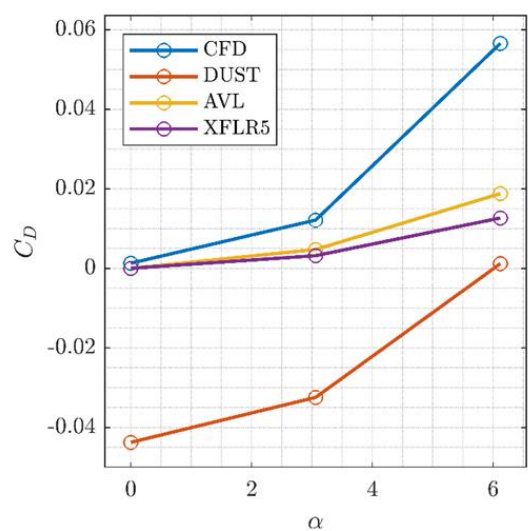
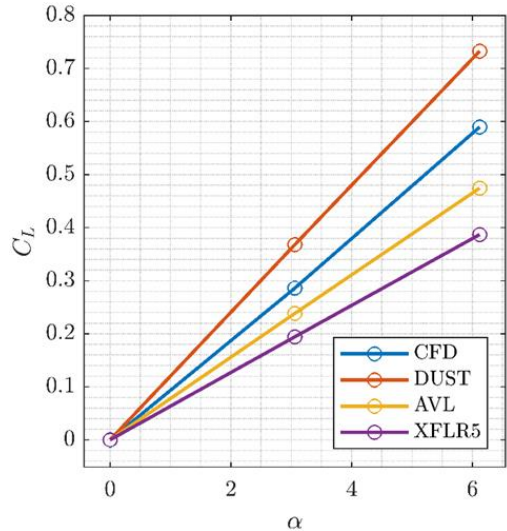
Has become a common CFD test case



Data available online to compare

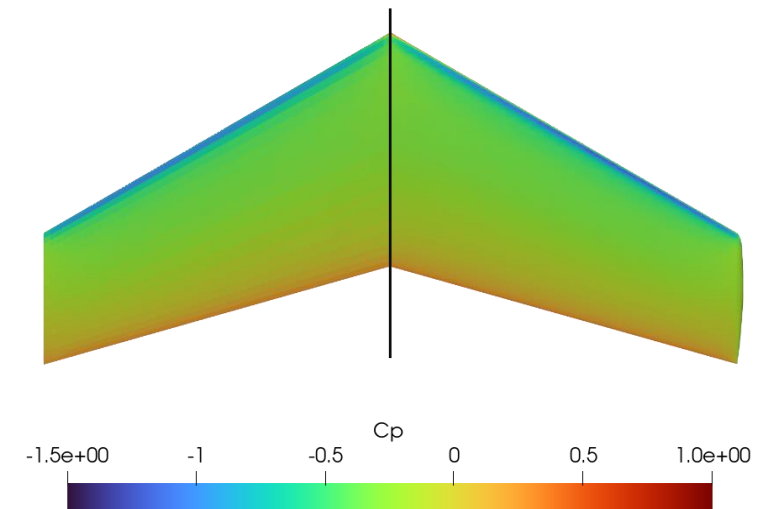
| MAC [m] | Span [m] | AR [-] | Taper | LE sweep [°] | TE sweep [°] |
|---------|----------|--------|-------|--------------|--------------|
| 0.646   | 1.196    | 3.800  | 0.562 | 30.0         | 15.8         |

# Onera M6: Subsonic Analysis

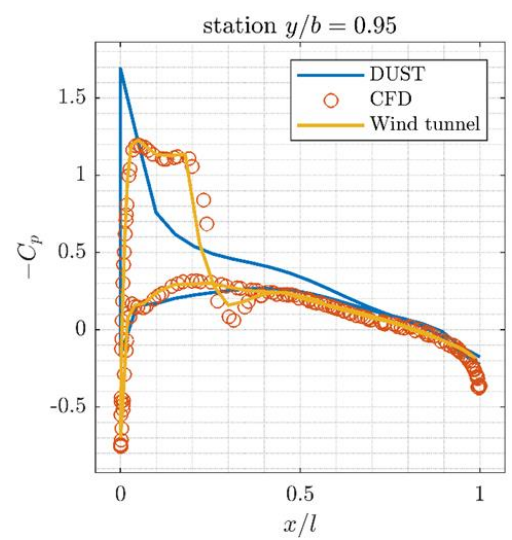
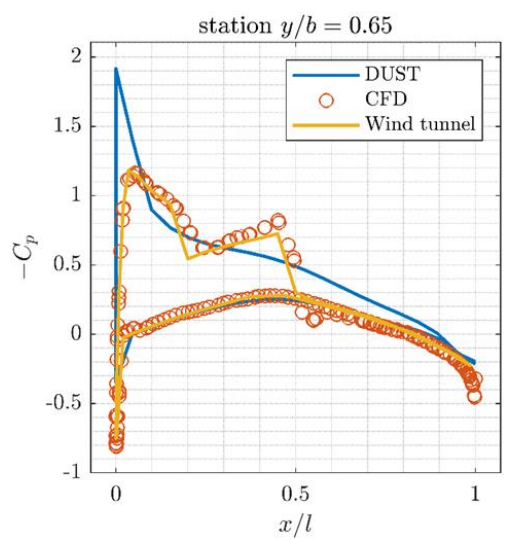
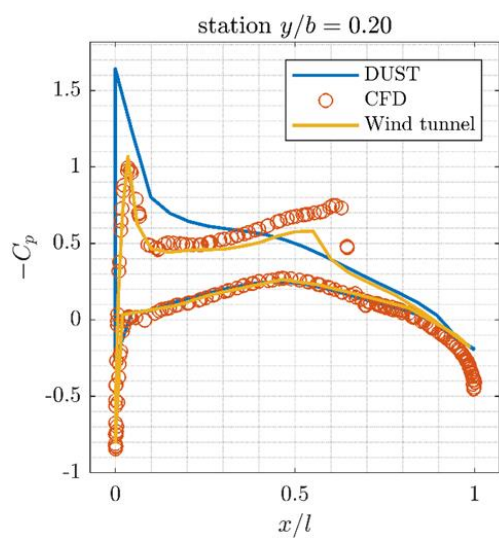
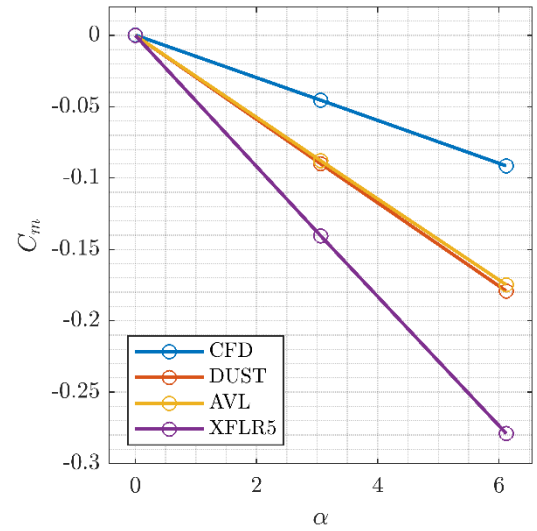
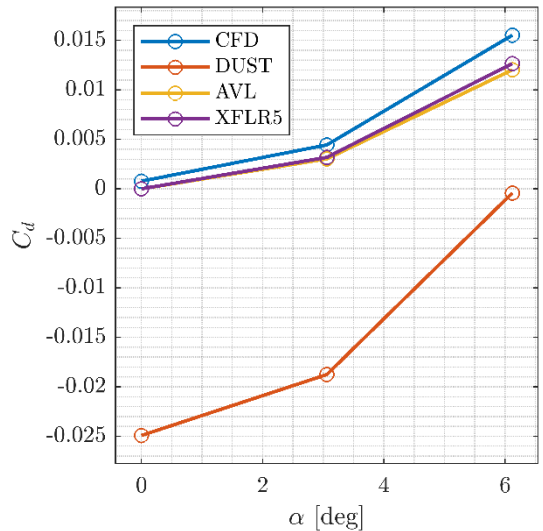
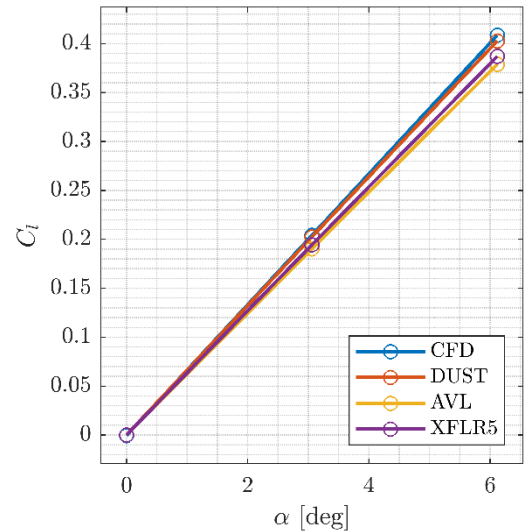


Free stream condition of both  
**DUST** and **SU2**:

| Ma [-] | P [Pa] | T [ $^{\circ}$ C] | $\alpha$ [ $^{\circ}$ ] |
|--------|--------|-------------------|-------------------------|
| 0.84   | 99974  | 15                | 0                       |
| 0.84   | 99974  | 15                | 3.06                    |
| 0.84   | 99974  | 15                | 6.12                    |



# Onera M6: Transonic Analysis



Free stream condition of both  
**DUST, SU2 and Wind tunnel:**

| Ma [-] | P [Pa] | T [ $^{\circ}$ C] | $\alpha$ [ $^{\circ}$ ] |
|--------|--------|-------------------|-------------------------|
| 0.30   | 12767  | 15                | 0                       |
| 0.30   | 12767  | 15                | 3.06                    |
| 0.30   | 12767  | 15                | 6.12                    |

